



# ESA CONTRACT REPORT

---

Contract Report to the European Space Agency

## **The technical support for global validation of ERS Wind and Wave Products at ECMWF**

**(April 2004 – June 2007)**

September 2007

*Authors: Saleh Abdalla and Hans Hersbach*

Final report for ESA contract 18212/04/I-OL

European Centre for Medium-Range Weather Forecasts  
Europäisches Zentrum für mittelfristige Wettervorhersage  
Centre européen pour les prévisions météorologiques à moyen terme

**Series: ECMWF - ESA Contract Report**

A full list of ECMWF Publications can be found on our web site under:  
<http://www.ecmwf.int/publications/>

**© Copyright 2007**

European Centre for Medium Range Weather Forecasts  
Shinfield Park, Reading, RG2 9AX, England

Literary and scientific copyrights belong to ECMWF and are reserved in all countries. This publication is not to be reprinted or translated in whole or in part without the written permission of the Director. Appropriate non-commercial use will normally be granted under the condition that reference is made to ECMWF.

The information within this publication is given in good faith and considered to be true, but ECMWF accepts no liability for error, omission and for loss or damage arising from its use.

Contract Report to the European Space Agency

---

**The technical support for global validation of  
ERS Wind and Wave Products at ECMWF  
(April 2004 - June 2007)**

*Authors: Saleh Abdalla and Hans Hersbach*

*Final report for ESA contract 18212/04/I-OL*

European Centre for Medium-Range Weather Forecasts  
Shinfield Park, Reading, Berkshire, UK

September 2007

	Name	Company
First version prepared by (10 July 2007)	S. Abdalla	ECMWF
	H. Hersbach	ECMWF
Quality Visa	P. Bougeault	ECMWF
Application Authorized by	P. Féménias	ESA/ESRIN

**Distribution list:****ESA/ESRIN**

Pierre Féménias  
Wolfgang Lengert  
Pascal Lecomte  
Betlem Rosich Tell  
ESA ESRIN Documentation Desk

**SERCO**

Raffaele Crapolichio  
Giovanna De Chiara

**ESA/ESTEC**

Paul Snoeij  
Evert Attema

**EUMETSAT**

Julia Figa-Saldaña  
Hans Bonekamp

**ECMWF**

HR  
Division Section Heads  
Lars Isaksen  
Ocean Wave Group

## Abstract

Contracted by ESA/ESRIN, ECMWF is involved in the global validation and long-term performance monitoring of the wind and wave Fast Delivery products that are retrieved from the Radar Altimeter (RA), the Synthetic Aperture Radar (SAR) and the Active Microwave Instrument (AMI), on-board the ERS spacecraft. Their geophysical content is compared with corresponding parameters from the ECMWF atmospheric and wave model as well as in-situ observations (when possible). Also, tests on internal data consistency are performed.

The project (18212/04/I-OL), which ran from 1 April 2004 to 30 June 2007, is the continuation of previous contracts initiated with ESA/ESRIN and ESTEC. This note presents the final report on the activities performed within the scope of this contract.

An ERS-2 on-board failure in January 2001 degraded attitude control. It had a negative, though acceptable, effect on the quality of the RA and SAR related products; however, a detrimental effect on AMI scatterometer winds. The problems in attitude control were gradually resolved, and since August 2003 the quality of all products is nominal. After 21 June 2003, ERS-2 lost its global coverage permanently due to the failure of both on-board tape recorders. However, the remaining coverage (North Atlantic and western coasts of North America and at a later stage the Southern Ocean, the coasts of East Asia and the northeastern parts of the Indian Ocean) provides valuable data for assimilation in atmospheric models. Major part of this report is dedicated for that period.

Furthermore, an overview evaluation of the wind and wave products from the entire ERS mission is carried out. The products involved are the fast delivery AMI scatterometer wind and SAR wave mode spectra and the off-line ocean product (OPR) wind and wave data from both ERS-1 and ERS-2 missions.

## 1 Introduction

The ERS mission is a great opportunity for the meteorological and ocean-wave communities. The wind and wave products from ERS-1/2 provide an invaluable data set. They form some kind of benchmarks against which model products can be validated. In addition, they are assimilated in the models to improve the predictions. On the other hand, consistent model products, especially first-guess products, can be used to validate and monitor the performance of the satellite products.

The European Centre for Medium-Range Weather Forecasts (ECMWF) has been collaborating with the European Space Agency (ESA) since the beginning of the ERS-1 mission in performing the global validation and long-term performance monitoring of the wind and wave products. These products are retrieved from three instruments, defining three Fast Delivery (FD) products that are received at ECMWF in BUFR format. Significant wave height and surface wind speed (URA product) are obtained from the Radar Altimeter (RA). Ocean image spectra (UWA product) are from the Synthetic Aperture Radar (SAR). Surface wind speed and direction (UWI product), finally, are retrieved from the Active Microwave Instrument (AMI) scatterometer. In-house developed monitoring tools are used for the comparison of these products with corresponding parameters from the ECMWF atmospheric (IFS) and wave (ECWAM) models (IFS Documentation, 2004). Whenever possible, these tools include a comparison with in-situ measurements. In addition, tests are performed on the internal consistency of the underlying observed quantities measured by the three instruments.

This support has been carried out within the framework of several consecutive contracts with ESA. The current contract (18212/04/I-OL), which is supervised by the European Space Research Institute (ESRIN), ran from 1 April 2004 to 30 June 2007. Findings from the monitoring activities described above are summarized in monthly or cyclic (depending on the product) data quality and validation reports. These reports are sent regularly to ESRIN. Besides giving an overview on instrument performance and scientific interpretation, these

reports also include recommendations to ESA for refinements of calibrations, further algorithm development and model tuning. Such recommendations are based on a long-term analysis of the relevant parameters.

In addition to these monitoring activities, dedicated studies on data quality and related scientific research have been carried out. These embrace, among others, collocation studies, algorithm development and the incorporation of ERS wind and wave data in the operational ECMWF assimilation system. As a result, ERS altimeter wave heights have been assimilated in the ECMWF wave model since 15 August 1993 (Janssen *et al.* 1997). It was replaced by ENVISAT Radar Altimeter-2 (RA-2) on 22 October 2003. Scatterometer winds were introduced in the atmospheric variational assimilation system on 30 January 1996 (for a description of its impact, see Isaksen and Janssen 2004). It was re-introduced on 8 March 2004 (Hersbach *et al.* , 2004), after the suspension in January 2001. The assimilation of SAR wave mode spectra in the ECMWF wave model, on the other hand, was realised on 13 January 2003. ERS-2 SAR assimilation was replaced by ENVISAT Advanced Synthetic Aperture Radar (ASAR) Level 1b wave mode spectra on 1 February 2006.

Since the ERS mission is approaching the end of its lifetime, it is thought opportune to make a review of the quality of the various products from both ERS-1 and ERS-2 satellites. Those products are the fast delivery (FD) scatterometer wind (UWI) product, FD SAR Wave Mode (UWA) product and both FD (URA) and the off-line OPR (Ocean Product) altimeter wind and wave products.

This document presents the final report of the present contract. It provides a focus on the operational performance of the wind and wave products over the last few years. Furthermore, an overview assessment of wind and wave products from the ERS mission since the start of the mission.

In Section 2, the performance of altimeter FD URA data in the North Atlantic will be considered. Section 3 presents the global performance of the altimeter OPR product for the whole lifetime of the ERS mission. An overview of the performance of the SAR significant wave height, both globally and in the North Atlantic, will be presented in Section 4, and of UWI wind data in Section 5. In Section 6, conclusions are formulated, and the report ends with a list of ECMWF model changes since November 2000.

## Acronyms

AMI	Active Microwave Instrument
ASPS	Advanced Scatterometer Processing System
AOCS	Attitude and Orbit Control System
ASAR	Advanced Synthetic Aperture Radar
ASCAT	Advanced SCATterometer
ASCII	American Standard Code for Information Interchange
BUFR	Binary Universal Form for the Representation of meteorological data
CERSAT	French ERS Processing and Archiving Facility (Centre ERS d'Archivage et de Traitement)
CMEDS	Canadian Marine Environmental Data Service
CMOD	C-band Geophysical MODEL function
EBM	Extra Back-up Mode
ECMWF	European Centre for Medium-range Weather Forecasts
ECWAM	ECMWF Wave Model (an enhanced version of WAM model)
ENVISAT	ENVIronmental SATellite
ERA-40	ECMWF 40-Year Reanalysis
ERS	European Remote sensing Satellite
ESA	European Space Agency
ESACA	ERS Scatterometer Attitude Corrected Algorithm
ESTEC	European Space research and TEchnology Centre
ESRIN	European Space Research INstitute
FD	Fast Delivery product
FEEDBACK	data to which information on usage in the ECMWF assimilation system has been added
FG	ECMWF First Guess with a time resolution of 3 hours
FGAT	First Guess at Appropriate Time
GMF	scatterometer Geophysical Model Function
GTS	Global Telecommunication System
HRES	High RESolution
IDL	Interactive Data Language
IFREMER	French Research Institute for Exploitation of the Sea (Institut français de recherche pour l'exploitation de la mer)
IFS	Integrated Forecast System
JPL	Jet Propulsion Laboratory
KNMI	Koninklijk Nederlands Meteorologisch Instituut
LRDPF	Low Rate Data Processing Facility
LBR	Low Bit Rate
MPI	Max-Planck-Institut for meteorology, Hamburg
NESDIS	National Environmental Satellite Data and Information Service
NDBC	U.S. National Data Buoy Center
NH	Northern Hemisphere
NRES	Nominal RESolution
NRT	Near-Real Time
NSCAT	NASA (National Aeronautics and Space Agency) Scatterometer
OPR	(ERS Radar Altimeter) Ocean PProduct



QC	Quality Control
QSCAT-1	QuikSCAT Scatterometer geophysical model function
RA	Radar Altimeter
RA-2	(ENVISAT) Radar Altimeter-2
RMSE	Root-Mean Square Error
SAR	Synthetic Aperture Radar
SH	Southern Hemisphere
SI	Scatter Index
STDV	STandard DeViation (of the Difference)
SWH	Significant Wave Height
UKMO	UK Met Office
URA	User FD Radar Altimeter product
UTC	Coordinated Universal Time
UWA	User FD SAR WAVE product
UWI	User FD scatterometer WInd product
WAM	third-generation ocean-WAVE Model
WMO	World Meteorological Organization
ZGM	Zero-Gyro Mode

## 2 The Radar Altimeter URA Product

Each URA (User fast delivery Radar Altimeter) product is sampled at 7 km along the satellite ground track. First the altimeter data stream is divided into sequences of 30 individual neighbouring observations. Erroneous and suspicious individual observations are removed and the remaining data in each sequence are averaged to form a representative super-observation, provided that the sequence has at least 20 "good" individual observations. Then, further monitoring is performed with respect to these super-observations, which, for this purpose are collocated with ECMWF model parameters and buoy data. Focus is on URA backscatter, URA wind speed and URA significant wave height.

### 2.1 Data Coverage after June 2003

The loss of the global coverage due to the failure of the on-board low-bit rate tape recorders in June 2003 reduced the number of observations received at ECMWF to about 13% of the full coverage data volume as can be seen in Figure 1 which shows the daily rate of total number of the altimeter super-observations processed at ECMWF. Assessment of the long-term quality of the product after the loss of the global coverage can not be done by comparing it with statistics when there was full coverage. For practical reasons it is not easy to re-process the product over a rather long period for the exact area under current coverage. Instead, readily available long-term statistics for the closest region is considered for comparison. The region covering the extra-tropical Northern Atlantic (north of latitude 20°N) is used as a common area with almost complete coverage before and after the loss of the global coverage. The 7-day running average of daily number of altimeter super-observations in the North Atlantic since the beginning of year 2000 is shown in Figure 2. It is clear that the current coverage in the North Atlantic is slightly lower than the usual coverage. The missing coverage is towards the southern edge of the region as can be seen in Figure 3. Comparing the coverage in Figure 3 with the corresponding one for last year (e.g. Figure 3 of Abdalla and Hersbach, 2006), it is possible to notice the extra coverage in the northeastern parts of the Indian Ocean received through the ground station at Singapore since late October 2006. The reduced coverage between the equator and latitude 20°N in the western parts of the Atlantic and the eastern parts of the Pacific cannot be missed. For the URA product, we will focus our attention on the quality of the altimeter products for the current coverage or specifically in the North Atlantic.

### 2.2 Monitoring of URA Significant Wave Height in the North Atlantic

As usual, URA significant wave heights (SWH) are rather stable and of good quality, apart from the overestimation of small SWH values. Figure 4 shows the time history of the 7- and 365-day running averages of the daily bias between the altimeter and the ECMWF operational model wave heights in the North Atlantic since the beginning of year 2000. After excluding the apparent anomalous altimeter behaviour during March-April 2000 and February 2001 one can distinguish a seasonal cycle of bias in Figure 4 with a minimum value taking place around April-May and a maximum value occurring around October-November before the loss of the global coverage. This seasonal cycle became stronger after the loss of the global coverage with the minimum and maximum values shifted earlier by about one month. Although it is difficult to pinpoint the reason for the stronger cycle, recent model changes like the unresolved bathymetry treatment introduced on 9 March 2004 and the change of wave model dissipation introduced on 5 April 2005 are possible candidates. Another possible reason could be related to the uncovered part towards the southern edge of the area (see Figure 3) which shows less variability than the higher latitudes. The 365-day running average in Figure 4 displays a clear general trend of reduced bias over the years as well. This is mainly due to the model improvements. Recently, the bias seems to fluctuate around the zero value. Apart from that, the bias between the altimeter and the model wave heights

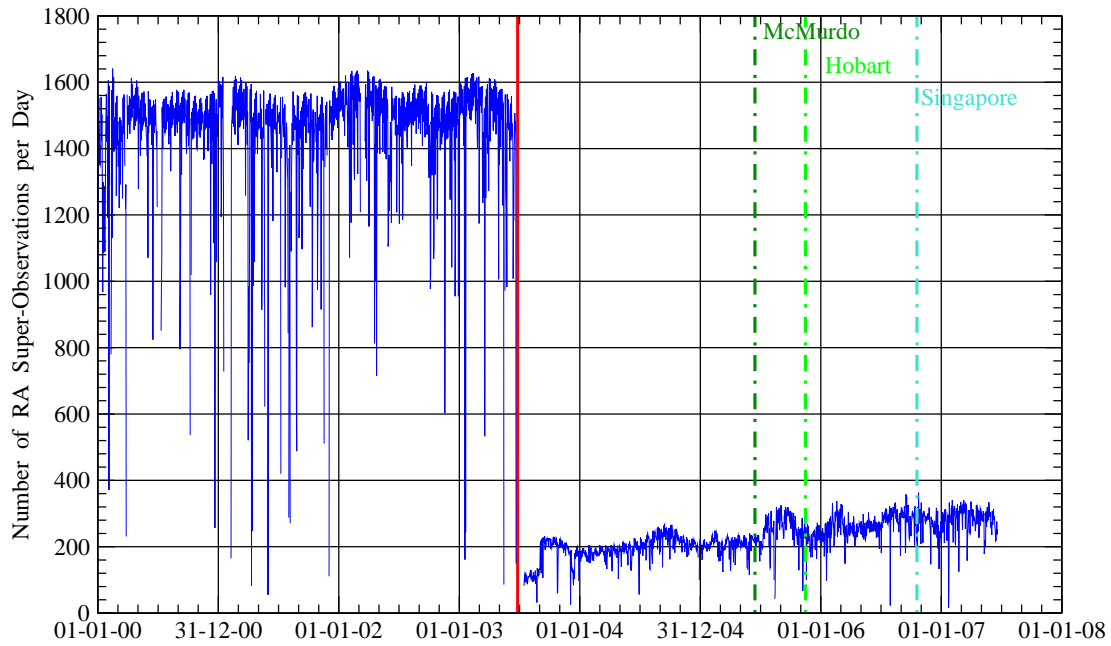


Figure 1: Time history of the total number of ERS-2 altimeter super-observations processed at ECMWF per day since 1 January 2000. Date of loss of global coverage is represented by a red thick vertical line.

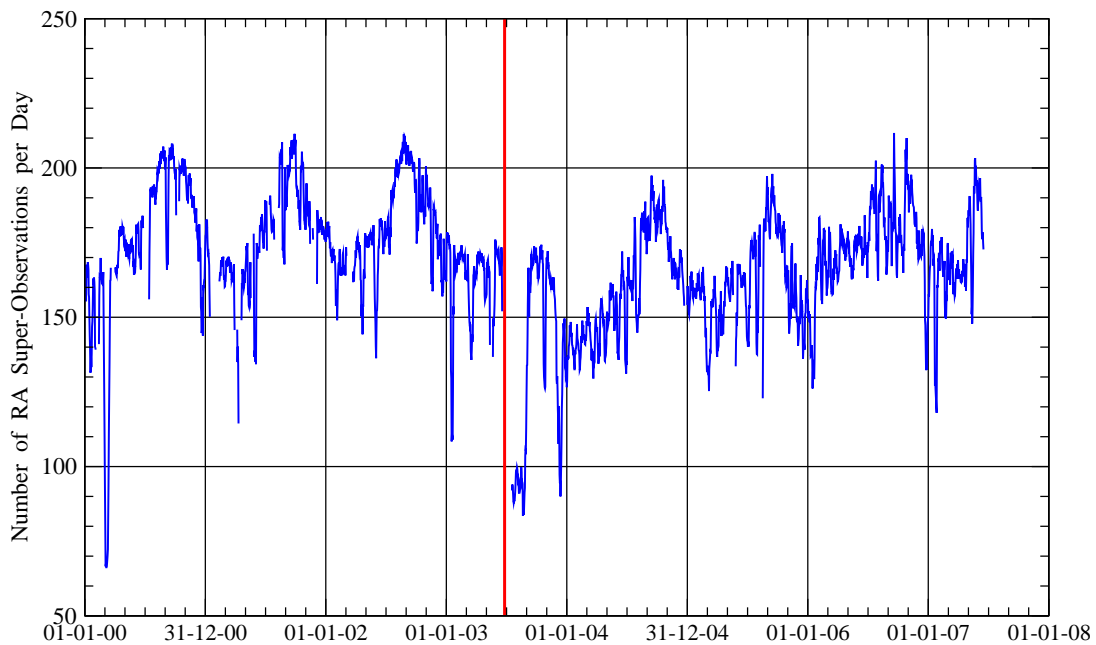


Figure 2: Time history of the 7-day running average of daily number of altimeter super-observations in the North Atlantic since 1 January 2000. Date of loss of global coverage is represented by a red thick vertical line.

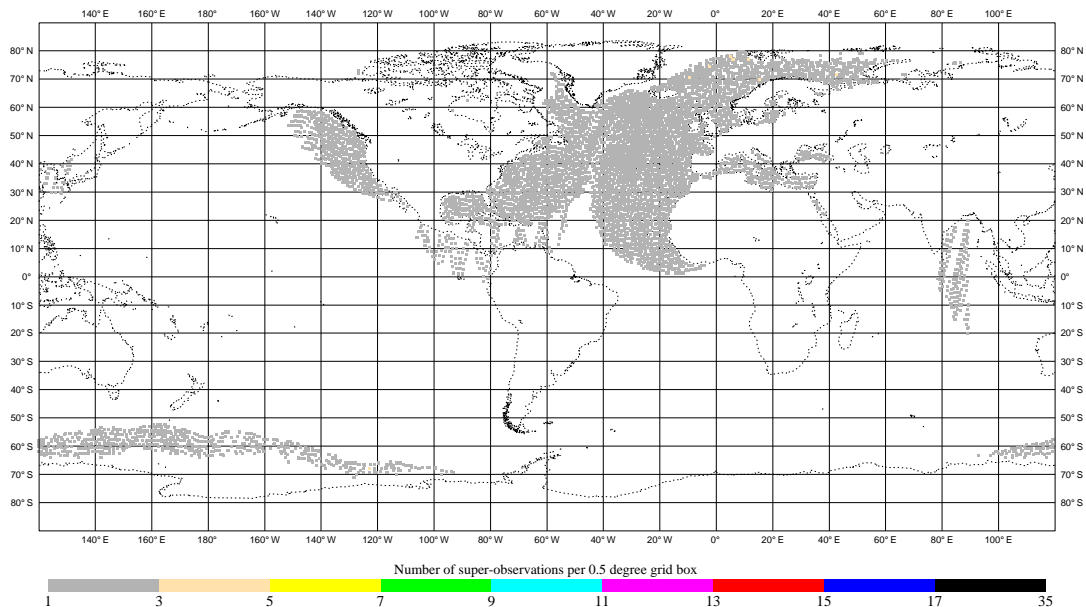


Figure 3: Typical recent ERS-2 radar altimeter monthly coverage (June 2007).

did not suffer any abrupt changes after the loss of the global coverage.

Figure 5 shows the time history of the 7- and 365-day running averages of the daily scatter index (SI) of the altimeter significant wave height with respect to the ECMWF wave model (ECWAM) in the North Atlantic since the beginning of year 2000. Both the seasonal variation (maximum during July-August and minimum during December-January) and the general trend of the reduction in the SI (the 365-day running average) can be seen. Again the seasonal variation seems to be stronger after the loss of global coverage. The higher SI values during July and August 2004 are due to a technical problem that prevented the ENVISAT RA-2 SWH product from being assimilated in the wave model.

In summary, it is possible to say that the altimeter significant wave height product is as good as it used to be. Other statistics (not shown) deliver the same message. It is worth mentioning that the ERS-2 altimeter wave height product was assimilated in the ECMWF wave model until it was replaced by the corresponding product from ENVISAT on 21 October 2003.

### 2.3 Monitoring of URA Surface Wind Speed in the North Atlantic

Before the loss of the global coverage, URA wind speed observations were not as good as the wave heights. They suffered several periods of degraded quality, especially after the start of the problems with the platform gyros early 2000 as will be described later in Section 3.4. The "sun blinding effect" is responsible for most of the degradation in the Southern Hemisphere (SH) during the period between mid-January to early March each year since year 2000.

Figure 6 shows the time history of the 7- and 365-day running averages of the daily bias of URA surface wind speed with respect to the ECMWF operational atmospheric model in the North Atlantic since 1 January

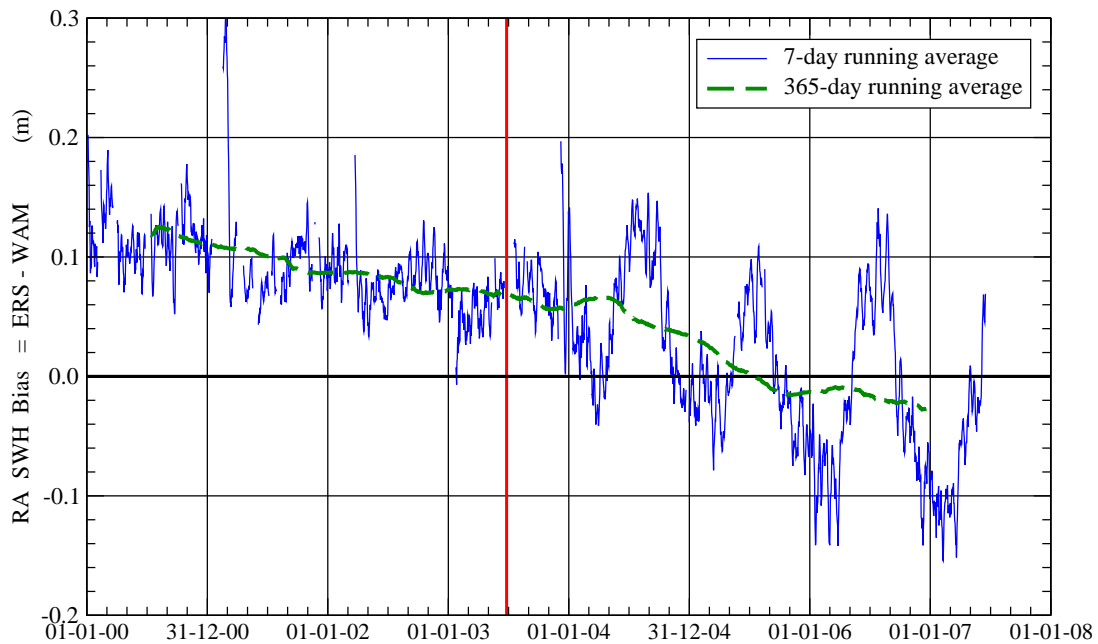


Figure 4: Time history of the 7- and 365-day running average of daily bias of altimeter significant wave height with respect to wave model in the North Atlantic since 1 January 2000. The thick green dashed line shows the bias trend (365-day running average). Date of loss of global coverage is represented by a red thick vertical line.

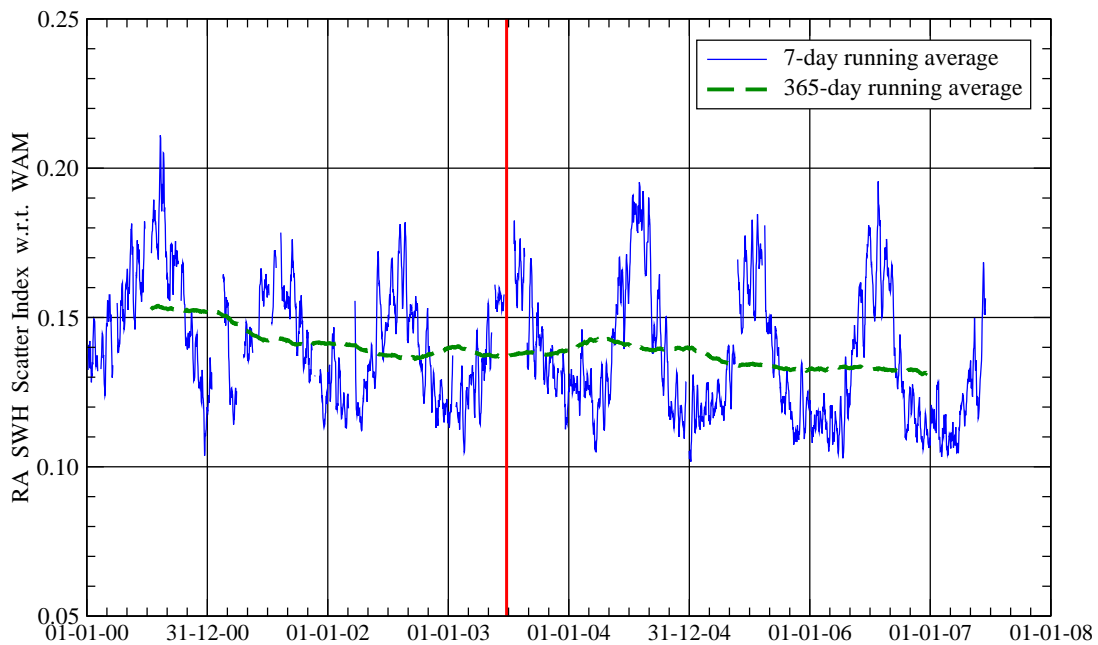


Figure 5: Time history of the 7- and 365-day running average of daily scatter index of altimeter significant wave height with respect to wave model in the North Atlantic since 1 January 2000. The thick green dashed line shows the SI trend (365-day running average). Date of loss of global coverage is represented by a red thick vertical line.

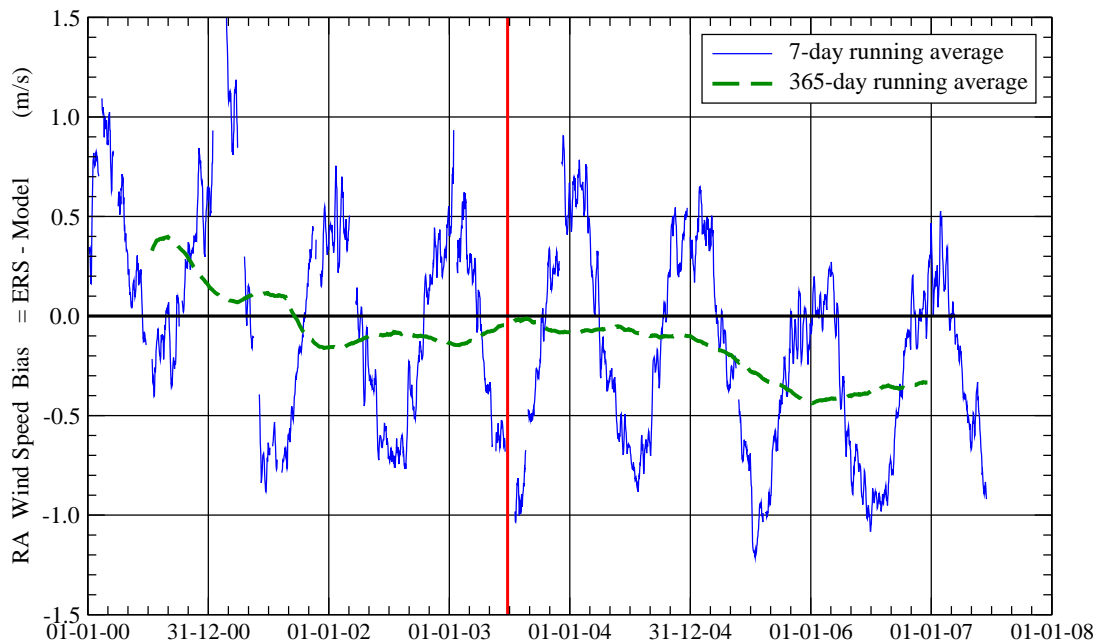


Figure 6: Time history of the 7- and 365-day running average of daily bias of altimeter surface wind speed with respect to the ECMWF atmospheric model in the North Atlantic since 1 January 2000. The thick green dashed line shows the bias trend (365-day running average). Date of loss of global coverage is represented by a red thick vertical line.

2000. The wind speed bias in the North Atlantic follows a seasonal cycle with positive bias (maximum) in the Northern Hemispheric (NH) winter and negative (minimum) in the NH summer can be clearly seen. Since early 2001, this seasonal cycle started to be symmetric around the zero line. This can be attributed to the ECMWF high-resolution model T511 implemented on 20 November 2000. The same behaviour continued after the loss of the global coverage. Another drop of bias, is witnessed in the middle of 2005 when the model convection was changed on 28 June 2005. On the other hand, Figure 7 shows the time history of the daily SI of surface wind speed with respect to the ECMWF operational atmospheric model in the North Atlantic since 1 January 2000. The SI follows a seasonal cycle with low values occurring during the NH winter and vice versa in summer. The exception to this cycle is the period from early January to early March each year since 2001. This may be due the residual effect of the "sun blinding effect". Continuous improvements of the ECMWF operational atmospheric model result in lower wind speed scatter index values between this model and the altimeter. A drop in SI (and bias) in early 2002 can be clearly recognised. This coincides with a model change including the assimilation of QuikSCAT wind speeds. The usual trend of the SI reduction continued after the reduction of ERS-2 coverage. The only exception is the relatively higher scatter index during January and February 2004.

## 2.4 Monitoring of URA Altimeter Backscatter

Altimeter backscatter is the raw observation that is translated into surface wind speed. Figure 8 displays the long-term monthly global mean backscatter coefficient values since December 1996. Before the loss of the global coverage, the monthly mean value used to be around 11.0 dB. However, the mean values used to increase to more than 11.4 dB for the month of July in years 1997 to 1999. Those peaks disappeared in year 2000 and later. Instead, the mean backscatter coefficient started to be rather low in the month of February (or March) each year from 2000. This is a direct result from the sun blinding effect.

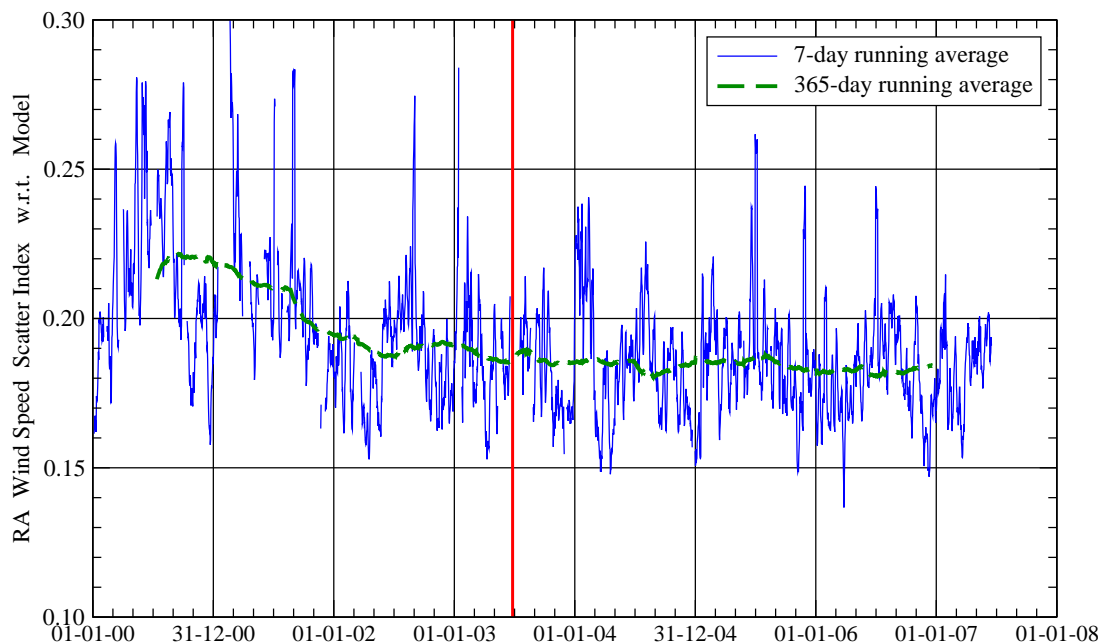


Figure 7: Time history of the 7- and 365-day running average of daily scatter index of altimeter surface wind speed with respect to the ECMWF atmospheric model in the North Atlantic since 1 January 2000. The thick green dashed line shows the SI trend (365-day running average). Date of loss of global coverage is represented by a red thick vertical line.

After the loss of the global coverage, the monthly mean started to have a strong seasonal cycle varies between 10.4 and 12.2 dB. This cycle has a peak during the NH summer (July-August) and a trough during winter (December-January). This is an expected behaviour in the NH. After the extension of the ERS-2 coverage by including more ground stations especially in the SH, the amplitude of the seasonal cycle of mean backscatter coefficient started to get smaller. The impact of including McMurdo, Hobart and Singapore ground stations can not be missed in Figure 8.

### 3 The Radar Altimeter OPR Product

#### 3.1 Introduction

The ERS missions started with the launch of ERS-1 (the first sun-synchronous polar-orbiting mission of ESA) on 17 July 1991. It was followed by ERS-2 which was launched on 21 April 1995. The Radar Altimeter (RA) and the Active Microwave Instrument (AMI) which consists of two separate radars; namely: the Synthetic-Aperture Radar (SAR) and the Scatterometer, are the instruments which are able to provide wind and wave data on-board both satellites.

According to ESA (2005), the launch and early orbit phase (LEOP) of ERS-1 began with the launch and ended with the satellite achieving nominal attitude and orbit. The duration of this initial phase was less than two weeks. A 3-day repeat cycle was adopted to provide frequent revisits to a number of dedicated sites for calibration purposes. The remaining effective life of the ERS-1 mission is sub-divided into the following phases:

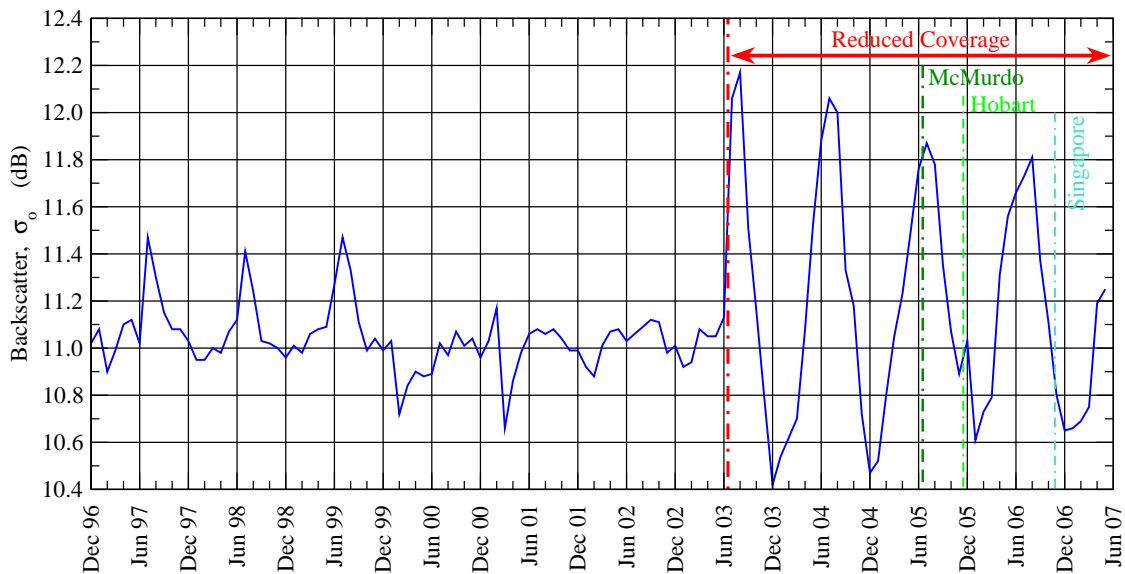


Figure 8: Time history of the monthly global mean of ERS-2 altimeter backscatter coefficient after QC since December 1996.

- **Phase A - Commissioning Phase:** 3-day repeat cycle. Lasted 138 days (from 25 July to 10 December 1991). Mainly to perform engineering calibration and geophysical validation.
- **Phase B - First Ice Phase:** 3-day repeat cycle. Lasted 93 days (from 28 December 1991 to 31 March 1992). Optimised for the specific requirements of Arctic ice experiments.
- **Phase R - Experimental Roll Tilt Mode Campaign:** 35-day repeat cycle. Lasted 12 days (from 2 to 14 April 1992). The satellite body was rotated by 9.5 degrees allowing operation of the SAR imaging mode at an incidence angle of 35 degrees. Performance of the RA Altimeter is slightly degraded because of the geocentric pointing instead of the local normal pointing.
- **Phase C - Multi-Disciplinary Phase:** 35-day repeat cycle. Lasted 20 months (14 April 1992 to 23 December 1993). Mean sea surface determination, ocean variability studies and surface mappings are among various uses during this phase.
- **Phase D - Second Ice Phase:** 3-day repeat cycle similar to the First Ice Phase (Phase B). Lasted 108 days (from 23 December 1993 to 10 April 1994).
- **Phase E - Geodetic Phase:** 168-day repeat cycle. Lasted about 5 months (from 10 April 1994 to 28 September 1994). Enables high-density measurements to improve the determination of the geode using RA.
- **Phase F - Shifted Geodetic Phase:** 168-day repeat cycle similar to the Geodetic Phase (Phase E) but with an 8 km spatial shift. Lasted about 6 months (from 28 September 1994 to 21 March 1995).
- **Phase G - Second Multi-Disciplinary Phase:** 35-day repeat cycle similar to the first Multi-Disciplinary Phase (Phase C). Lasted about 14 months (from 21 March 1995 to 2 June 1996). Tandem mission with ERS-2 (from 17 August 1995 to 2 June 1996) was within this phase.

Phase G concluded the nominal ERS-1 mission. ERS-1 stayed in this configuration while serving as a back up for ERS-2. ERS-1 finally retired on 10 March 2000 after a failure in its on-board attitude control system.

On the other hand, ERS-2 had only two phases of operations both with the same orbital configuration of 35-day repeat cycle:

- **Phase A - Commissioning Phase:** Lasted from 2 May 1995 to 17 August 1995. Mainly to perform engineering calibration and geophysical validation.
- **Phase B - Routine Phase:** Started on 17 August 1995 and still going on. Similar to ERS-1 Phases C and G. This phase started with the tandem mission from 17 August 1995 to 2 June 1996.

ERS-2 was unfortunate to start losing its gyroscopes in early 2000. This led to the implementation of the Attitude and Orbit Control System (AOCS) mono-gyro attitude software early February 2000 (c.f. Féménias and Martini, 2000). Further loss of gyroscopes on 17 January 2001, which left a single working gyroscope, forced the piloting of the spacecraft without any gyroscopes in the Extra Back-up Mode (EBM). This led to degradation of some ERS-2 products. The implementation of the zero-gyro mode (ZGM) was introduced in June 2001 to assist the piloting of the spacecraft without any need for the frequent use of the only available gyroscope.

Finally, the permanent failure of the ERS-2 low bit rate (LBR) tape recorders on 21 June 2003 prevented the continuation of the ERS-2 global coverage. ERS-2 LBR data coverage is limited within the vicinity of the ground stations. The recent coverage map is shown in Figure 3.

### 3.2 Data Sources and Collocations

ERS altimeter OPR data products were obtained from the French ERS Processing and Archiving Facility (CER-SAT) of the French Research Institute for Exploitation of the Sea (IFREMER). The data were converted into BUFR format. The same operational pre-processing and quality control procedures (c.f. Abdalla and Hersbach, 2004) were applied before the use of the data. The only exception is that the number of 1-Hz observations averaged to produce one super-observation was selected to be 11 (rather than the value of 30 used operationally for ERS-2).

As both operational atmospheric and wave models at ECMWF are changing frequently, the operational ECMWF data archive does not represent a consistent data set to be used for the evaluation of the ERS products. The quality of both wind and wave fields are improving with time. Since we are after a long-term evaluation of ERS products, a more consistent data set (free of other changes) is needed. Therefore, it was found appropriate to use the ECMWF 40-Year Reanalysis (ERA-40) wind fields for the validation. ERA-40 fields were produced using the same atmospheric model for the entire period of the reanalysis from September 1957 to August 2002. The model used in the reanalysis has a spectral resolution of T159 (c.f. Uppala et al., 2005) which corresponds to about 125 km. Although this is much coarser than the operational resolution during the last few years, ERA-40 resolution is much higher than the operational resolutions at earlier times. Furthermore, ERA-40 represents a rather consistent data set as far as the model is concerned. The amount and quality of the observations assimilated in ERA-40 varied by time during the ERA-40 period. This, of course, has some (hopefully minor) impact on the consistency of ERA-40 products. However, in the absence of another alternative, one can make use of this data set.

The wave model used in ERA-40 was of rather coarser resolution (1.5 degree which is about 166 km). Although this may not be a major concern in the open ocean, it has a definite detrimental impact on wave fields in the inner seas and near the coasts. Therefore, we decided not to use ERA-40 wave fields for the evaluation of ERS OPR wave products. Instead a long term stand-alone wave model hindcast run (without any data assimilation) was used. The model used for this run is the latest version of the ECMWF wave model (ECWAM) which

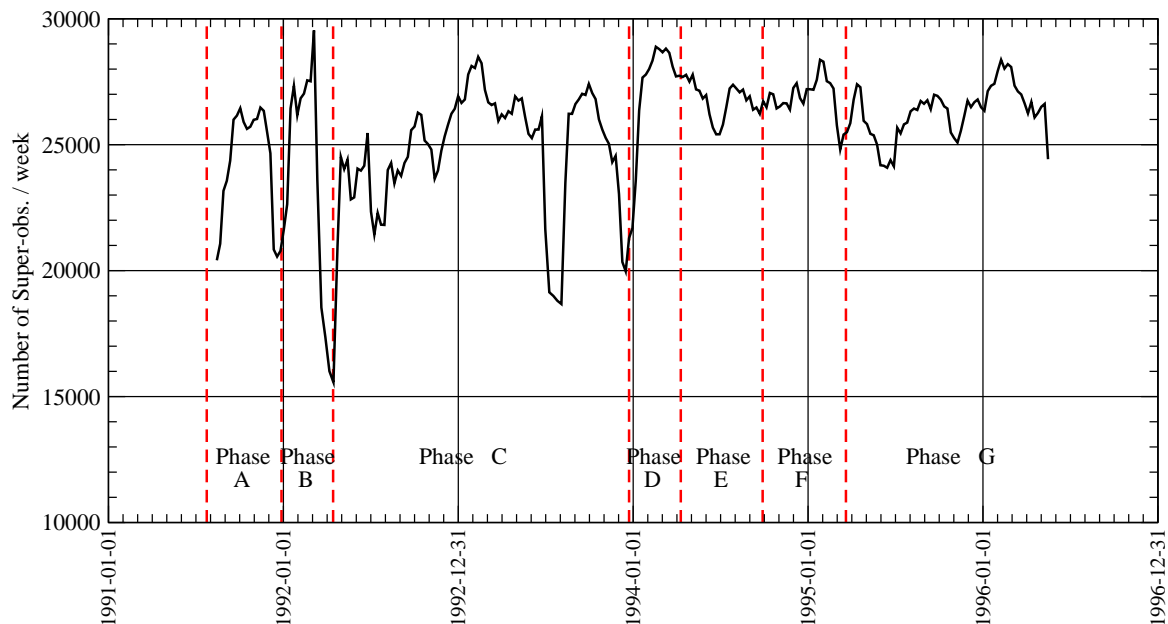


Figure 9: Time history of the 5-week running average of weekly number of ERS-1 altimeter super-observations during the effective lifetime of ERS-1 (August 1991 to May 1996). Various ERS-1 phases are displayed.

includes several enhancements, both physics and numerics, over the standard WAM model (c.f. Janssen, 2004, Janssen et al., 2005 and Bidlot et al., 2006). The model resolution is 0.5 degrees (about 55 km). ERA-40 wind fields were used to force the model.

The ERA-40 data set covers the period until 31 August 2002. After that date, operational wind fields were used for ERS-2 wind speed products. The same wind fields were used to force the wave model beyond ERA-40 period. It is important to note that the operational wind fields are of much better quality than ERA-40 due to the recent model enhancements and to the higher resolution. Naturally one should expect better wave fields as a result of using such wind fields for the hindcast run.

The radar altimeter super-observations were collocated with the corresponding model counterparts. Each week worth of collocations are used to compute various statistics. The time histories of those statistics are examined to draw conclusions related to the altimeter wind and wave products. To concentrate on long-term changes it was necessary to filter out the short term variability (noise) of those plots by using 5-weekly running averages.

### 3.3 ERS-1 Altimeter OPR Product

Figure 9 shows the time history of the weekly number of super-observations of ERS-1 altimeter OPR products during the effective lifetime of ERS-1 (August 1991 to May 1996). Note that the number of 1-Hz observations averaged to form each super-observation is 11. This is the reason for the higher number of super-observations compared to the operational plots of URA product (e.g. ERS-2 URA plot of Figure 1).

Figure 10 shows the time history of the weekly bias of ERS-1 altimeter significant wave height with respect to the ECWAM model hindcast (using ERA-40 reanalysis wind fields) during the effective lifetime of ERS-1. Both (absolute) bias and bias relative to the model mean (relative bias) are shown. It is clear that ERS-1 OPR SWH is in general lower than the model by about 18 cm (about 7%). The seasonal cycle of the bias

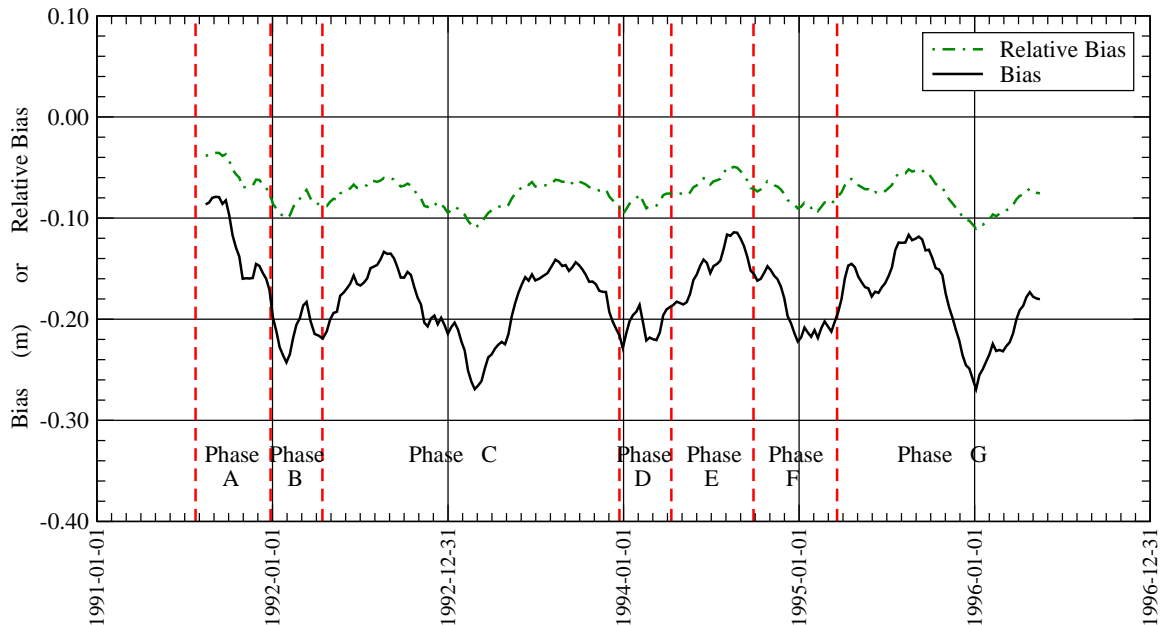


Figure 10: Time history of the 5-week running average of weekly global bias and relative bias (i.e. the bias normalised by the model mean) of ERS-1 altimeter significant wave height with respect to the ECWAM model hindcast (using ECMWF ERA-40 reanalysis wind fields) during the effective lifetime of ERS-1 (August 1991 to May 1996). Various ERS-1 phases are displayed.

can not be missed. Normalising with the mean model wave height does not totally eliminate this seasonal cycle. The underestimation of ERS-1 SWH with respect to the model varies between about 12 cm (during the NH summer) and about 24 cm (in NH winter). This corresponds to about 5% and 11%, respectively. It is worthwhile mentioning that during the first two months of the ERS-1 mission (August-September 1991), the SWH bias was the smallest ever during the entire mission. It seems that the various ERS-1 phases do not have any impact on SWH bias.

The time history of the weekly SI of ERS-1 OPR SWH with respect to the same wave model hindcast during the whole effective lifetime of ERS-1 is shown in Figure 11. The SI fluctuated around a mean value of about 16% with a seasonal cycle especially for the period starting from early 1993. Before that the SI was fluctuating at a higher level of about 17%. Unlike the SWH bias, SI was the highest during the first two months of the mission. Again, there is no clear evidence on any impact of orbit configuration changes (phases) on the SWH SI.

Figure 12 shows the time history of the weekly bias of ERS-1 altimeter surface wind speed with respect to ERA-40 wind fields during the entire effective lifetime of ERS-1 (August 1991 to May 1996). It is clear that the ERS-1 lifetime can be divided into four main distinct periods in terms of wind speed bias characteristics. The limits of each period coincide with ERS-1 orbital configuration changes (phases). During the Commissioning (Phase A) and the First Ice (Phase B) phases, which share the same orbital configurations of 3-day repeat cycle, the wind speed bias was around  $-0.10 \text{ m s}^{-1}$ . The start of the Multi-Disciplinary Phase (Phase C), which has a 35-day repeat cycle, coincides with a jump in the wind speed bias to about  $+0.40 \text{ m s}^{-1}$ . Within the above two periods, there is a linear increase in the wind speed bias. A bias drop occurred at the beginning of the Second Ice Phase (D), which has a 3-day repeat cycle, to about  $+0.07 \text{ m s}^{-1}$ . The same bias continued until the end of

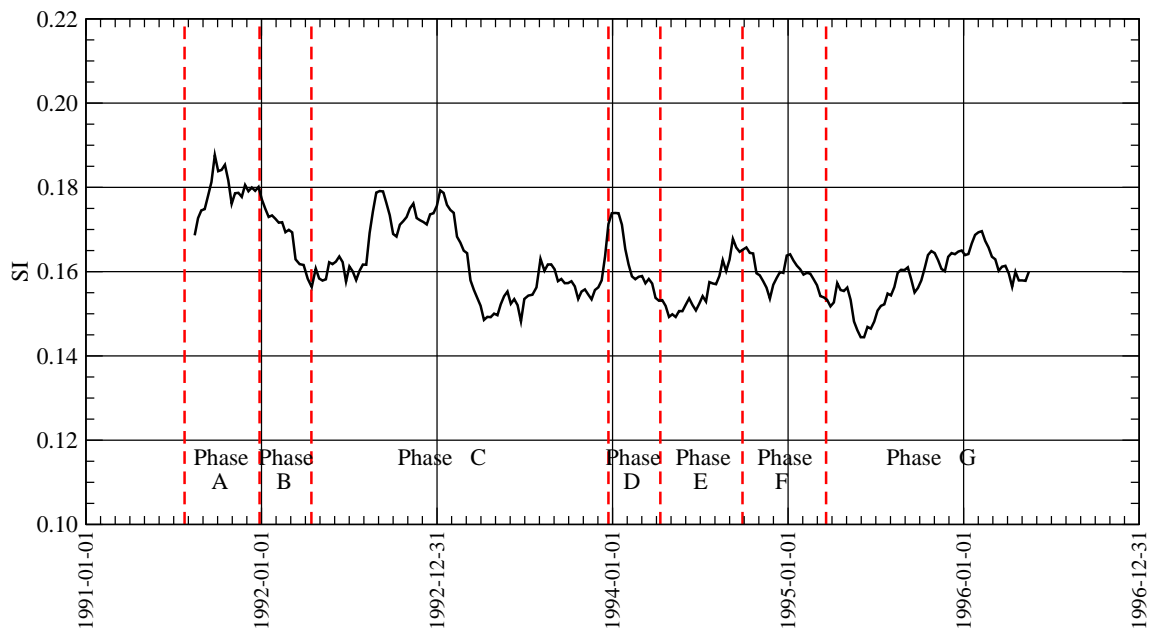


Figure 11: Time history of the 5-week running average of weekly global scatter index of ERS-1 altimeter significant wave height with respect to the ECWAM model hindcast (using ECMWF ERA-40 reanalysis wind fields) during the effective lifetime of ERS-1 (August 1991 to May 1996). Various ERS-1 phases are displayed.

the Shifted Geodetic Phase (F), when the repeat cycle was 168 days. One can even notice a slight change in bias (drop to about  $+0.13 \text{ m s}^{-1}$ ) in the transition from Phase E to Phase F. Finally, with the start of the 35-day repeat-cycle Phase G (Second Multi-Disciplinary), the wind speed bias jumped to about  $+0.50 \text{ m s}^{-1}$ . Even within Phase G, there is also a systematic trend in the bias.

The above correlation may suggest some dependency of the wind speed bias on the orbit configuration. However, it is difficult to explain the different bias levels between Phases B and D which have same repeat cycle of 3 days and between Phases E and F which have repeat cycles of 168 days. Furthermore, Phases D and E have different repeat cycles (3 for the former and 168 for the latter) but have the same level of bias.

The use of a rather consistent model wind data set (ERA-40) reduces the responsibility of the model for the abrupt changes in wind speed bias. Furthermore, the coincidence of the wind speed bias jumps with the change of ERS-1 phases, make us confident that the problem lies in the ERS-1 OPR wind speed product.

Figure 13 displays the long-term 5 week running average of weekly global mean backscatter coefficient values over the effective lifetime of ERS-1. The mean backscatter coefficient is slightly below 11 dB. It is possible to distinguish periods similar to those described in the wind speed bias (Figure 12). This confirms that the changes of wind speed bias are due to the changes in the altimeter instrument or the processing algorithms to provide the backscatter coefficients.

The time history of the weekly SI of the ERS-1 OPR surface wind speed with respect to ERA-40 is shown in Figure 14. During the Commissioning Phase, the wind speed SI was relatively high and reached about 25%. With the start of Phase B (the First Ice Phase), the SI reduced considerably to about 22%. During Phases B and C, there seems to be a seasonal cycle with high SI during the NH winter and low values during the summer. This cycle was interrupted with local peaks at the start of each phase. During the Second Multi-Disciplinary Phase the wind speed SI was stabilised at a level slightly below 22%.

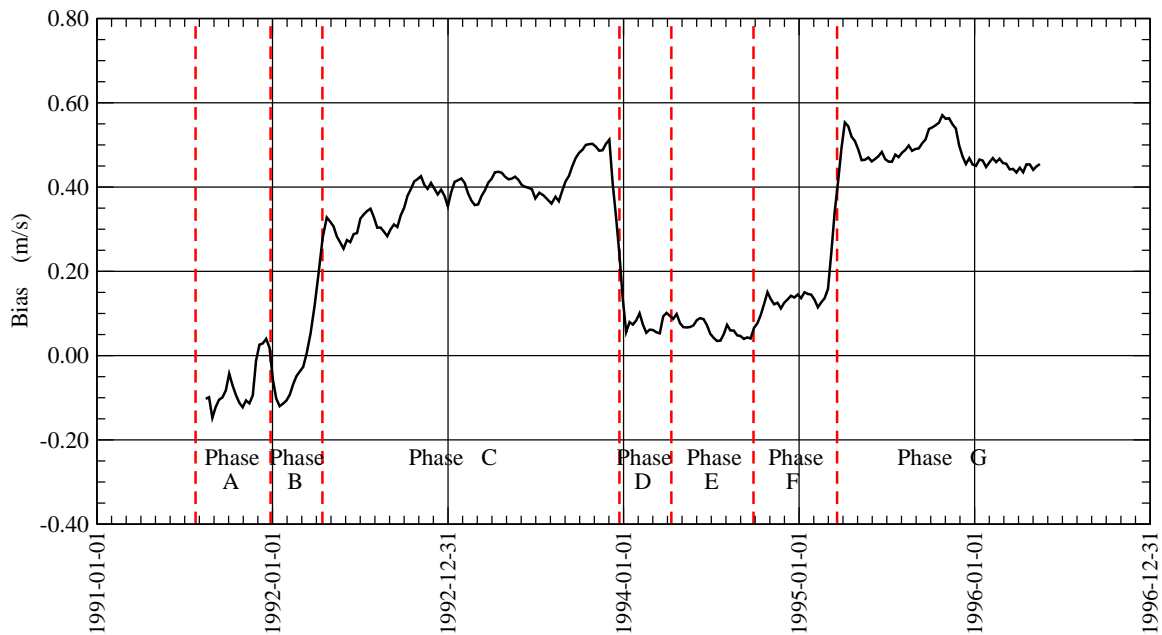


Figure 12: Time history of the 5-week running average of weekly global bias of ERS-1 altimeter surface wind speed with respect to the ECMWF ERA-40 re-analysis during the effective lifetime of ERS-1 (August 1991 to May 1996). Various ERS-1 phases are displayed.

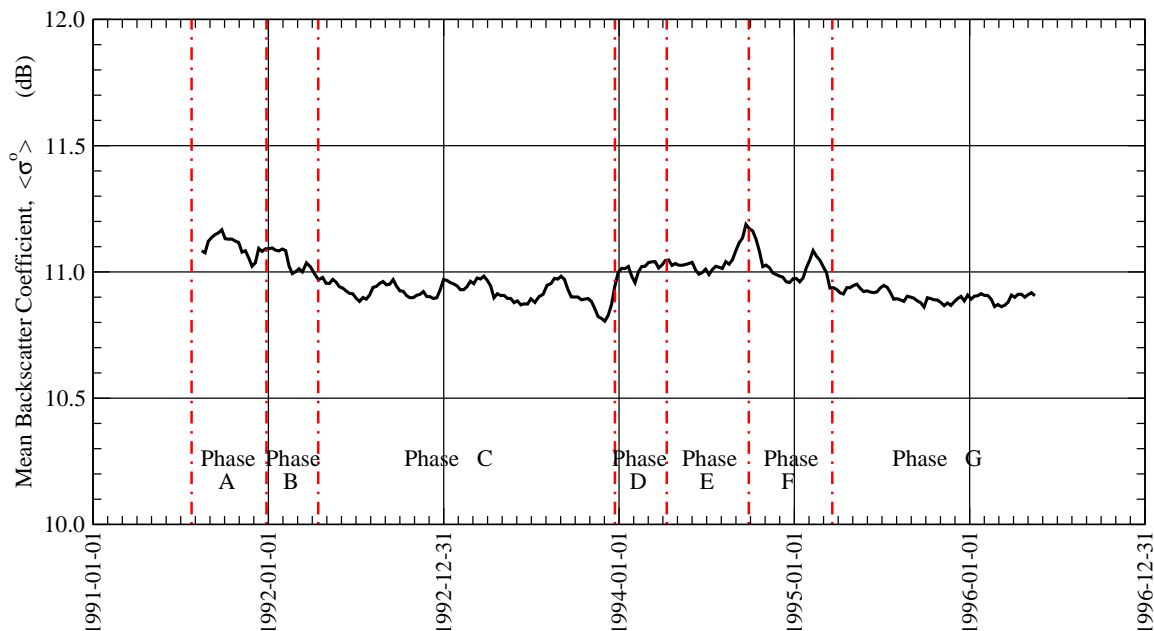


Figure 13: Time history of the 5-week running average of weekly global mean ERS-1 altimeter backscatter coefficient after QC during the effective lifetime of ERS-1 (August 1991 to May 1996). Various ERS-1 phases are displayed.

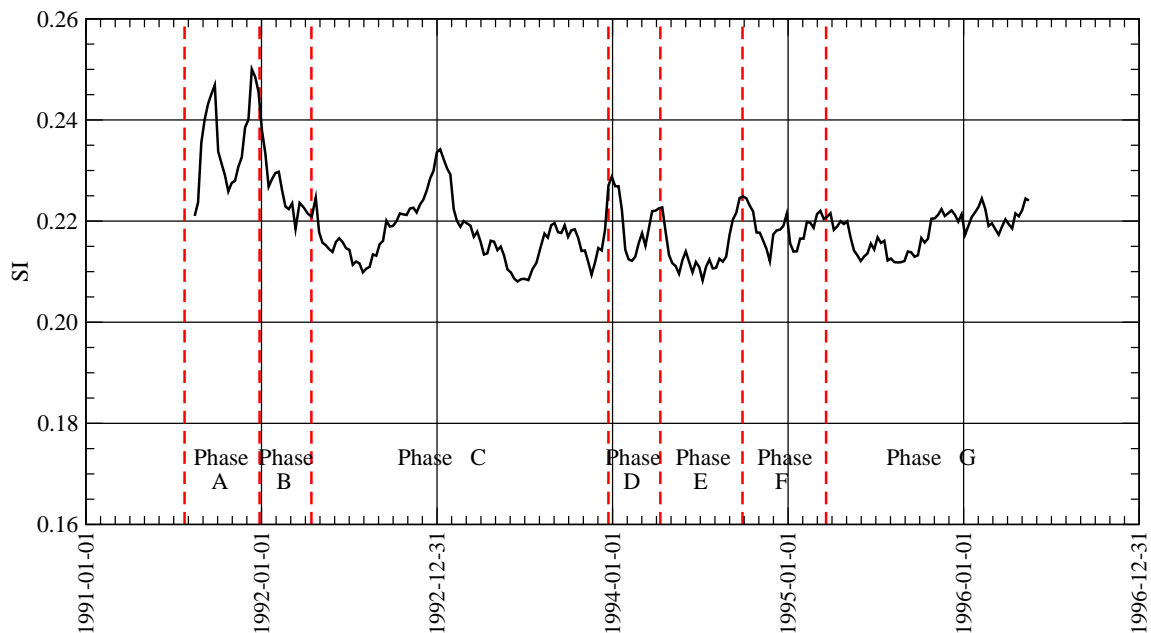


Figure 14: Time history of the 5-week running average of weekly global scatter index of ERS-1 altimeter surface wind speed with respect to the ECMWF ERA-40 re-analysis during the effective lifetime of ERS-1 (August 1991 to May 1996). Various ERS-1 phases are displayed.

### 3.4 ERS-2 Altimeter OPR Product

Figure 15 shows the time history of the weekly number of super-observations of ERS-2 altimeter OPR products during the period from May 1995 to June 2003. Note that the number of 1-Hz observations averaged to form each super-observation is 11 as was the case for Figure 9. It is clear that apart from several short gaps, the volume of observations was rather constant.

Figure 16 shows the time history of the weekly bias and SI of ERS-2 altimeter SWH with respect to the wave model hindcast (using ERA-40 wind fields before the end of August 2002 and operational wind fields afterwards) during the period from May 1995 to June 2003. In general, ERS-2 OPR SWH seems to be of consistent quality over the whole effective lifetime of spacecraft. The bias shows a seasonal cycle with peaks as high as 16 cm (about 20 cm in 1995 and 1996) in the NH summer and troughs as low as a few centimetres in the winter. The drastic change in bias is due to the use of the higher-quality operational wind fields on 1 September 2002. The SWH SI level is about 16%. There is also a seasonal cycle which is anti-phased with respect to the bias cycle. The amplitude of this cycle is rather small. Again a noticeable change in SI is due to the use of the operational wind fields. It seems that the loss of gyroscopes has no impact on ERS-2 SHW quality.

Figure 17 shows the time history of the weekly relative bias (normalised with model mean wind speed) and SI of ERS-2 altimeter OPR surface wind speed with respect to ERA-40 before the end of August 2002 and the operational wind fields afterwards during the effective lifetime of the satellite (from May 1995 to June 2003). It is clear that until the beginning of 2000, both wind speed bias and SI values were stable. The bias was about +2% of the model mean (about  $0.20 \text{ m s}^{-1}$ ) and the SI was about 21%. Due to an unknown reason, the wind speed bias jumped on 16 January 2000 to more than 10% (about  $0.80 \text{ m s}^{-1}$ ) together with a slight increase in SI. Although a few days earlier, this may not have any connection with the AOCS mono-gyro piloting in early February 2000 (c.f. Féménias and Martini, 2000). However, it is possible that this was an indication of the

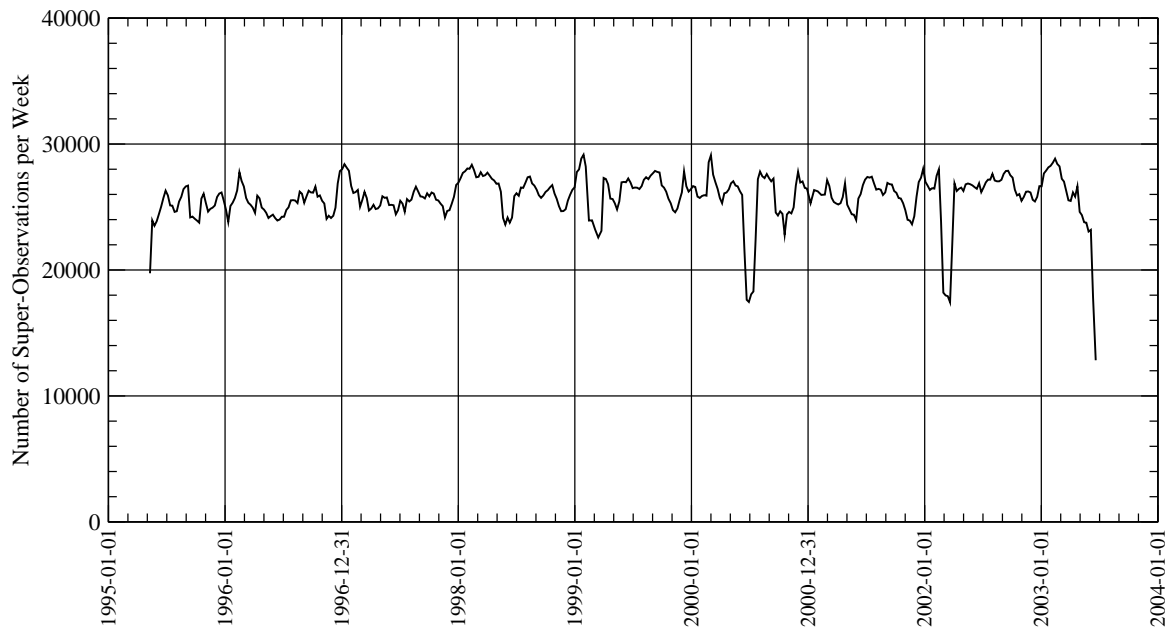


Figure 15: Time history of the 5-week running average of weekly number of ERS-2 altimeter super-observations during the period from May 1995 to June 2003.

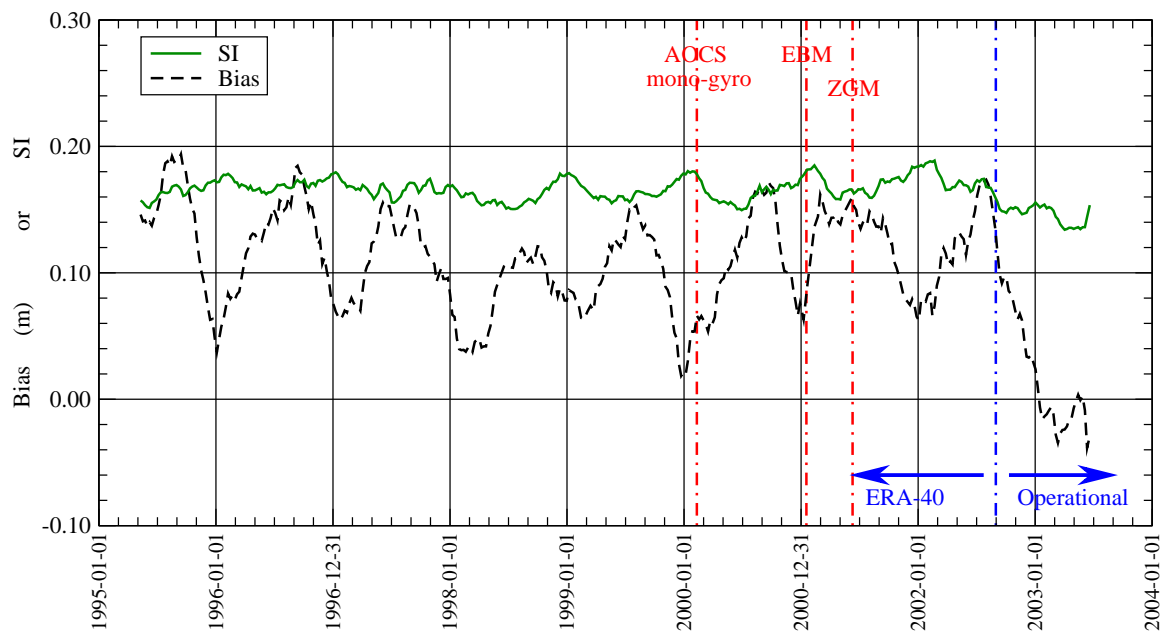


Figure 16: Time history of the 5-week running average of weekly global bias and scatter index of ERS-2 altimeter significant wave height with respect to the ECWAM model hindcast (using ECMWF ERA-40 reanalysis wind fields before the end of August 2002 and operational winds afterwards) during the period from May 1995 to June 2003. Important ERS-2 gyroscope related events are displayed.

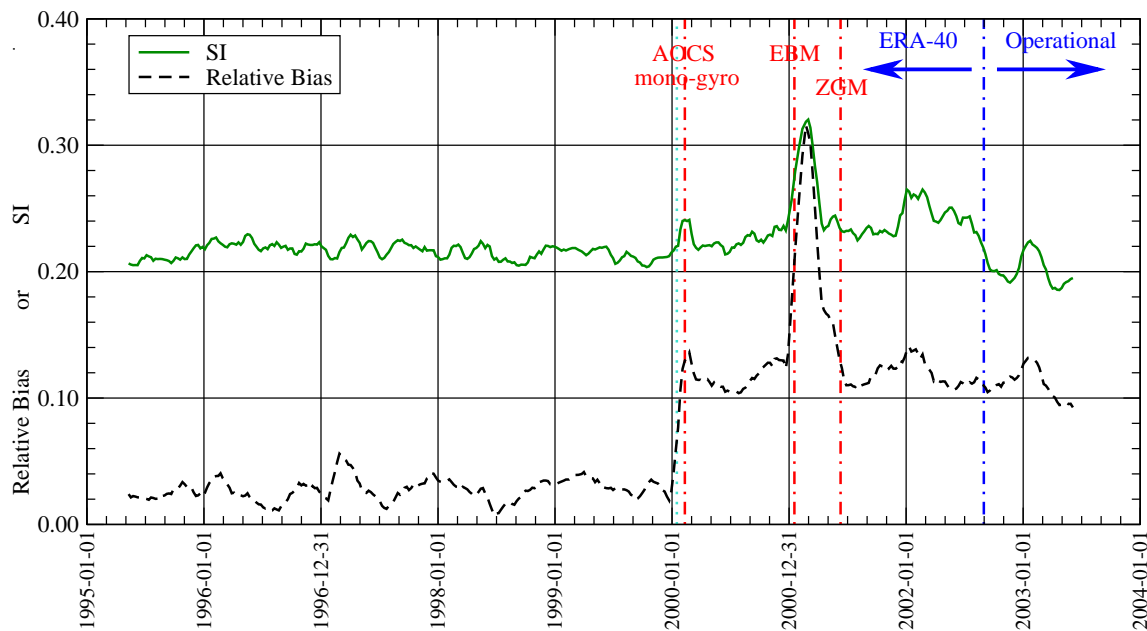


Figure 17: Time history of the 5-week running average of weekly global relative bias and scatter index of ERS-2 altimeter surface wind speed with respect to the ECMWF ERA-40 re-analysis (before the end of August 2002 and operational winds afterwards) during the period from May 1995 to June 2003. Important ERS-2 gyroscope related events are displayed.

forthcoming gyro problems. Further loss of gyroscopes in January 2001, which led to the EBM piloting, further degraded the altimeter wind speeds. An uploaded wrong configuration file after the recovery is responsible for the spike degradation of the product. The impact of using better model wind fields on the bias and SI can be seen after August 2002. The sun blinding effect, which is only effective in the SH, can be noticed in the small spikes around the month of February each year since 2000.

The long-term 5 week running average of weekly global mean backscatter coefficient values over the effective lifetime of ERS-2 shown in Figure 18 is in line with the developments with the wind speed product. The mean backscatter coefficient before January 2000 was stable and fluctuating around a value slightly above 11 dB. After the January 2000 event, the mean value reduced by about 0.2 dB. During the EBM operations the mean backscatter was not stable. The ZGM stabilised this parameter after June 2001.

## 4 The Synthetic Aperture Radar (SAR) UWA product

For the UWA product, SAR records are provided at 200 km intervals, each containing an image spectrum for an area of about 5 km x 5 km. Records for which all parameters are within an acceptable range are collocated with ECWAM model spectra. The SAR image spectra are then transformed into corresponding ocean-wave spectra using an iterative inversion scheme based on the forward closed integral transformation (MPI scheme, Hasselmann and Hasselmann, 1991). For this procedure the collocated ECWAM model spectra serve as a first-guess. Depending on the outcome of the inversion process, further QC is applied. Long-term monitoring is based on integrated parameters such as the significant wave height, mean wave period and mean directional spread. Monitoring of the one-dimensional energy spectrum is performed as well.

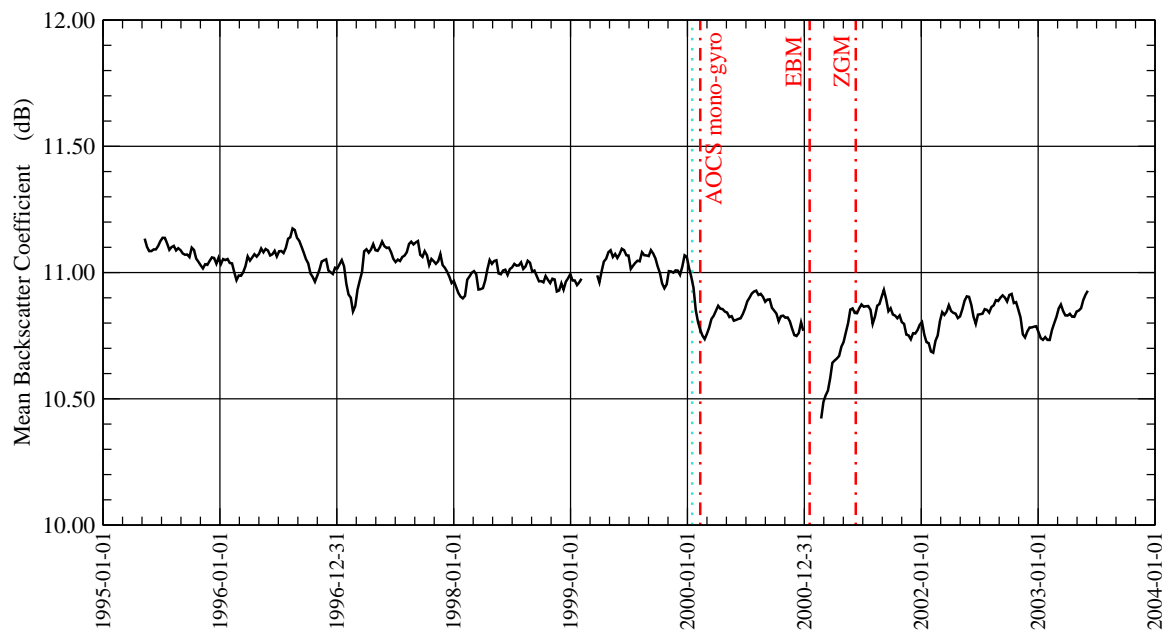


Figure 18: Time history of the 5-week running average of weekly global mean ERS-2 altimeter backscatter coefficient after QC during the period from May 1995 to June 2003. Important ERS-2 gyroscope related events are displayed.

#### 4.1 ERS-2 SAR Data Coverage after June 2003

The loss of the global coverage due to the failure of the on-board low-bit rate tape recorders in June 2003 reduced the number of observations received at ECMWF to about 13% of the full coverage data volume as can be seen in Figure 19 which shows the global weekly number of SAR wave mode spectra processed at ECMWF. The current ERS-2 SAR coverage can be seen in Figure 20. The extra coverage in the northeastern parts of the Indian Ocean (received by Singapore ground station) can be clearly seen when comparing Figure 20 with the corresponding one of last year (Figure 20 of Abdalla and Hersbach, 2006). As was done for the altimeter, the extra-tropical Northern Atlantic (north of latitude  $20^{\circ}\text{N}$ ) is used for monitoring the FD SAR wave mode UWA product. This is very close to the bulk of the current coverage. The weekly number of SAR wave mode spectra in the North Atlantic since the beginning of the ERS-2 mission is shown in Figure 21. It is clear that the current coverage in the North Atlantic is slightly less than the nominal coverage. The difference is small and is due to the small gap at the southern edge of the North Atlantic. The quality of the products in this area is investigated here.

#### 4.2 ERS-2 SAR Wave Height in the North Atlantic

A long-term monitoring of the significant wave height computed from the inverted ERS-2 SAR spectra was performed. It is worthwhile mentioning that on 28 June 1998 the SAR inversion software was unable to properly handle the SAR data with the new calibration procedure introduced around that time. This was fixed with the implementation of the ECWAM model change on 20 November 2000. Furthermore, SAR wave mode data were assimilated in the wave model from 13 January 2003 to 31 January 2006. Further related events are mentioned in Section 4.4.

Figure 22 shows the time history of the weekly bias of the significant wave height computed from the inverted SAR wave mode spectrum with respect to the model wave height in the North Atlantic since April 1996. By ignoring the period with the inversion bug (from 28 June 1998 to 20 November 2000) and the period with EBM

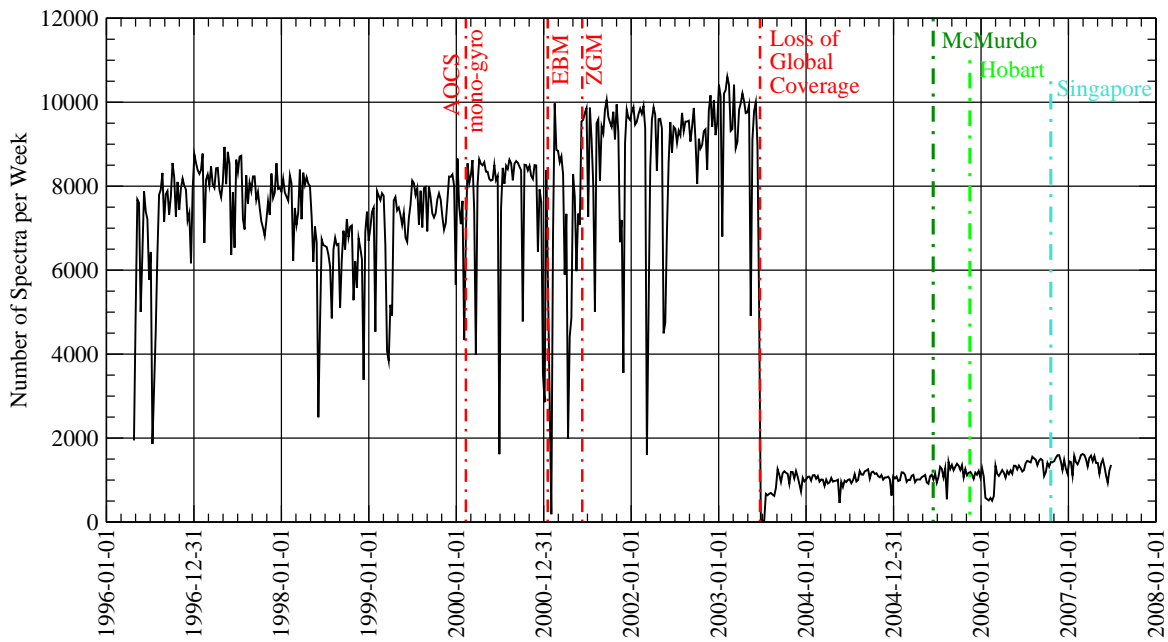


Figure 19: Time history of the global weekly number of ERS-2 UWA spectra during the period since April 1996. Important ERS-2 gyroscope related events are displayed.

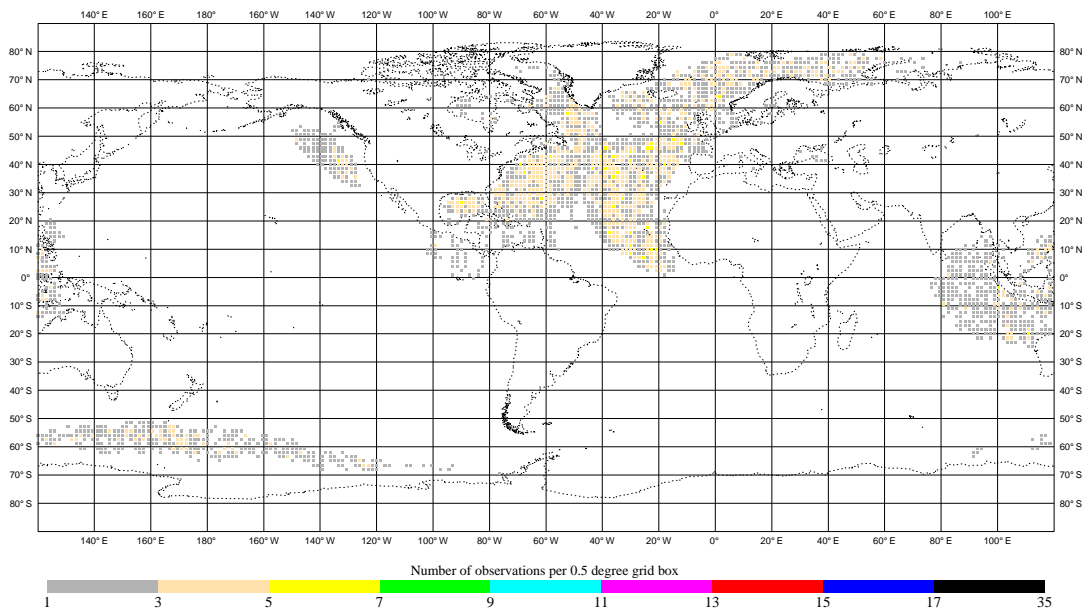


Figure 20: Typical recent ERS-2 SAR wave mode monthly coverage (June 2007).

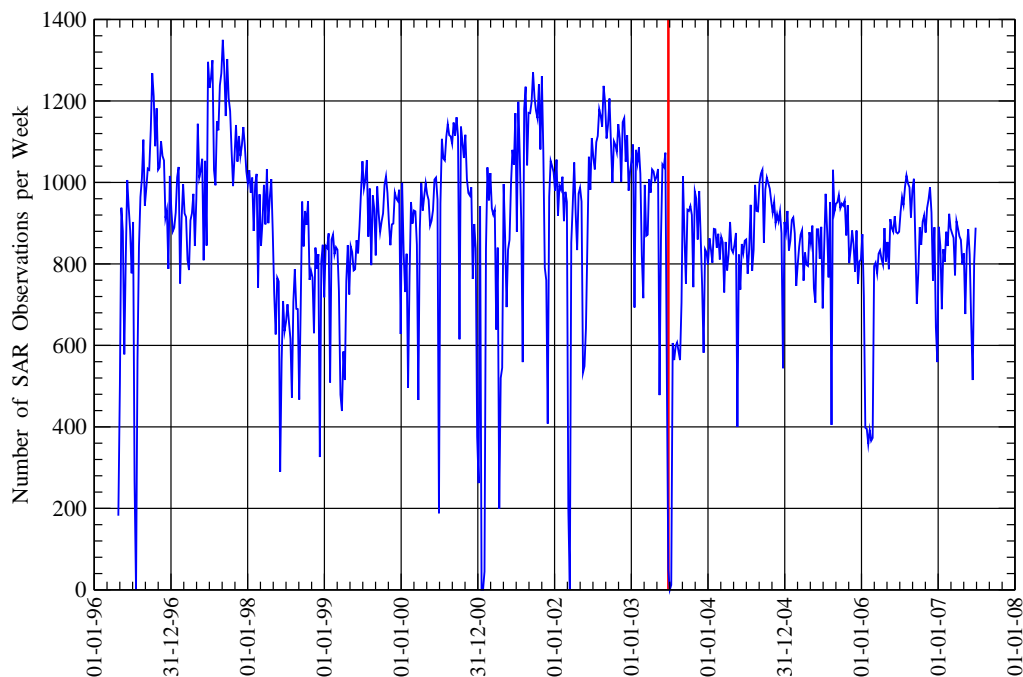


Figure 21: Time history of the weekly number of SAR wave mode spectra in the North Atlantic since 1 January 1996. Date of loss of global coverage is represented by a red thick vertical line.

(from 17 January 2001 to mid June 2001), it is possible to recognise a seasonal cyclic variation similar to the altimeter SWH (i.e. with minima during the NH winter and maxima during the summer). It is clear that the bias behaviour since the loss of the global coverage is similar to that of 2-3 years before.

Figure 23 shows the time history of the daily scatter index of the SWH of the inverted SAR wave mode product with respect to the operational wave model in the North Atlantic since April 1996. The period with the inversion bug can be clearly recognised by the high SI values. There tends to be a kind of seasonal cycle (in phase with the bias cycle) of variation in SI after the recovery from the EBM using the ZGM. This seasonal cycle continued after the loss of the global coverage. Furthermore, the general trend of SI reduction continued over the period of limited coverage. Even the errors became smaller than ever; especially during the winter. This may be a consequence of assimilating the SAR wave mode product in the ECMWF operational wave model from 13 January 2003 to 31 January 2006. A step change in SI can not be seen at that specific date. However, the SI peak values started to be the lowest during the NH summer of 2003.

### 4.3 Global ERS-1 SAR Significant Wave Height

Figure 24 shows the time history of the weekly number of ERS-1 FD SAR Wave Mode spectra (UWA) products over the entire globe during the period from April 1993 to April 1996. There is no UWA data available at ECMWF before April 1993. The number of observations increased slightly towards the end of 1993.

Figure 25 shows the time history of the weekly bias and scatter index of the SWH derived from the inverted ERS-1 SAR spectra with respect to the operational ECMWF wave model during the period from April 1993 to April 1996. The bias started at a level of about 27 cm before it increased linearly to about 44 cm during July 1993. The reason of this change could not be correlated with any model or SAR related changes. Another linear increase occurred during Phase D (the Second Ice Phase). The bias then fluctuated around 50 cm. The

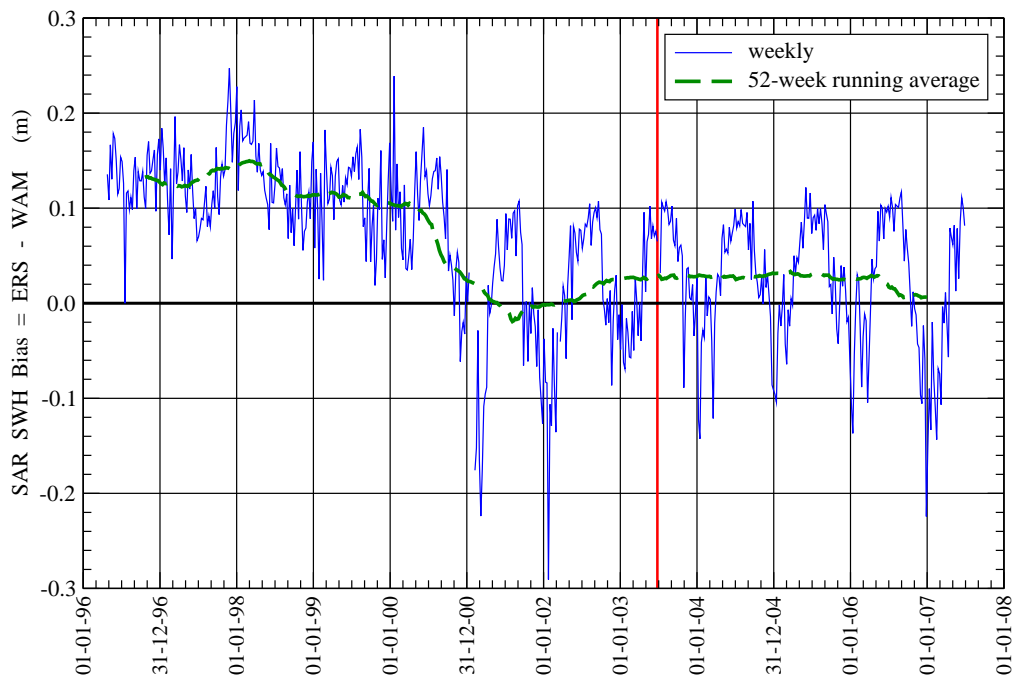


Figure 22: Time history of the weekly bias of SAR wave mode significant wave height with respect to wave model in the North Atlantic since April 1996. 52-week running average is shown by a thick green dashed line. Date of loss of global coverage is represented by a red thick vertical line.

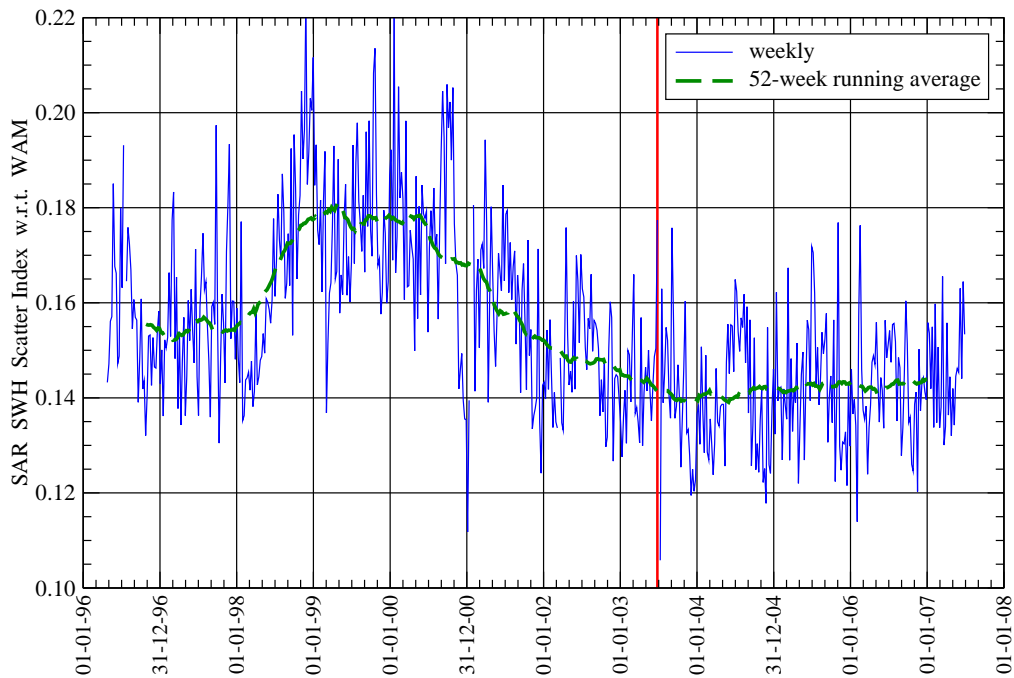


Figure 23: Time history of the weekly scatter index of SAR wave mode significant wave height with respect to wave model in the North Atlantic since April 1996. 52-week running average is shown by a thick green dashed line. Date of loss of global coverage is represented by a red thick vertical line.

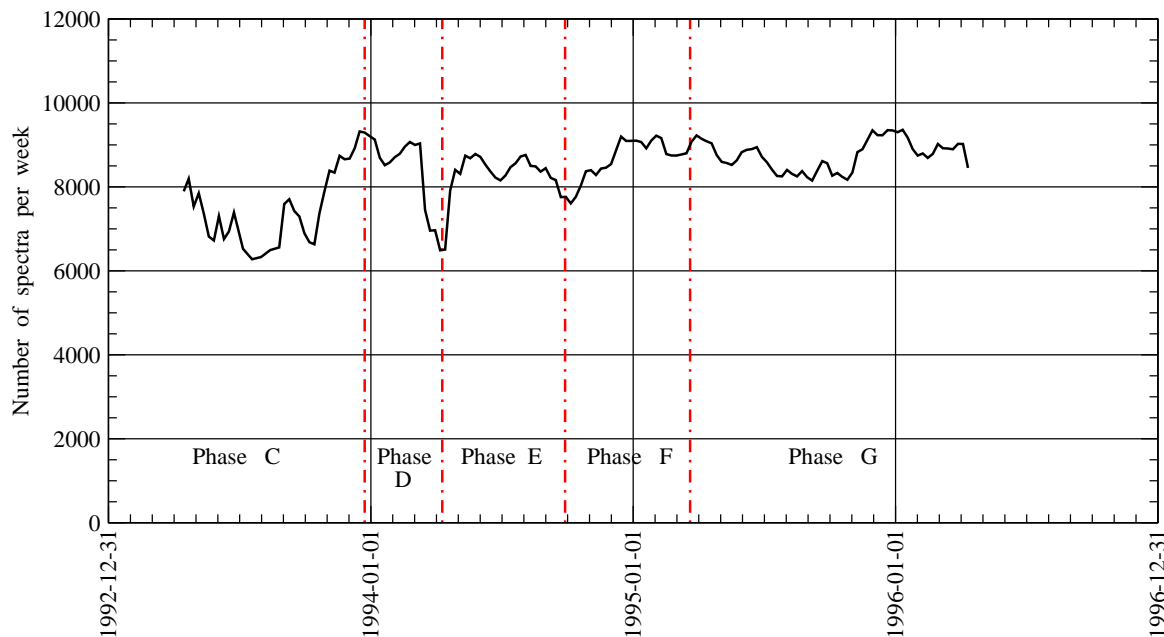


Figure 24: Time history of the 5-week running average of weekly number of ERS-1 UWA spectra during the period from April 1993 to April 1996. Various ERS-1 phases are displayed.

beginning of Phase G (the Second Multi-Disciplinary Phase) witnessed another bias increase to the level of 60 cm. It is clear that almost all phase changes were associated with a local bias change (drop).

On the other hand, the SI values were small (about 21%) at the beginning. Gradual, but small, increase of SI can be noticed. A significant SI jump happened at the beginning of Phase G together with the last bias jump mentioned above. The SI exceeded 32% during the period from May to September 1995.

It should be noted that one can not rule out the impact of possible undocumented model changes on the observed changes in Figure 25.

#### 4.4 Global ERS-2 SAR Significant Wave Height

The time history of the weekly number of global ERS-2 SAR Wave Mode spectra products during the period from April 1996 to May 2006 is shown in Figure 19. It should be noted that the LBR data coverage of ERS-2 was significantly reduced after the failure of the on-board tape recorders on 21 June 2003. Therefore, as described earlier, any comparison after that date does not represent the global situation.

Figure 26 shows the time history of the global weekly bias and scatter index of the SWH computed from ERS-2 SAR wave mode spectra with respect to the operational ECMWF wave model during the period from April 1996 to May 2006. It is worthwhile reminding that on 28 June 1998 a change in the SAR calibration procedure adversely impacted the SAR inversion process. This was fixed on 20 November 2000. The impact of this bug can be clearly seen in Figure 26. Unfortunately, less than two months after the recovery from this bug, the spacecraft lost its gyroscopes on 17 January 2001 and was piloted, as a result, in the EBM. This resulted in a degraded UWA product during the period of EBM as can be clearly seen in Figure 26. The introduction of the ZGM later that year (June 2003), restored the UWA quality. The loss of the global coverage in June 2003 limited the data to be mainly in the Northern Hemisphere. This fact is reflected into a strong seasonal bias cycle and a mild SI cycle both in phase. Another point to note is the gradual reduction of the SI by time.

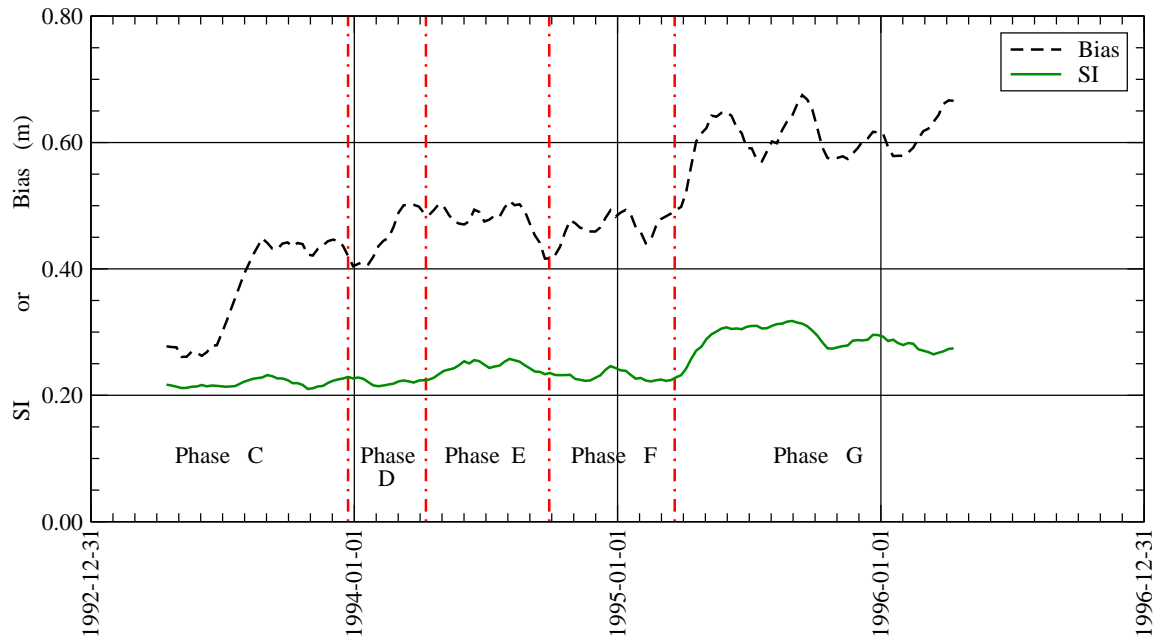


Figure 25: Time history of the 5-week running average of weekly global bias and scatter index of ERS-1 SAR significant wave height with respect to the operational ECMWF wave model during the period from April 1993 to April 1996. Various ERS-1 phases are displayed.

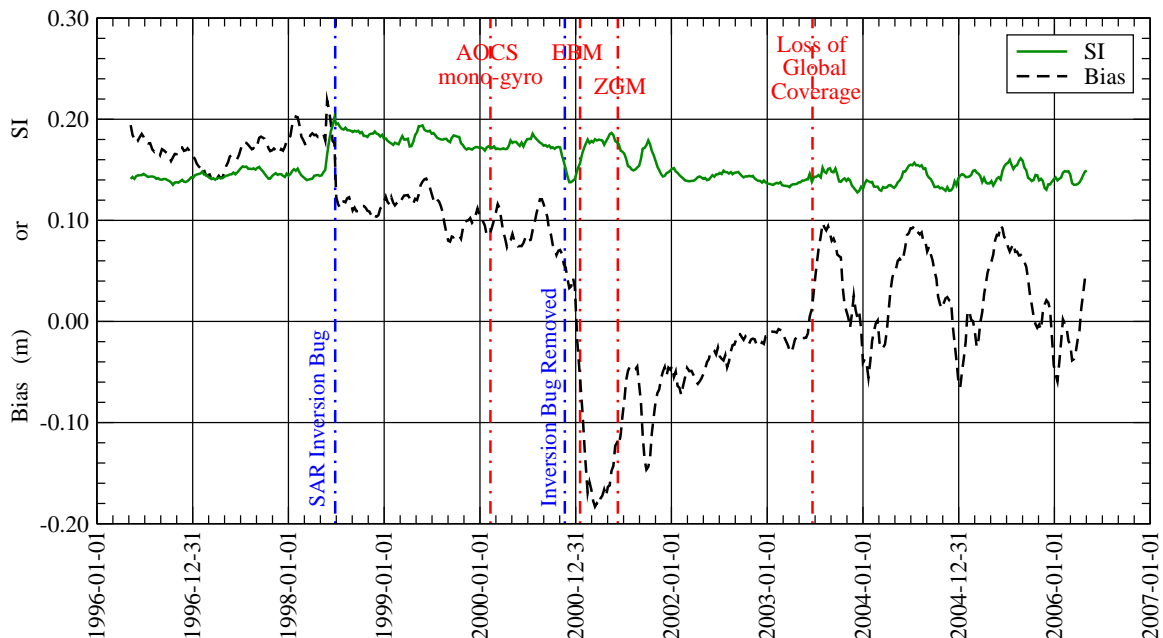


Figure 26: Time history of the 5-week running average of weekly global bias and scatter index of ERS-2 SAR significant wave height with respect to the operational ECMWF wave model during the period from April 1996 to May 2006. Important ERS-2 gyroscope related events and relevant model changes are displayed.

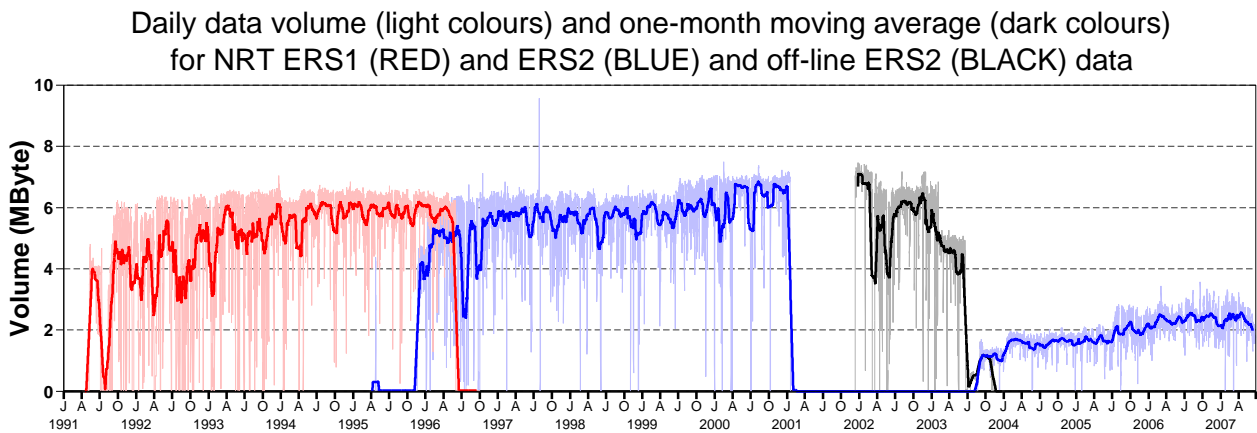


Figure 27: Volume of received ERS-1 and ERS-2 UWI data at ECMWF subject to the data cut-off time in Mbyte per day.

## 5 The Scatterometer UWI product

### 5.1 Overview

The AMI instrument on board ERS-2, and previously ERS-1, obtains backscatter measurements from three antennas, illuminating a swath of 500 km, in which 19 nodes, or wave-vector cells (WVC), define a 25 km product (for details on configuration and geometry see Attema, 1986). From these backscatter triplets, two wind solutions are retrieved one of which is reported in a by ESA disseminated near-real time product, called UWI. For this the geophysical model function CMOD4 (Stoffelen and Anderson, 1997) is used.

ERS-1 was launched on 17 July 1991 and has provided scatterometer data from September 1991 until December 1999. At ECMWF, ERS-1 UWI data was received from 9 May 1991 to 3 June 1996 (red curve in Figure 27), i.e., including some pre-launch test data from 9 May to 4 July 1991. In April 1995 ERS-2 was launched and is still operational. At ECMWF some preliminary data was received on 24 April 1995, while operational data flow started on 22 November 1995 (left-hand blue curve in Figure 27). Due to an on-board anomaly in January 2001, ESA was forced to suspend data dissemination between 18 February 2001 and 21 August 2003. However, off-line data was obtained from ESRIN between 12 December 2001 and 7 November 2003 (black curve in Figure 27). Two months before public re-dissemination, ERS-2 had lost its storage capacity of LBR data, including scatterometer data. After this event, data only remained available when in contact with a ground station. As a consequence, global coverage was lost for the newly disseminated stream, resulting in much lower data volumes (right-hand blue curve in Figure 27).

Within the framework of various contracts with ESA and ESRIN, ECMWF has been monitoring UWI data for a number of years. By passing derived scatterometer winds to the ECMWF operational assimilation system (initially passively, since January 1996 actively), an accurate comparison with model winds can be obtained. Findings of such comparison are, amongst other quality checks, recorded in cyclic reports on 5-weekly intervals. Elements of these reports are described in Section 5.2.

A summary of the monitoring of the entire ERS-2 period will be presented in Section 5.3.

Besides operational assimilation since January 1996, scatterometer data from ERS-1 and ERS-2 have been

actively used in the ECMWF re-analysis project (ERA-40) from January 1993 to January 2001. This extended period of assimilation in the homogenous ERA-40 model context forms an ideal test bed for the assessment and inter-comparison of the long-term behaviour of both scatterometers. In order to allow for an in-depth analysis, a triple collocation set had been created between ERS data, ERA-40 first-guess winds and surface winds from a carefully screened buoy network (Abdalla and Hersbach 2006). As a follow-up of this work two periods of each three years of stable behaviour for ERS-1 respectively ERS-2 have been selected and analysed using a non-parametric method. This allows for an assessment of both a bias in the ERA-40 first-guess winds and ERS winds based on CMOD5. Comparison with other collocation studies all indicate a negative bias for CMOD5 varying between  $0.3 \text{ ms}^{-1}$  and  $0.55 \text{ ms}^{-1}$ . It appears possible to make a refit of the 28 tunable parameters of CMOD5 such that inverted wind speed becomes  $0.48 \text{ ms}^{-1}$  stronger for all wind-speed domains and WVC's. This will be the subject of Section 5.4.

Given the estimates for the bias in the ERA-40 winds and the improved coefficients for CMOD5 (which will be called CMOD5.4), the collocation set between ERS and ERA40 winds was extended to the entire globe. The period before active assimilation was analysed as well, embracing a set from September 1991 until January 2001. From this set it could be confirmed that most changes in the behaviour of the ERS-1 and ERS-2 wind product can be attributed to changes in calibration of the underlying level 1B backscatter product. After a proper re-calibration, an unbiased, stable wind product of high quality is obtained from 15 April 1992 onwards for ERS-1 and from 22 November 1995 onwards for ERS-2. This subject (see also Hersbach *et al.* 2007b) will be addressed in Section 5.5.

The high-quality re-calibrated scatterometer winds are currently assimilated in an experimental configuration of a future reanalysis project at ECMWF (Simmons *et al.* 2007), and CMOD5.4 was introduced in the operational ECMWF model on 7 June 2007. Also on 7 June 2007, the screening on sea ice was revised. Some details will be presented in Section 5.6. On 12 June 2007, data from the ASCAT scatterometer on-board MetOp-A was introduced in the operational assimilation suite at ECMWF.

## 5.2 5-weekly cyclic UWI ERS-2 monitoring reports

The routine monitoring of the ERS-2 UWI product at ECMWF is summarized in the form of 5-weekly cyclic reports. At <http://earth.esa.int/pcs/ers/scatt/reports/ecmwf/>, these reports are available from Cycle 41 (start date 14 July 1998) up to, at the time of this writing, Cycle 126 (end date 11 June 2006).

Up to Cycle 60 (nominal period) the UWI product has been compared with ECMWF first-guess winds as available within the assimilation system. These FGAT (first-guess at appropriate time) winds are well collocated with the scatterometer observation time and location. From Cycle 69 onwards, e.g., with the start of the reception of offline data from ESRIN, collocation was performed with archived first-guess wind fields instead (available at 3-hourly resolution; and will be called FG winds). Collocation errors are slightly larger, but on the other hand it enables the monitoring of data that does not pass pre-screening quality control.

From Cycle 69 onwards, the quality of winds inverted on the basis of CMOD5 are monitored as well. At ECMWF, such retrieved ERS-2 scatterometer winds have been assimilated from 9 March 2004 onwards.

The ECMWF scatterometer cyclic monitoring reports contain the following elements:

- An introduction, giving a general summary of the quality of the UWI data and trends w.r.t. previous cycles. Data coverage, and interruptions in data reception are listed. Also, since Cycle 69 (12 November 2001) it is mentioned whether there was an enhancement of solar activity, and whether it could have affected the UWI wind product. Finally, it is informed whether the ECMWF assimilation system has changed and whether this had an anticipated impact on the quality of the ECMWF surface winds.

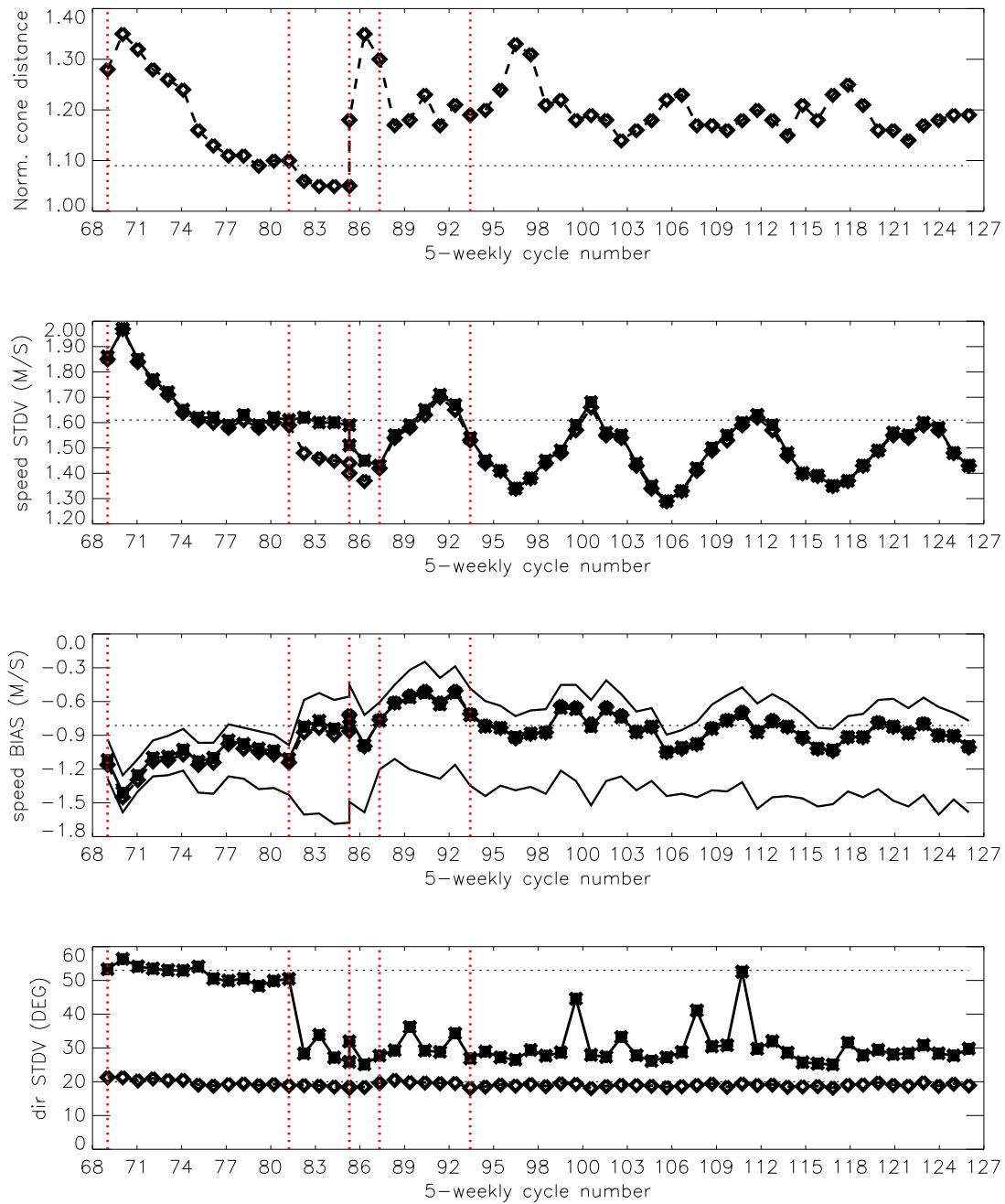


Figure 28: Evolution of the performance of the ERS-2 scatterometer averaged over 5-weekly cycles from 12 December 2001 (Cycle 69) to 11 June 2007 (end Cycle 126) for the UWI product (solid, star) and de-aliased winds based on CMOD4 (dashed, diamond). Results are based on data that passed the UWI QC flags. For Cycle 85 two values are plotted; the first value for the global set, the second one for the regional set (see text for more details). Dotted lines represent values for Cycle 59 (5 December 2000 to 17 January 2001), i.e. the last stable cycle of the nominal period. From top to bottom panel are shown the normalized distance to the cone (CMOD4 only) the standard deviation of the wind speed compared to FG winds, the corresponding bias (for UWI winds the extreme inter-node averages are shown as well), and the standard deviation of wind direction compared to FG.

- A section giving a detailed description of performance during the cycle. It includes the following plots.
- Evolution of 5-weekly averaged performance of the cone distance, bias and standard deviation of UWI and CMOD4 wind speed and direction compared to ECMWF FG winds starting from Cycle 69. The plot for Cycle 126 is given in Figure 28.
- Data coverage and geographical averages of UWI wind speed, and relative bias and standard deviation compared to ECMWF FG winds (Cycle 91 onwards; for Cycle 123, see Figure 29).
- Backscatter ( $\sigma_0$ ) bias for the three antennas (fore, mid, aft) as function of WVC (1 to 19) and stratified with respect to ascending and descending tracks:

$$dz = \langle z \rangle / \langle z_{\text{CMOD}}(\theta, \text{FGAT}) \rangle, \quad (1)$$

where  $z = \sigma_0^{0.625}$ , and  $\theta$  the WVC and antenna-dependent incidence angle. Note that the in this way estimated bias depends on the underlying model function. Results are produced on the basis of CMOD4. Trends in the inter-node and inter-antenna relationship indicate changes in the antenna patterns, because trends in the normalizing ECMWF winds would appear as integral shifts. Examples are provided in Figures 30 and 32.

- Time series of the difference between the fore and aft incidence angle of node 10 (Cycle 81 onwards), and the UWI  $k_p$ -yaw quality flag (Cycle 88 onwards). Asymmetries indicate errors in yaw attitude control.
- Plots of time series of quantities averaged over 6-hourly data batches and stratified w.r.t. six classes of nodes (1-2, 3-4, 5-7, 8-10, 11-14 and 15-19) of
  - The normalized distance to the cone, the fraction of rejected data on the basis of CMOD4 inversion, ESA flags or ECMWF land and sea-ice mask, and the total number of received data over sea.
  - Bias and standard deviation of UWI versus ECMWF first-guess winds for wind speed and direction.
  - The same for CMOD4 winds as inverted at ECMWF from level 1b.
- Global plots of locations where UWI winds were more than  $8 \text{ ms}^{-1}$  weaker or stronger than ECMWF FG winds (included from Cycle 79). Usually two specific cases are highlighted in a separate plot.
- Accumulated histograms (scatterplots) between UWI and ECMWF first-guess wind speed and direction. Scatterplots for FG winds versus de-aliased CMOD4 winds and CMOD5-based winds have been produced from Cycle 74 onwards. Examples for a one-year accumulation period (July 2006 to June 2007) are presented in Figure 33.
- Time series for at ECMWF assimilated CMOD5 winds, and QuikSCAT winds relative to ECMWF FGAT winds for a region covering the North Atlantic and part of Europe (Cycle 94 onwards; for Cycle 126 see Figure 31).

### 5.3 General Overview for ERS-2

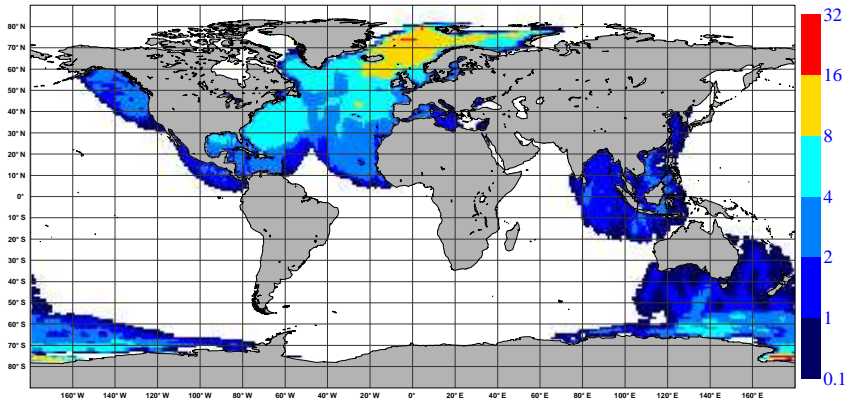
#### 22 November 1995 - 19 March 1996

Pre calibration phase. Large but constant  $\sigma_0$  biases were encountered.

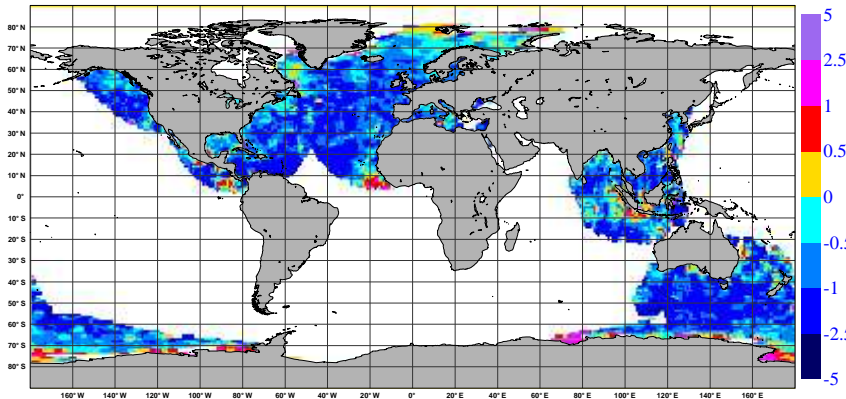
#### 19 March 1996 - 6 August 1996

End of commissioning phase. A thorough calibration has resulted in revised look-up tables. Scatterometer data

NOBS ( ERS-2 UWI ), per 12H, per 125km box  
average from 2007012300 to 2007022618 GLOB:2.45



BIAS ( ERS-2 UWI vs FIRST-GUESS ), in m/s.  
average from 2007012300 to 2007022618 GLOB:-0.8



STDV ( ERS-2 UWI vs FIRST-GUESS ), in m/s.  
average from 2007012300 to 2007022618 GLOB:1.2

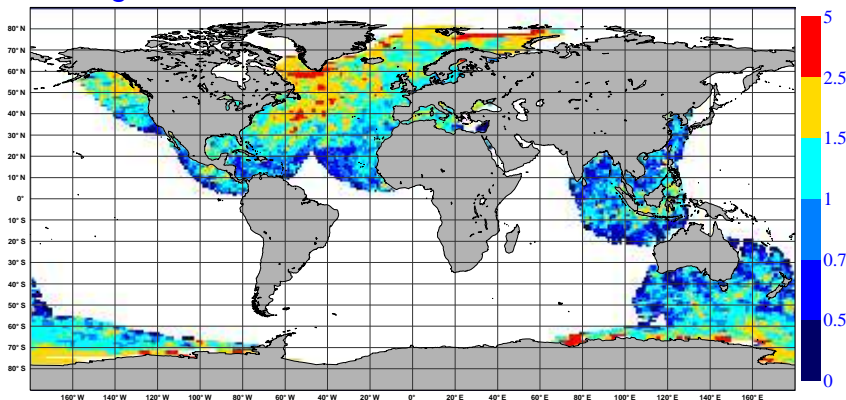


Figure 29: Average number (top) of observations per 12H and per N80 reduced Gaussian grid box ( $\sim 125$  km), relative bias (middle) respectively standard deviation (lower panel) compared to ECMWF FG 10-meter winds, ( $\sim 125$  km) of UWI winds that passed quality control at ECMWF for data in Cycle 123 (23 January to 26 February 2007). Only data are plotted for grid cells that contained at least 5 observations.

from ERS-2 (bias-corrected CMOD4 winds) is included in the ECMWF assimilation system on 1 June 1996, replacing the assimilation from ERS-1 that had been used from 30 January 1996. Details may be found in Isaksen and Janssen (2004).

#### **6 August 1996 - 18 June 1997**

Due to an erroneous switch to a redundant calibration subsystem  $\sigma_0$  values decrease by 0.2 dB.

#### **18 June 1997 - 17 January 2001 (Cycle 22 to Cycle 60)**

Nominal period. Backscatter values return to old, well-calibrated levels.

The performance of the UWI product is stable, although in the fall of 2000 there are some problems with the functioning of several of the six gyroscopes on-board the spacecraft. On average, backscatter levels are around 0.5 dB too low, leading to winds that are on average  $0.7\text{--}0.8\text{ m s}^{-1}$  slower than FGAT winds. Although the inter-node and inter-antenna sigma biases are small, the UWI wind-speed bias does depend on node number (from  $-1.1\text{ m s}^{-1}$  for low to  $-0.6\text{ m s}^{-1}$  for high incidence angle). It is induced by imperfections in the CMOD4 model function (and do not appear for CMOD5). Standard deviation between UWI and FGAT winds are around  $1.6\text{ m s}^{-1}$ . For Cycle 59, values of the average cone distance, (UWI - FGAT) and (CMOD4 - FGAT) statistics are displayed by the horizontal dotted lines in Figure 28.

#### **17 January 2001 - July 2001 (Cycle 60 to 65)**

As a result of the on-board failure there are no gyroscopes left for the platform's attitude control. The control system is switched to Extra Back-up Mode. The dissemination of scatterometer data is suspended after 2 February 2001; empty cyclic reports are made for Cycles 62 to 68.

#### **July 2001 - 12 December 2001 (Cycle 65 to 69)**

Introduction of the Zero-Gyro Mode (ZGM). Satellite pointing is achieved through payload data and the digital earth sensor. Although pitch and roll can be controlled accurately, large errors in the yaw attitude (several degrees) still occur. Such errors especially affect the quality of the scatterometer measurements. Dissemination of scatterometer data remains suspended.

#### **12 December 2001 - 4 February 2003 (Cycle 69 to 81).**

Restart of dissemination of UWI data, however, to a restricted group of users only. At ECMWF, the monitoring is resumed. Existing tools are updated where necessary.

Large errors in yaw, which especially seem to occur around periods of enhanced solar activity, have a large negative impact on the data quality. During these events, part of the backscatter signal is destroyed, which, after inversion, results in far too low winds. Peaks of more than  $-3\text{ m s}^{-1}$  frequently occur, especially in January 2002 (Cycle 70), which marks a period of considerable solar activity. These incorrect data are also visible in the scatter diagrams of UWI versus FG wind speed as anomalously large numbers of collocations between strong ECMWF winds and weak UWI winds. For later cycles the situation improves.

Initially, also extremely large negative biases are observed in the backscatter levels, including data that was less affected by yaw errors. Large inter-node and inter-antenna differences induce large cone distances. The situation is worst for Cycle 70 but later slowly improves. However, the increasing negative bias towards higher nodes remains. In line with the average reduction in  $\sigma_0$  bias, the cone distance and wind-speed biases gradually improve (see Figure 28).

For the random error of the UWI and CMOD4 wind speeds a similar trend is observed: worst for Cycle 70 (almost  $2\text{ m s}^{-1}$ ) and then first improving rapidly and later stabilizing. From Cycle 75 onwards its level is around the value obtained for the nominal period (see Figure 28). In general best results are obtained for winds inverted on the basis of CMOD5. Both the negative bias level and standard deviation are smaller for such derived winds.

The performance in wind direction is found to be much less affected. Although initially wind direction performs somewhat worse, at Cycle 72 it is on the level of the nominal period, and after Cycle 75 it has even become better (see lower panel of Figure 28).

#### **4 February 2003 - 22 June 2003 (Cycle 81 to 85)**

Start of the validation phase of ESACA, the new processor. Aim of this complete revision of the original LRDPF, was to bring the quality of the UWI product back to its nominal level. It is capable of the interpretation of on-board filter characteristics appropriately according to an estimation of the yaw attitude error. During the test phase, ESACA data is distributed for Kiruna station only, which leads to daily data gaps between approximately 21 UTC and 06 UTC.

The new de-aliasing algorithm, being part of ESACA, (and developed at DNMI) appears to perform well. The UWI winds agree considerably more often to the wind solution that is closest to the ECMWF FG wind direction. Values of standard deviations drop from 50 to less than 30 degrees (see Figure 28).

The UWI winds do not coincide anymore with one of the two solutions from the CMOD4 inversion at ECMWF. At ECMWF inverted CMOD4 winds appear to be of much higher quality than the by ESRIN disseminated UWI winds (see Figure 28). At ESRIN, the cause for this non-ideal situation is tracked down quickly. At the beginning of April 2003 appropriate corrections to ESACA are implemented and since then UWI winds are in line with CMOD4 again (though not yet for Kiruna station; i.e., the discrepancy in winds remains for the data as received at ECMWF). The standard deviation w.r.t. FGAT winds are below  $1.50 \text{ ms}^{-1}$ , i.e., about  $0.1 \text{ ms}^{-1}$  better than it used to be during the nominal period.

Large fractions of high  $k_p$  values are found, especially for nodes at high incidence angles (more than 50%). Consideration between the (UK) MetOffice and ESRIN reveals that there is a problem with the BUFR encoding algorithm. A solution is formulated and implemented (again, not yet at Kiruna).

In the near range the fore and aft antenna show large negative biases in the average backscatter levels. As a result, very large negative wind-speed biases are found for low nodes ( $-1.6 \text{ ms}^{-1}$ ). At ESRIN its cause is identified and resolved (though, not visible at Kiruna). Apart from the initially large near-range biases, the inter-node and inter-antenna differences in backscatter levels are small. Their level is comparable to that during the nominal period.

The incidence angles between the fore and aft antenna are not equal anymore. They now show a rapid variation in time and peaks up to 7 degrees are observed. This asymmetry is a direct result of errors in yaw attitude. A large anomaly on April 1 2003 (while the Earth was inside a gusty solar wind stream, source: [www.spaceweather.com](http://www.spaceweather.com)) results in low-quality winds. This event illustrates the potential usefulness of a yaw flag in the UWI product.

Along with improved quality of the CMOD4 winds, the normalized distance to the cone is now below the level of the nominal period.

#### **22 June 2003 - 21 August 2003 (Cycle 85 to 87)**

On 22 June 2003 the second Low Bit-Rate recorder on-board ERS-2 fails, and is found to be beyond repair. As the first recorder had become unusable in December 2002, this means that now there is no facility left to store LBR data, including scatterometer data. After a data-void period of three weeks, data flow is resumed on 16 July 2003, however, only for observations for which there is a direct contact with a ground station. For the Kiruna test data received at ECMWF, this means that coverage is limited to the Atlantic north of  $40^\circ\text{N}$ , making statistics very sparse.

#### **21 August 2003 - 11 June 2007 (Cycle 88 to 126)**

On 21 August 2003, the public dissemination of UWI data is restarted. This fortunate event makes an end to the

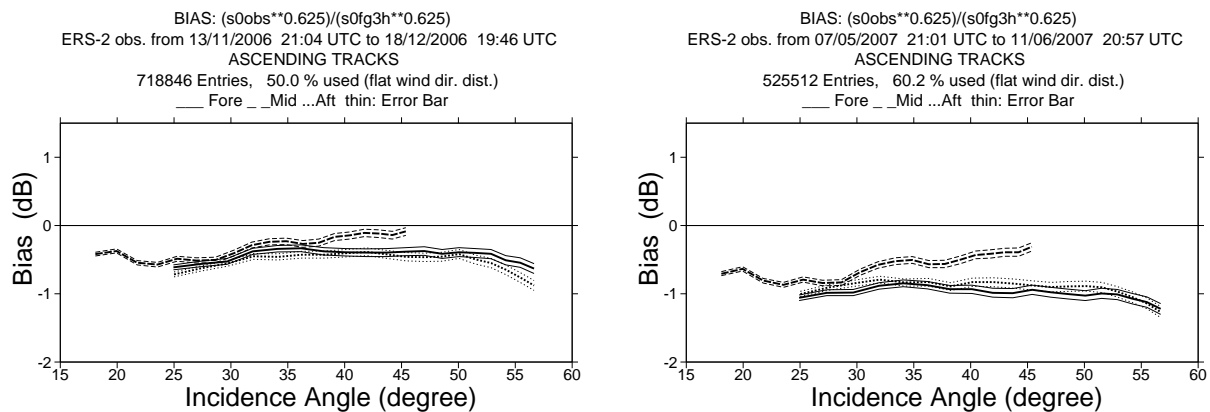


Figure 30: Ratio of  $\langle \sigma_0^{0.625} \rangle / \langle \text{CMOD4}(\text{FGAT})^{0.625} \rangle$  converted in dB for the fore antenna (solid line), mid antenna (dashed line) and aft antenna (dotted line), as a function of incidence angle for ascending tracks of data within Cycles 121 (left panel) and 126 (right panel). The thin lines indicate the error bars on the estimated mean.

restricted distribution. From this date onwards data is received in the original manner (via the UK Met-Office), and is stored in the usual ECMWF analysis-input archives (the restricted data had been archived at a less accessible location). The original monitoring in the assimilation system (e.g., comparison with FGAT winds) is restored. However, cyclic reports are still based on the off-line monitoring (FG winds), since it includes data that is rejected in an early stage of the assimilation system. Besides Kiruna station, data is now also received from Maspalomas, Gatineau and Prince Albert, which, bearing in mind the loss of the LBR recorders, results in a coverage over the North Atlantic, part of the Mediterranean, the Gulf of Mexico, and a small part of the Pacific north-west from the US and Canada. An initial gap in the North Atlantic is resolved on 15 January 2004, when a station at West Freugh (Scotland) is included. Coverage in the Caribbean is obtained by a station at Miami (February 2005), in the Chinese Sea by a station at Beijing (July 2005), and partial coverage over the Southern Hemisphere by the inclusion of McMurdo (Antarctica, June 2005) and Hobart (Tasmania, February 2006) stations, and coverage over the Bay of Bengal and the North-Eastern part of the Indian Ocean by a station in Singapore (October 2006). Since 8 March, 2007, however, no data from Hobart has been acquired because of an anomaly of the ground station antenna. The areas covered by Miami and Beijing station allow for the accurate observation of a number of tropical cyclones. All stations joined together lead to a (for Cycle 123) coverage as indicated in Figure 29.

The recording by separate ground stations means that in certain areas observations are reported more than once. For each ground station gridding into 25-km cells and de-aliasing is performed separately. It is found that overlapping cells may be dislocated (by 12.5 km), and that regularly not the same wind solution is selected for all ground stations.

The operational ESACA processor has resolved all non-optimal features that had been detected during the validation period. Data quality is found to be high, although the cone distance has increased and is now 10% higher than for nominal data (see top panel of Figure 28). Assimilation experiments with winds inverted on the basis of CMOD5, show a small positive impact in global forecast skill (Hersbach *et al.* 2004). It leads to the re-introduction of ERS-2 scatterometer data in the ECMWF assimilation system on 8 March 2004.

An original flag for high  $k_p$  values is now also set for yaw attitude  $k$  errors exceeding 2 degrees. It appears to work well and a close correlation with the asymmetry in incidence angle is observed. It is routinely checked whether peaks in attitude errors coincide with enhanced solar activity. Magnetic storms influence the outer part of the atmosphere, which in turn could affect the ERS-2 platform. Although sometimes collocations between anomalies and solar storms occur, the relation is not obvious. Besides, since mid 2006 the Sun resides near its

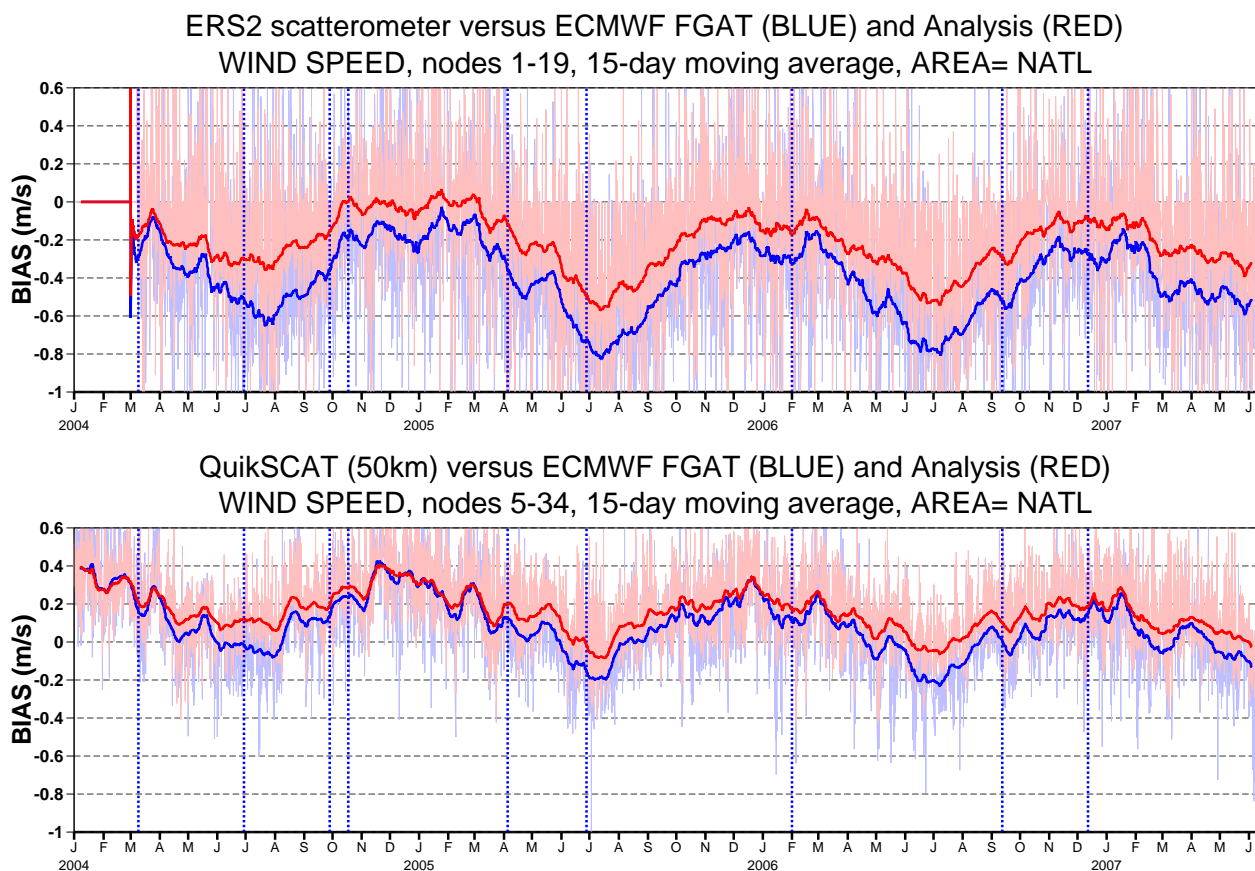


Figure 31: Wind-speed bias relative to FG winds for actively assimilated ERS-2 winds (based on CMOD5) for nodes 1-19 (top panel) respectively 50-km QuikSCAT (based on the QSCAT-1 model function and reduced by 4%) for nodes 5-34 (lower panel), averaged over the area (20N-90N, 80W-20E), and displayed for the period 01 January 2004 - 26 June 2006. Fat curves represent centred 15-day running means, thin curves values for 6-hourly periods. Vertical dashed blue lines mark ECMWF model changes.

minimum of its (chaotic) 11-year solar cycle, and, as a result, magnetic storms have been relatively sparse.

Since the loss of global coverage, a seasonal trend has been introduced in the now regional data set, making objective monitoring more difficult. A clear example of such a trend is observed for the relative standard deviation of the UWI wind speed compared to FG winds (see second panel of Figure 28); a more intense and volatile wind climate in winter time will naturally lead to an increased RMSE.

A seasonal trend also appears for bias levels of both wind speed and backscatter. For backscatter, bias patterns are found to be flat in winter time, but large asymmetries emerge during summer. Typical examples for this consistent yearly trend are given in Figure 30. For wind speed, bias relative to ECMWF FG winds, are found to be (like backscatter) most negative around July ( $\sim 1.1 \text{ m s}^{-1}$ ) and least negative around January ( $\sim 0.7 \text{ m s}^{-1}$ ). The seasonal fluctuations, which are also observed for QuikSCAT (see e.g. Figure 31) are thought to be related to seasonal variations in the stability of the marine boundary layer. For a discussion, see Section 5.4 of Abdalla and Hersbach 2006.

In order to filter out seasonal effects, relative biases in backscatter space are presented in (the right-hand panels of) Figure 32 for the one-year period July 2006 to June 2007. For Cycle 59 (end 2000) similar plots are

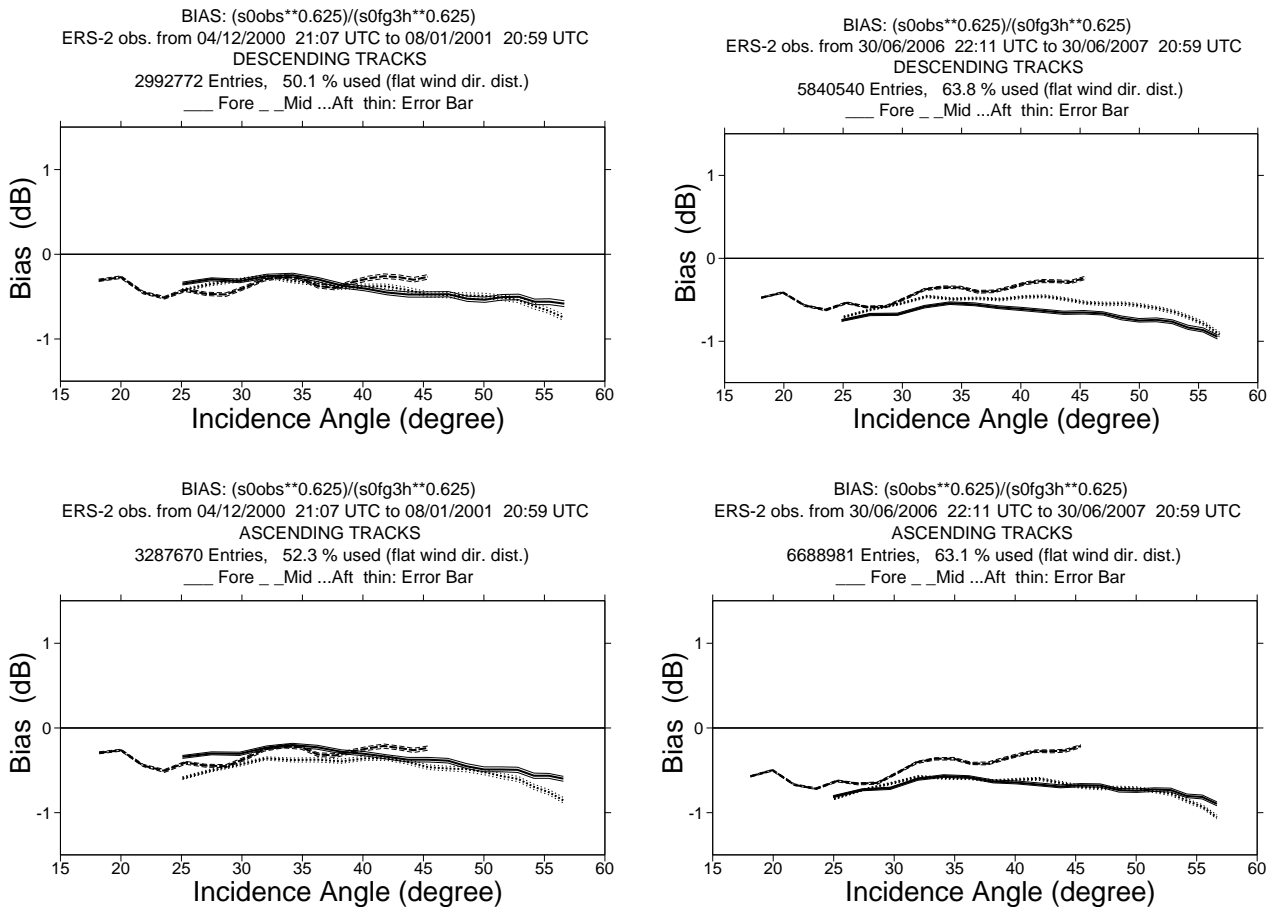


Figure 32: The same as Figure 30, but now averaged over Cycle 59 (left-hand panels) and the one-year period July 2006 to June 2007 (right-hand panels) for descending (top panels) respectively ascending (lower panels) tracks.

presented in the left-hand panels. Although accumulated over the limited 5-weekly period for this Cycle, seasonal effects are still filtered out by the fact that data was globally available (other cycles in 2000 display a similar pattern, not shown). Comparison between the two sets of plots shows that current bias levels are about 0.2 dB more negative than for nominal data. It is a reflection of the enhancement of ECMWF surface winds by about  $0.2\text{m s}^{-1}$  over the last 6 years. This trend emerges, e.g., from longterm monitoring of QuikSCAT winds and buoy winds (not shown). The inter-antenna asymmetry has increased. For higher incidence angles the bias level of the mid antenna is less negative than for the other two antennas; especially for the ascending tracks. This asymmetry is most prominent during the Summer as can e.g., be seen from the right-hand panel of Figure 30. Its origin is not known.

For wind the accumulation over the one-year period July 2006 - June 2007 (and all 19 nodes), indicates that UWI winds are on average  $0.8 - 0.9\text{ m s}^{-1}$  biased low compared to ECMWF FG winds (top left-hand panels of Figure 33). This is slightly more negative than for nominal data (before January 2001), and matches the gradual increase ( $\sim 0.2\text{m s}^{-1}$ ) in average wind speed of the ECMWF first-guess winds since 2000 as mentioned above. Compared to a yearly average from July 2005 - June 2006 (Figure 34), the situation is very stable. For both wind speed and wind direction, scatterplots with respect to ECMWF FG winds are remarkably similar in detail. Although, standard deviation in wind direction has improved from 32.8 degrees to 28.8 degrees. Reason for this is that during the last year less events of evident degradation of the de-aliasing software have been observed (e.g., as had occurred between 29 November and 7 December 2005; see Cyclic report 111 for details). For

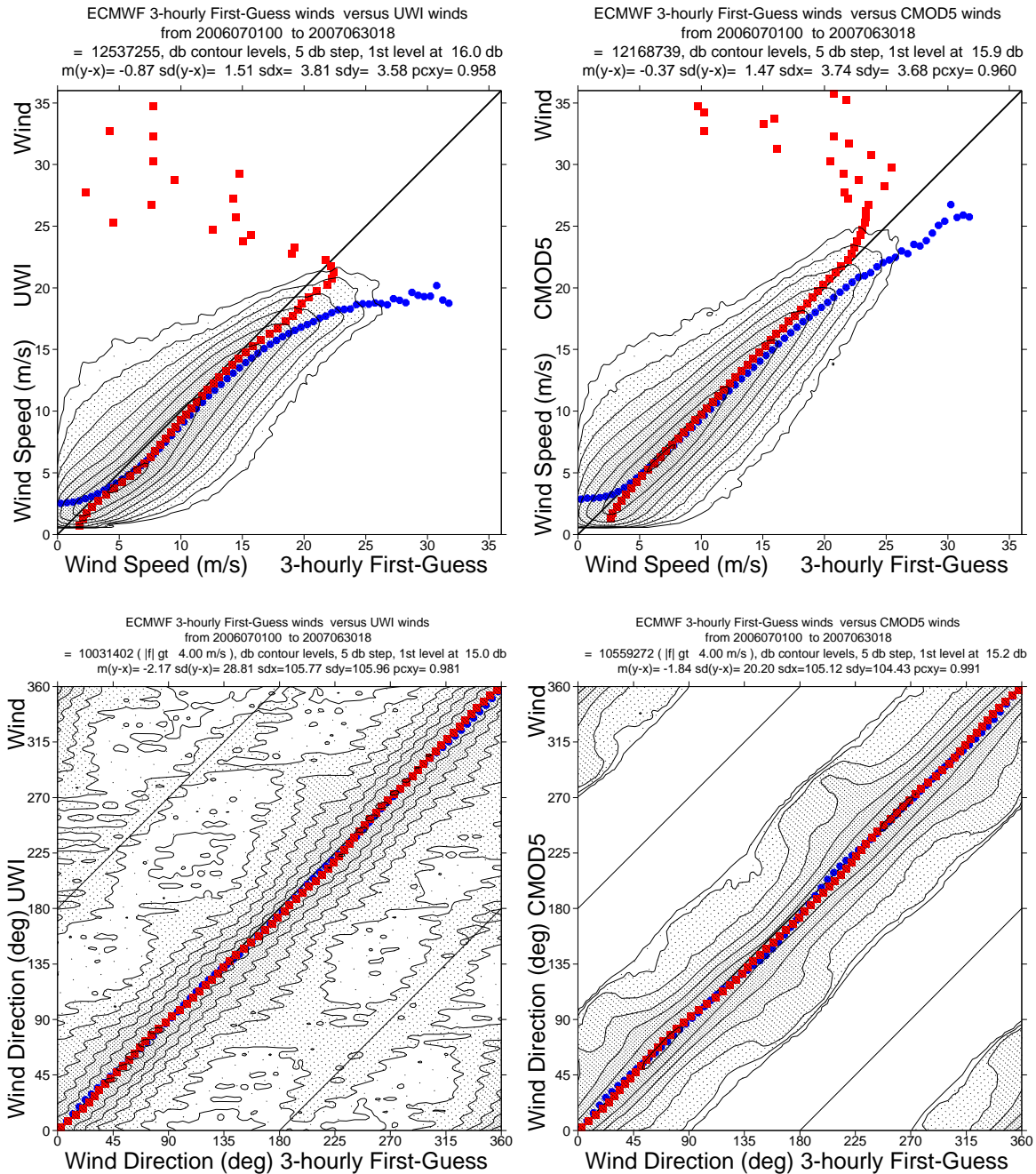


Figure 33: Two-dimensional histogram of UWI (left hand panels) or de-aliased CMOD5 (right hand panels) relative to ECMWF FG for wind speed (top panels) and wind direction (lower panels) over the one-year period from July 2006 to June 2007. Blue circles denote averages for bins in the x-direction, and red squares averages for bins in the y-direction.

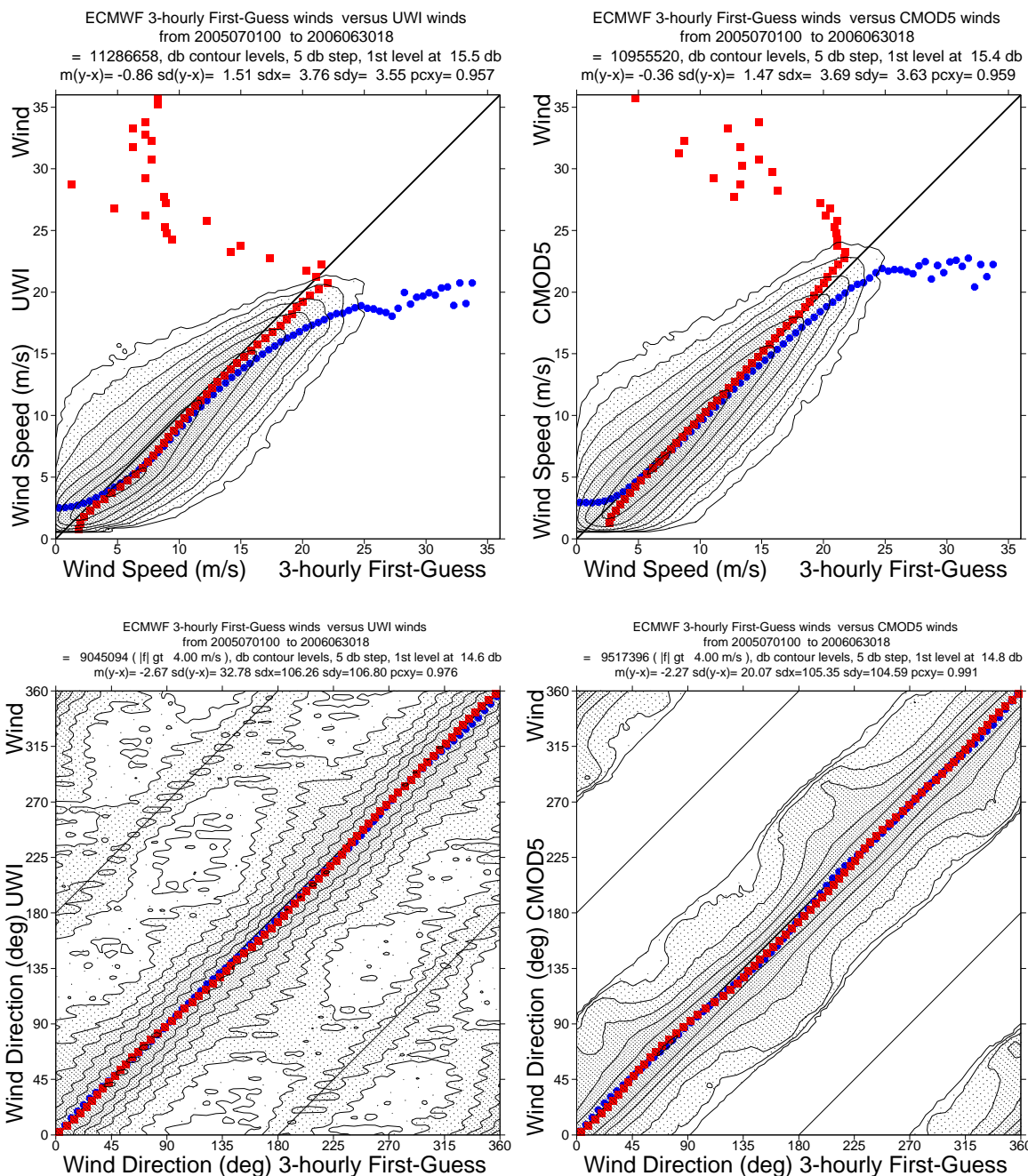


Figure 34: The same as Figure 33, but now for the period 1 July 2005 - 30 June 2006.

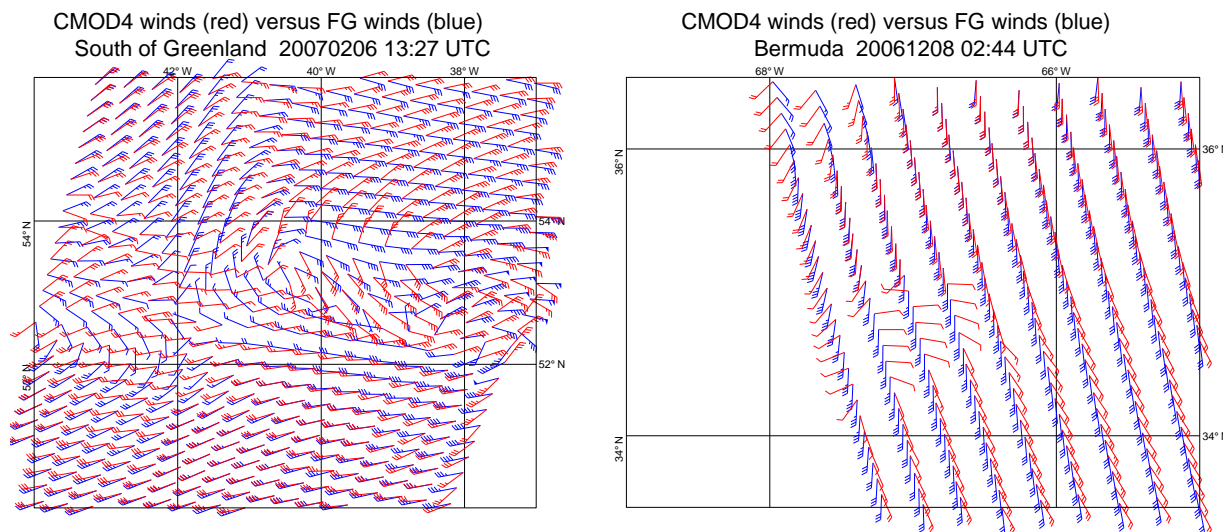


Figure 35: Two examples for situations where scatterometer and ECMWF winds differ significantly.

de-aliased CMOD4 winds, no noticeable difference in performance for wind direction is observed between the two yearly data sets. The same holds for winds derived from CMOD5. Average relative wind bias is around  $-0.35 \text{ m s}^{-1}$ , which seems fairly independent on wind speed, as e.g. can be seen from the histogram displayed in the top right-hand panel of Figures 33 and 34.

Compared to the situation of nominal data (e.g., before 2001), the current one-year accumulated relative standard deviation of UWI winds is about  $0.1 \text{ m s}^{-1}$  lower ( $1.5 \text{ m s}^{-1}$  versus  $1.6 \text{ m s}^{-1}$ ). It is difficult to state whether the quality of the UWI product has improved, since the lower STDV can well be the result of the current omission of strong (e.g. volatile) winds in the Southern Hemispheric storm tracks, combined with the gradually improved quality of ECMWF winds.

As observed during the ESACA test phase, the quality of UWI wind direction is (as a result of the improved de-aliasing algorithm) superior to that of nominal data (see lower panel of Figure 28). Nevertheless, incorrect wind solutions are still frequently reported as can be seen from the lower panels of Figure 33. Occasionally, peaks of degraded performance have occurred (latest between 12-16 August 2006; see report for Cycle 118 for details), which usually can be traced back to temporarily missing input (model winds) in the ESACA de-aliasing software. Such peaks are not observed for at ECMWF de-aliased CMOD5 winds.

A previously non-existing bias is observed for wind direction. On average, (de-aliased) ERS-2 winds are found to be rotated by 2 to 3 degrees counter-clockwise compared to ECMWF first-guess fields. One reason for this consistent bias appears the lack of cross-isobar flow (Hollingsworth 1994) at warm advection of ECMWF surface winds. A similar, opposite, effect is found on the Southern Hemisphere, and, therefore, this bias is almost averaged out in a global verification, but not in an unequally distributed data set as for ERS-2. A study for QuikSCAT data versus model winds may be found in Brown *et al.* 2005.

Locations for large differences between UWI (or CMOD5) winds are usually isolated. They often indicate meteorologically active regions, for which UWI data and ECMWF model field show reasonably small differences in phase and/or intensity. Tropical cyclones and frontal systems are typical candidates. One example (left-hand panel of Figure 35) was a complex situation of two merging low pressure systems south of Greenland for 6 February 2007. For the right-hand system the scatterometer winds show a less elongated and slightly shifted

U.S. National Data Buoy Center (NDBC)							
41001	41002	41010	42001	42002	42003	44011	46002
46004	46005	46006	46035	51001	51003	51004	46059
Canadian Marine Environmental Data Service (CMEDS)							
46036	46184						

Table 1: Five-digit WMO identifiers of buoys that were taken in consideration for the collocation with ERS winds, grouped into originating data provider.

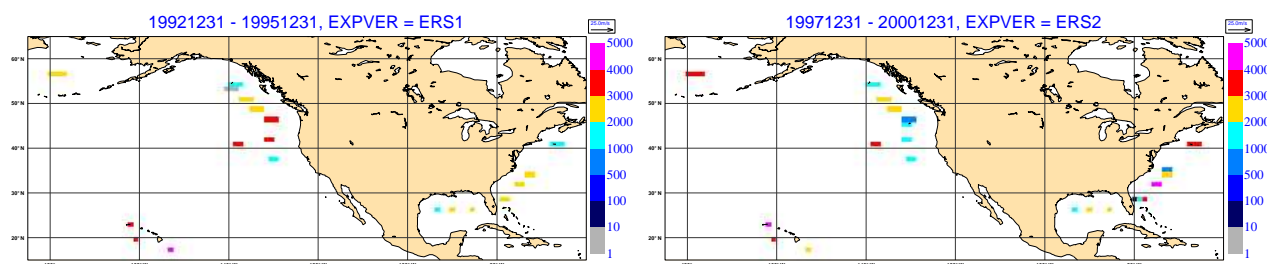


Figure 36: Number of collocations accumulated over the indicated period (and mapped on a N80 reduced Gaussian grid) for which buoy and ERS-1 (left) respectively ERS-2 (right) are positioned within 30 minutes and 50 km. Adjacent non-empty grid boxes expose buoy displacements.

vortex. Although the UWI winds look sensible, they do suffer from incorrect de-aliasing near the centre.

Besides large differences that pin point errors in the ECMWF first-guess field, occasionally cases are observed in which UWI winds seem clearly incorrect. This is often manifested as odd patches within a surrounding wind field of presumably good quality. An example is shown in the right-hand panel of Figure 35. Problems are found most likely to occur at light wind conditions relatively close to land, and at lower incidence angles in general.

## 5.4 Re-calibration of the CMOD5 coefficients

CMOD5 (Hersbach *et al.* 2007) provides an improvement on the original C-band model function CMOD4 (Stoffelen and Anderson 1997). Although, the latter is still used for the determination of the wind solution provided in the UWI product, CMOD5 gives rise to a more uniform performance across the AMI swath. Improvements are especially obtained for extreme cases, and CMOD5 extends the dynamical range for C-band scatterometer data from  $24 \text{ m s}^{-1}$  to  $35 \text{ m s}^{-1}$ .

The CMOD5 model function was derived on the basis of a collocation study between ERS-2 AMI triplets and ECMWF FGAT winds. Here it was assumed that ECMWF FGAT winds represent an unbiased reference for surface winds over the global oceans. However, being a function of time (i.e., depending on the ECMWF model version), biases in these fields are known to exist (for a comparison with QuikSCAT winds see e.g., Chelton and Freilich, 2005). A triple collocation with buoys (which are generally believed to provide the best unbiased estimate of the ground truth) for a one-year period (August 1998 to July 1999) showed that both CMOD5 and ECMWF FGAT winds were biased low by about  $0.35 \text{ m s}^{-1}$ . This bias is found to be uniform, i.e., independent on wind speed itself (see Fig. 13 of Hersbach *et al.* 2007). Similar results were obtained by a study of Portabella and Stoffelen (2007), though with a negative bias for CMOD5 of around  $0.50 \text{ m s}^{-1}$ .

In Abdalla and Hersbach (2006), the ERS archive as used in the ECMWF 40-year reanalysis system (Uppala, 2005; denoted by ERA-40), had been collocated with a carefully selected buoy network. Although several

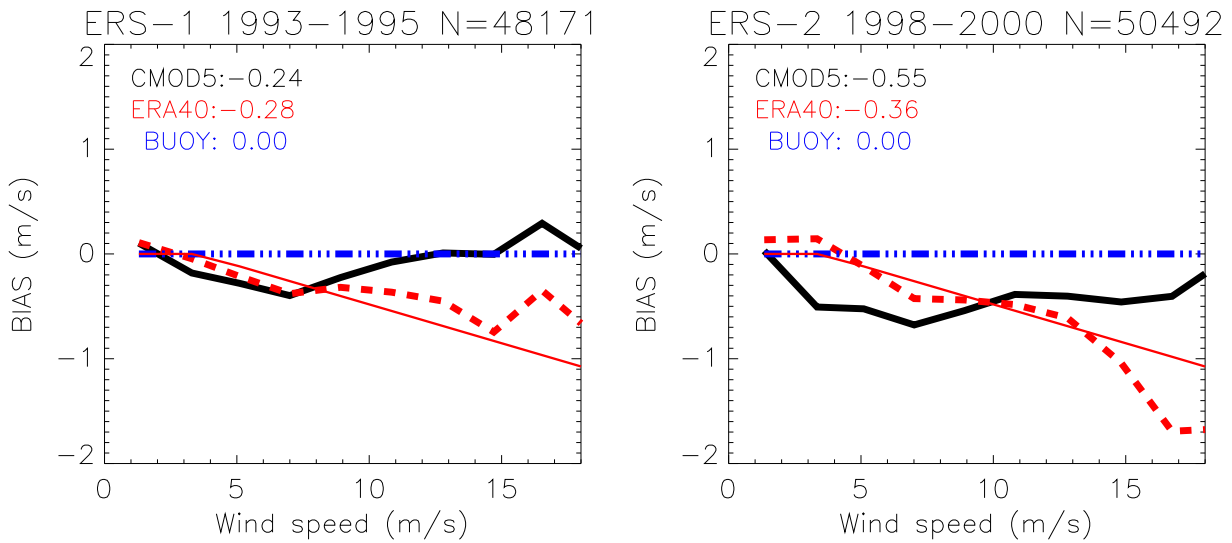


Figure 37: Bias of AMI wind speed inverted on the basis of CMOD5 (black), and the ERA-40 FGAT wind speed (red), relative to buoy wind speed, for the period 1993-1995 for ERS1 (left-hand panel), respectively for the period 1998-2000 for ERS-2 (right-hand panel). The thin solid red line represents relation (2).

periods of clearly non-ideal performance of the UWI archive were identified, long periods of stable behaviour were found as well. This analysis provides an ideal situation to repeat a triple collocation for an extended period for both ERS-1 and ERS-2. In order to minimize the effect of seasonal fluctuations (see Figure 37 of Abdalla and Hersbach 2006) two stable periods of exactly three years were selected: 1993-1995 (with the exclusion of an anomalous period between 23 December 1993 and 14 January 1994; see Section 5.5 for details) for ERS-1 and 1998-2000 for ERS-2. Maximum collocation error was set to 50km in position and 30 minutes in time. Since among the original set of 27 buoys (see table 1 of Abdalla and Hersbach 2006) persistent biases have in the meantime been found for some buoys, either due to possible calibration problems, or the presence of ocean currents, the number of buoys was further reduced to 18. A list may be found in Table 1; their location and the number of collocations in Figure 36. Relative biases and random errors were estimated on the basis of a non-parametric method (some details may be found in Abdalla and Hersbach 2006). In case the buoy network can be regarded as an unbiased reference (which is the usual choice), biases for ERA-40 FGAT winds, and AMI winds inverted on the basis of CMOD5 are displayed in Figure 37.

For the ERA-40 winds (red curves in Figure 37) similar results are found between both periods. For light winds ERA-40 seems to be unbiased, while towards strong winds ERA-40 (increasingly) under estimates wind speed. A posteriori, the wind-speed dependent bias can by reasonable approximation be parametrized with the following relation (thin red line in Figure 37):

$$s_{\text{unbiased}} = \begin{cases} s & s \leq 3.5 \text{ m s}^{-1} \\ 1.08s - 0.28 \text{ m s}^{-1} & s > 3.5 \text{ m s}^{-1} \end{cases}, \quad (2)$$

where  $s$  is the ERA-40 wind speed, and  $s_{\text{unbiased}}$  the unbiased value it should have represented.

Note that there is a small difference in the average ERA-40 bias level (i.e.,  $-0.28 \text{ m s}^{-1}$  versus  $-0.36 \text{ m s}^{-1}$ ) between both periods. It is difficult to assess whether this indicates an evolution of the ERA-40 wind product, or is to be attributed to possible changes and/or fluctuations in the buoy network. Since the results are probably not statistically significant within  $0.1 \text{ m s}^{-1}$ , the reason for the difference will not be investigated.

For the CMOD5 winds differences between both sets are larger. For ERS-2 a reasonably flat bias of  $-0.55 \text{ m s}^{-1}$  is

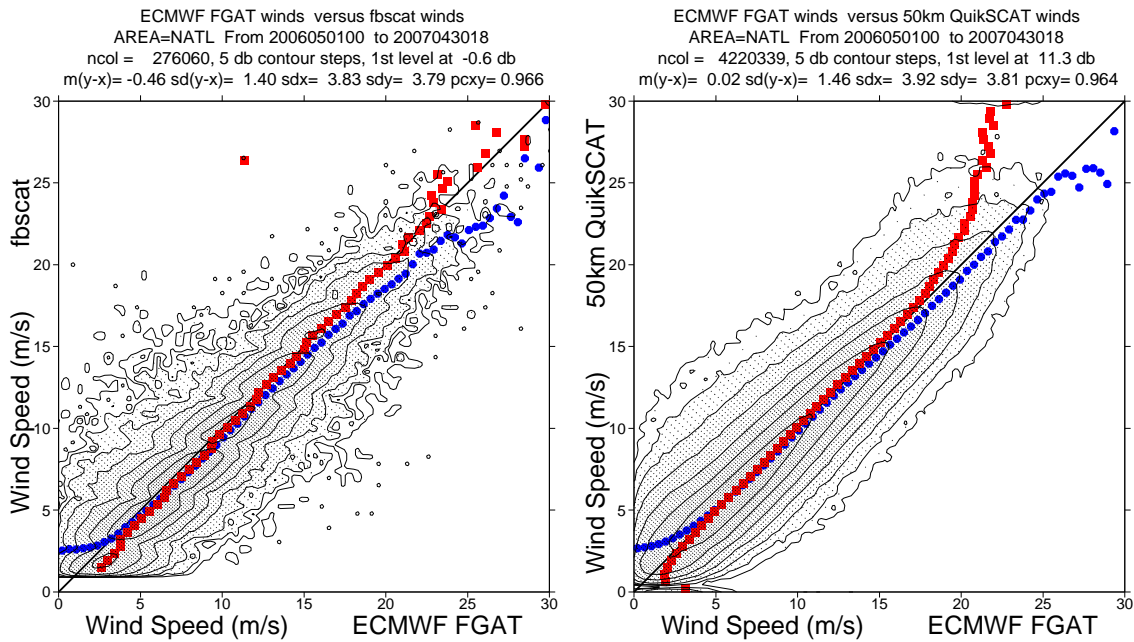


Figure 38: Scatterplot of actively assimilated ERS-2 (left-hand panel) and QuikSCAT (right-hand panel) data versus ECMWF FGAT surface wind speed for data within the area (20N-90N, 80W-20E) and accumulated over the 1-year period between 1 May 2006 and 30 April 2007. Blue circles denote averages for bins in the x-direction, and red squares averages for bins in the y-direction.

observed, while for ERS-1 a wind-speed dependent bias of on average  $-0.24\text{ m s}^{-1}$  emerges. The difference of  $0.31\text{ m s}^{-1}$  is likely to be statistically significant, and, as such, indicates a (small) difference in calibration between ERS-1 and ERS-2.

Another way to investigate a bias in CMOD5 can be found from a comparison with QuikSCAT winds. For QuikSCAT, validation studies performed by Freilich and Dunbar (1999) and Ebuchi *et al.* (2002), conclude that winds compare well with buoy measurements. On average, no bias is observed. However, QSCAT-1 (the Ku-band geophysical model function used) has been tuned to provide neutral equivalent winds, i.e., the wind at 10-m height in case of a neutrally stratified marine boundary layer. In practice, such winds are on average about  $0.2\text{ m s}^{-1}$  stronger than real winds at 10-metre height. To incorporate this difference, inverted QuikSCAT (neutral) winds are reduced by 4% in the ECMWF assimilation system.

Long-term monitoring shows that ERS-2 winds are typically  $0.4$  to  $0.5\text{ m s}^{-1}$  weaker than QuikSCAT winds. As an example, histograms accumulated over a one year period within an area in the North Atlantic well covered by both ERS-2 and QuikSCAT are presented in Figure 38. Although the two plots do not represent data that exactly collocate in space and time, the relative bias between ERS-2 and QuikSCAT is realistic and clear. From the right-hand panel it emerges that ECMWF FGAT winds are nearly unbiased with respect to QuikSCAT winds. Although for a number of years ECMWF winds have been biased low by up to  $-0.4\text{ m s}^{-1}$  (see e.g., Chelton and Freilich, 2005), they seem unbiased since the increase of the horizontal and vertical model resolution in February 2006 and changes in the convective momentum transport in September 2006. The left-hand panel of Figure 38 indicates a negative bias of  $-0.48\text{ m s}^{-1}$  for ERS-2 relative to QuikSCAT, independent of wind speed.

Although all analyses presented above confirm that CMOD5 is biased low, they disagree in the exact amount. For ERS-1 a bias of  $-0.28\text{ m s}^{-1}$  is found, while for ERS-2 estimates vary between  $-0.35\text{ m s}^{-1}$  and  $-0.55\text{ m s}^{-1}$ . As a compromise, it seems reasonable to assume a bias of  $-0.45\text{ m s}^{-1}$ . It appears that this difference can be

Coefficient	Original	Updated	Coefficient	Original	Updated
$c_1$	-0.688	-0.688	$c_{15}$	0.007	0.007
$c_2$	-0.793	-0.795	$c_{16}$	0.330	0.326
$c_3$	0.338	0.339	$c_{17}$	0.012	0.012
$c_4$	-0.173	-0.172	$c_{18}$	22.00	22.524
$c_5$	0.000	0.000	$c_{19}$	1.950	2.026
$c_6$	0.004	0.004	$c_{20}$	3.000	3.000
$c_7$	0.111	0.110	$c_{21}$	8.390	8.380
$c_8$	0.0162	0.0160	$c_{22}$	-3.440	-3.375
$c_9$	6.340	6.583	$c_{23}$	1.360	1.332
$c_{10}$	2.570	2.701	$c_{24}$	5.350	5.899
$c_{11}$	-2.180	-2.240	$c_{25}$	1.990	2.238
$c_{12}$	0.400	0.451	$c_{26}$	0.290	0.312
$c_{13}$	-0.600	-0.690	$c_{27}$	3.800	4.025
$c_{14}$	0.045	0.045	$c_{28}$	1.530	1.632

Table 2: Original and updated CMOD5 coefficients

incorporated in the original CMOD5 empirical functional estimate of scatterometer backscatter  $\sigma_0$  given wind speed  $u_{10}$ , wind direction  $\phi$  and incidence angle  $\theta$ :

$$\sigma_0 = \text{CMOD5}(u_{10}, \phi, \theta, \mathbf{c}) \quad (3)$$

without changing its general form (a full specification may be found in Hersbach *et al.* 2007). It only requires a refit  $\mathbf{c}'$  of the original set  $\mathbf{c}$  of 28 tunable parameters such that:

$$\text{CMOD5}(u_{10}, \phi, \theta, \mathbf{c}') = \text{CMOD5}(u_{10} - 0.45 \text{ms}^{-1}, \phi, \theta, \mathbf{c}). \quad (4)$$

It appears possible to make such a refit within 0.002 dB for all winds between  $3 \text{ms}^{-1}$  and  $50 \text{ms}^{-1}$  and incidence angles between 18 and 56 degrees, i.e., for the entire range that could be encountered in practise. This is well within the level of data discretization (of 0.01 dB). The resulting set  $\mathbf{c}'$ , which is to be denoted by CMOD5.4, is presented in Table 2 together with the original set of coefficients.

In order to test the wind inversion for the newly obtained set of coefficients, ERS-2 backscatter triplets were inverted for the one-year period from August 1998 to July 1999. For this, the inversion software (the PRESCAT algorithm, see Stoffelen and Anderson 1997) uses a pre-calculated look-up table, in which CMOD5 based  $\sigma_0$  is tabulated at discretized values for wind speed, wind direction and incidence angle. An updated table was calculated for the new set of coefficients, and inverted winds appeared to be stronger by  $0.48 \text{ms}^{-1}$  compared to inversion using the original table. The extra  $0.03 \text{ms}^{-1}$  is probably due to the non-linear relationship between wind and backscatter and possibly systematic rounding errors in wind speed selection (steps of  $0.5 \text{ms}^{-1}$ ). Given the range of uncertainty in the bias level of CMOD5 as found above, it was not thought necessary to redo the fit. The same value of  $0.48 \text{ms}^{-1}$  was found for the entire range in wind speed and for all 19 WVC's, i.e., the updated model function truly provides winds that are  $0.48 \text{ms}^{-1}$  stronger for all situations. Retrieved wind direction was basically unaltered.

## 5.5 Re-calibration of the ERS wind archive

The collocation set of the ERS archive and ERA-40 winds confined to buoy location allowed for a re-calibration of CMOD5 and for an estimate of the bias in the ERA-40 surface wind speed. Although strictly speaking these

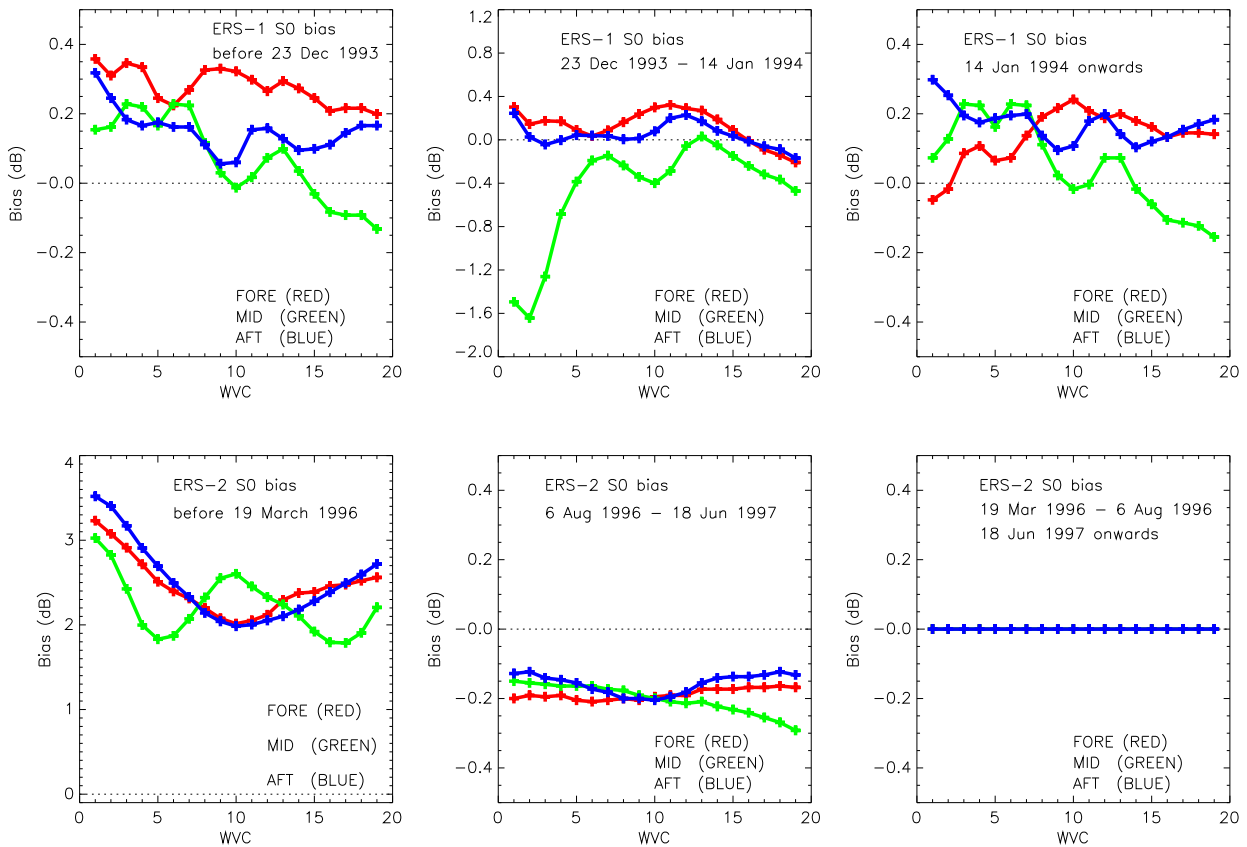


Figure 39: Biases observed in backscatter levels, based on ocean calibration for ERS-1 (top panels), respectively ERS-2 (lower panels) for the indicated periods, and relative to the nominal period for ERS-2 (lower right-hand panel). The vertical scale varies between the plots.

findings have been established near buoy location only, it is assumed that they are also valid elsewhere. Hence, it is assumed that both CMOD5.4 and re-calibrated ERA-40 winds as given in (2) provide unbiased estimates of surface wind over all global oceans. When doing so, the entire ERS archive within the ERA-40 period becomes available to detect changes in the behaviour of the ERS wind product. This typically enlarges the monthly number of 2,000 collocations near buoy locations to about 4,000,000 collocations globally. During assimilation of ERS scatterometer data in ERA-40 (1 January 1993 to 17 January 2001) collocations with ERA-40 surface wind are readily available at appropriate time (FGAT). For the period prior to assimilation, collocations have been created offline (FG) back to the start of the ERS-1 data flow in August 1991. In total this amounts to a data set of around 500,000,000 collocations.

Goal is to provide a homogeneous wind product for the entire archive up to January 2001 for both ERS-1 and ERS-2. Changes in the wind product are usually the reflection of changes in calibration of the underlying backscatter triplets. Therefore, only bias corrections in backscatter space are to be adapted; bias corrections in wind space are not to be changed. In a first iteration, CMOD5.4 winds were determined for the entire period, without applying any bias correction in backscatter levels.

For each WVC, time series of bias and STDV relative to the bias-corrected ERA-40 winds (2) were produced. This clearly indicated several (mostly known) phases of varying data quality for ERS-1 and ERS-2. Each such period was then studied separately. Biases in backscatter space were estimated on the basis of ocean calibration as given in (1), but summed over all tracks, and using modelled backscatter from bias-corrected ERA-40 winds

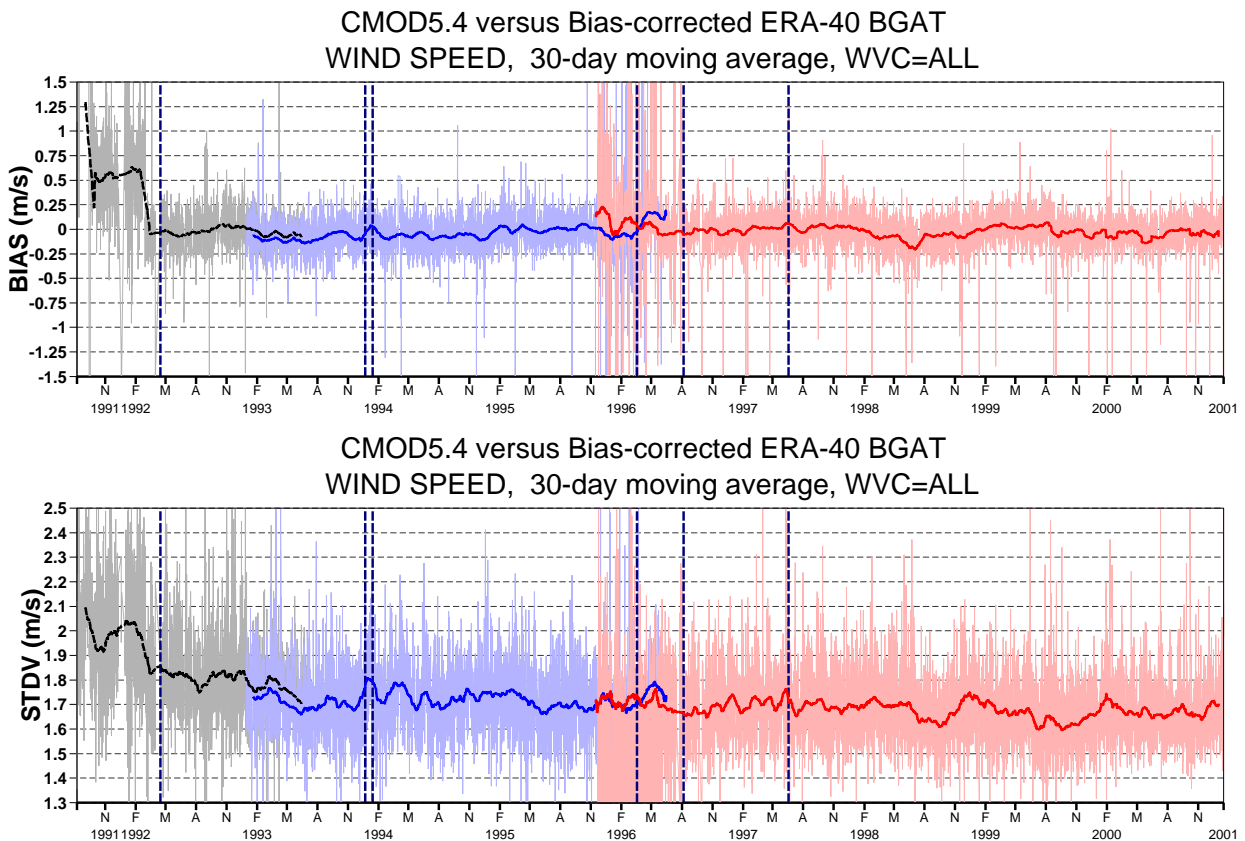


Figure 40: Relative bias between the re-calibrated AMI wind speed and bias-corrected ERA-40 First guess wind speed for ERS-1 before assimilation (black), ERS-1 during assimilation (Blue) and ERS-2 during assimilation (red) in the ERA-40 reanalysis. Vertical dashed lines mark changes in calibration of backscatter levels.

subject to CMOD5.4. Results were transformed back to dB space, and normalized such that for the nominal period of ERS-2 no corrections are to be applied (by choice). The in this way determined biases are displayed in Figure 39. For ERS-1 the following phases were identified:

- **Before 24 December 1993 and after 14 January 1994.** Small biases of around 0.2 dB which reflect the difference in calibration from ERS-2 as found in Figure 37. Although for the mid and aft antenna similar patterns are obtained for both periods, there is a noticeable difference at lower WVC's for the fore antenna.
- **24 December 1993 to 14 January 1994.** Large negative bias in the mid antenna at low WVC. Bias levels for the fore and mid antenna are small and similar. This period of anomalous behaviour at low WVC had been previously identified by Portabella and Stoffelen (2007).

For ERS-2 the following periods were observed:

- **Before 19 March 1996:** Known pre-calibration period. Bias levels are quite high, though after correction, a descent product is obtained.

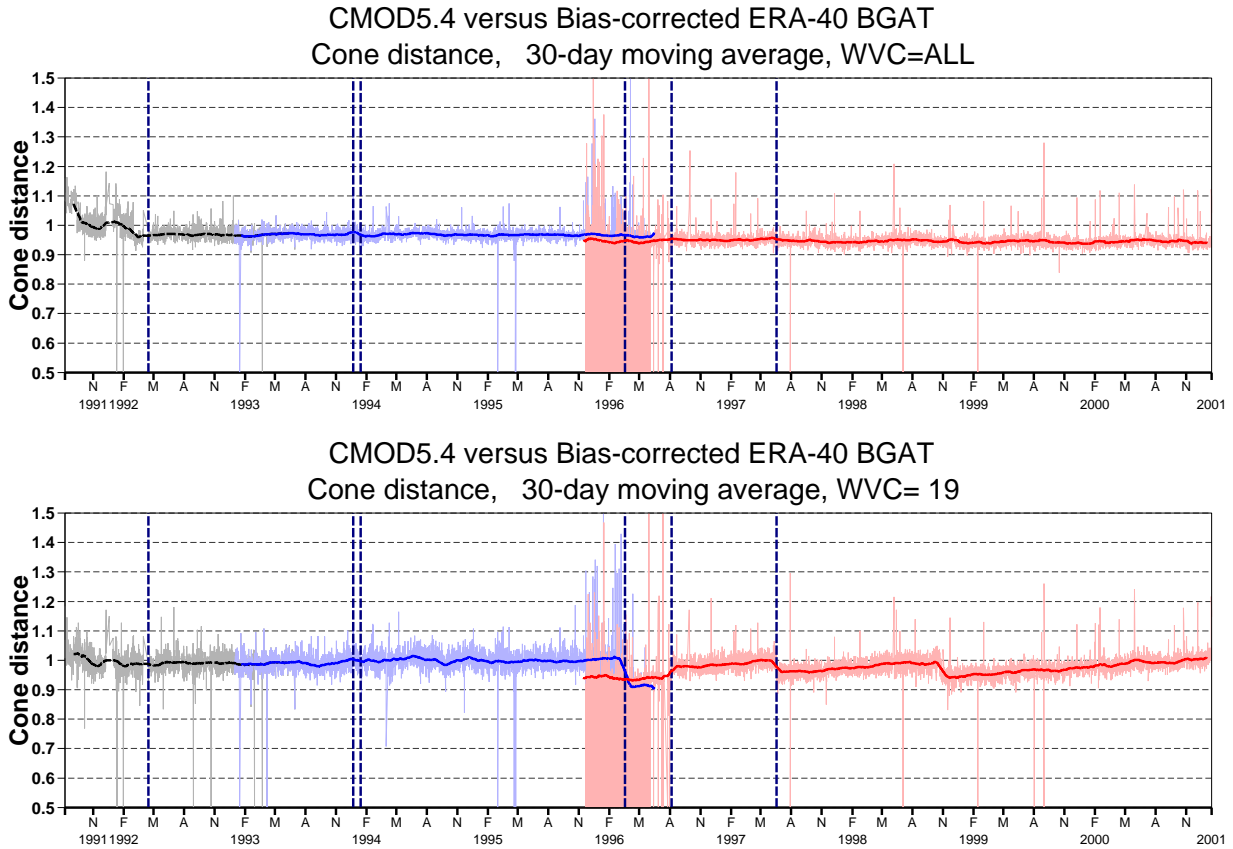


Figure 41: Time series of normalized distance to the cone averaged over all WVC's (top panel) respectively WVC 19 (lower panel) for ERS-1 before (black) respectively during (blue) assimilation, and for ERS-2 during assimilation (red) in the ERA-40 re-analysis. Vertical dashed lines mark changes in calibration of backscatter levels.

- **6 August 1996 to 18 June 1997:** Also known period; negative biases of around 0.2 dB are indeed confirmed.
- **19 March 1996 to 6 August 1996, and 18 June 1997 onwards:** Nominal period for ERS-2. By construction, no biases in backscatter space are applied.

After this exercise, CMOD5.4 winds were determined once again, but now after correction for the established biases in backscatter. In this manner a homogeneous wind product of consistent high quality for each WVC was obtained for ERS-1 from 15 April 1992 onwards, and for ERS-2 from the start of data reception on 22 November 1995. As an example a time series for the sum over all 19 WVC's is presented in Figure 40. Relative bias compared to bias-corrected ERA-40 winds is generally within  $0.2 \text{ ms}^{-1}$  for all WVC's, and STDV is typically around  $1.7 \text{ ms}^{-1}$ . The reason why this STDV is higher than what is observed for the routine monitoring of recent ERS-2 data as presented in Section 5.3 ( $\sim 1.5 \text{ ms}^{-1}$ ), is to be found in the lower quality of the ERA-40 winds compared to current operational winds.

Time series for the cone distance appeared to be homogeneous as well. Dependencies on wind speed and WVC appear reasonably well described by the following empirical relation:

$$\frac{\|\mathbf{z}^o - \mathbf{z}^m(\mathbf{s}, \phi)\|^2}{\|\mathbf{z}^o\|^2} \approx D \equiv \|\mathbf{k}_p\|^2 \left( \frac{25}{\theta_m - 5} \right) \left( \frac{s'}{1 + 2/s'} \right), \quad (5)$$

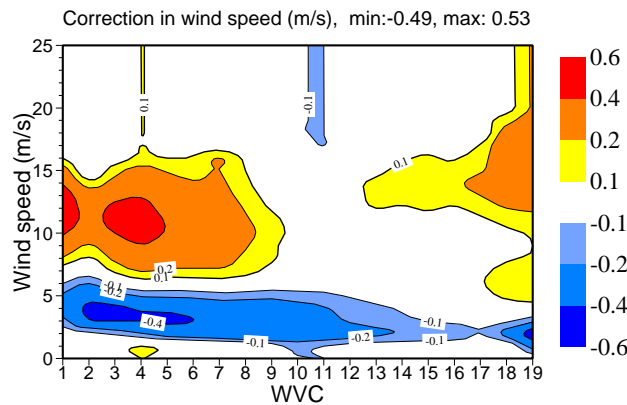


Figure 42: Correction ( $\text{ms}^{-1}$ ) applied in wind speed for ERS1 and ERS2 during the entire period of assimilation in the ERA-Interim system.

where  $\mathbf{z} = (z_{\text{fore}}, z_{\text{mid}}, z_{\text{aft}})$ , with  $z = (\sigma_0)^p$ ,  $p = 0.625$ ,  $\mathbf{k}_p = p(k_{p \text{ fore}}, k_{p \text{ mid}}, k_{p \text{ aft}})$ , where  $k_p$  is the antenna-wise reported noise level,  $\theta_m$  the incidence angle of the mid antenna, and where  $s'$  is retrieved wind speed  $s$ , though limited to the range of  $1 \text{ ms}^{-1}$  to  $25 \text{ ms}^{-1}$ . Average deviation from (5) is as function of incidence angle and wind speed around 10% respectively 30%. Note that (5) is different from the original normalization as described by Stoffelen and Anderson (1997) which had been tuned to CMOD4. On average slightly lower values are found for ERS-2. This is demonstrated by the top panel of Figure 41 which shows a time series of the cone distance normalized by  $D$  as given in (5). Although this average over all WVC's does not show a noticeable evolution in time, it does for WVC's at higher incidence angles. As demonstrated in the lower panel of Figure 41, for ERS-2 cone distance for WVC 19 slowly grows as function of time. During the erroneous switch to the redundant calibration subsystem between 6 August 1996 and 18 June 1997, the distance was temporally enhanced. After an increase in emitted power of 2dB on 26 October 1998, the average level was suddenly reduced, after which it started growing again. Clearly for this low-backscatter WVC, the cone distance is sensitive to the instrument noise, while this appears less an issue for other WVC's.

Scatterometer winds based on the here described re-calibration are currently assimilated in an experimental configuration of a future reanalysis project at ECMWF (ERA-Interim, Simmons *et al.* 2007). Before wind inversion on the basis of CMOD5.4, backscatter is corrected as described above. After wind inversion, an additional bias correction in wind speed is applied such that confined to each WVC, cumulative distributions between scatterometer and bias-corrected ERA-40 wind speed match. When doing so, it is effectively assumed that both wind sources have a similar random error. In hindsight this choice may not have been optimal, since the quality of the ERA-40 winds is lower than that of the scatterometer winds (see Section 5.5 of Abdalla and Hersbach, 2006). The resulting bias is shown in Figure 42. The more or a less WVC independent dipole correction up to  $-0.5 \text{ ms}^{-1}$  at low wind speed and  $+0.5 \text{ ms}^{-1}$  at high wind speed is induced by the (incorrect) assumption that the quality of the ERA-40 and scatterometer winds are equal. The WVC-dependent features, though, indicate residual biases that are not resolved by CMOD5.4.

At the time of writing, re-calibrated ERS winds have been assimilated in the ERA-Interim system up to May 1997. A time series of the bias and STDV compared to the new reanalysis FGAT surface winds is displayed in Figure 43. It confirms a stable homogenous wind product of high quality. Scatterometer winds are between  $0.1 \text{ ms}^{-1}$  and  $0.2 \text{ ms}^{-1}$  stronger than the FGAT winds, which indicates a small negative bias in the model winds. Relative standard deviation is in between  $1.4 \text{ ms}^{-1}$  and  $1.5 \text{ ms}^{-1}$ , which is on the level of the monitoring of recent ERS-2 scatterometer data. The improvement of  $1.7 \text{ ms}^{-1}$  for ERA-40 to  $1.5 \text{ ms}^{-1}$  for the ERA-Interim reflects the improved quality of the latter model surface winds. There is no noticeable difference in the relative STDV between ERS-1 and ERS-2. Both scatterometers seem to perform equally well.

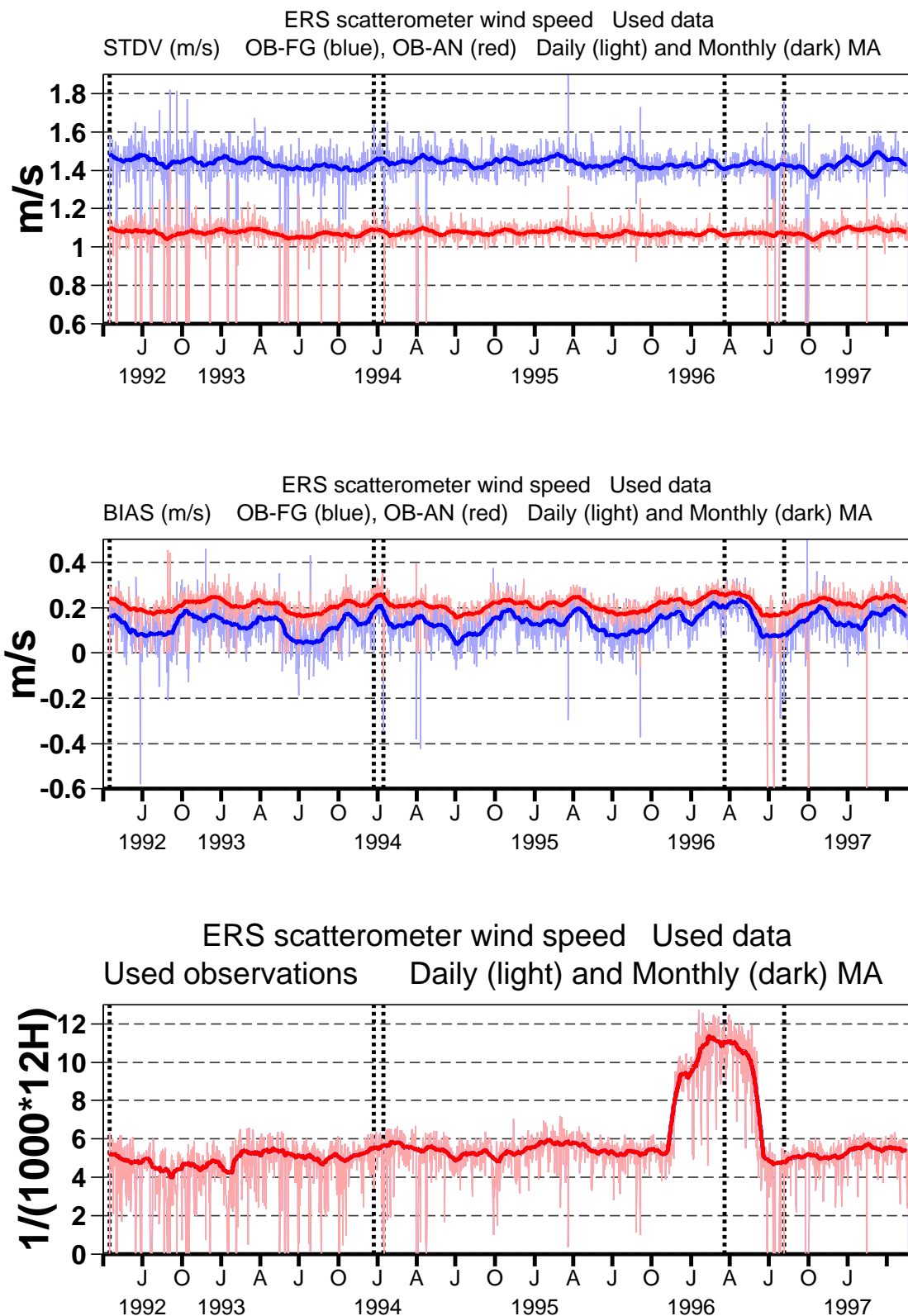


Figure 43: STDV, BIAS and number of ERS scatterometer winds used sofar in the ERA-Interim system before (blue) and after (red) assimilation. Vertical dashed lines mark changes in calibration of backscatter levels.

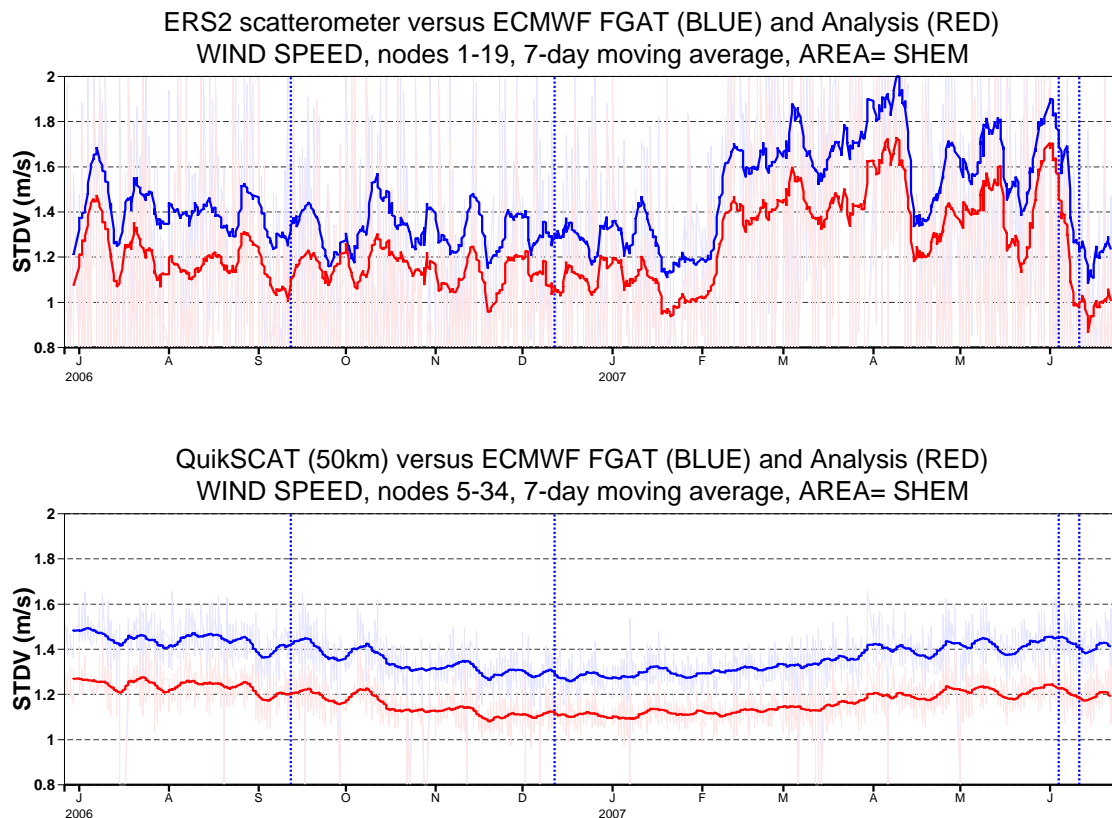


Figure 44: Time series of relative standard deviation of actively assimilated ERS-2 (top panel) and QuikSCAT (lower panel) scatterometer data versus ECMWF FGAT (in blue) and ECMWF analysis (in red) surface winds. Light colours are 6-hourly averages, dark lines the 30-day moving average. Vertical dotted lines indicate ECMWF model changes CY30R1 (1 February 2006), CY31R1 (12 September 2006) and CY31R2 (12 December 2006).

## 5.6 Screening on sea-ice

Scatterometer data is sensitive to the presence of sea ice. Over open ocean, backscatter provides information on the amplitude of capillary waves, which themselves are generated by the instantaneous surface wind fields. Observed triplets (AMI instrument on-board ERS) or quadruplets (SeaWinds instrument on-board QuikSCAT) appear distributed around a two-dimensional cone surface (Cavanié and Offiler, 1986), that represent variations in wind speed and wind direction. Over sea ice backscatter response is typically stronger and, besides, more isotropic (Cavanié A., and Gohin F., 1992, Early D. S., and Long D. G., 1997). In backscatter space these data follow an ice line, which is parametrized by a quantity that is denoted by ice age. In addition, sea ice and open ocean show a different variation of backscatter as function of incidence angle. Thanks to the differences in characteristics in backscatter response, continuous ingestion of scatterometer data can be used for the update of sea ice maps and sea ice drift (see e.g. Ezraty *et al.*, 2007)

In the screening part of the ECMWF integrated assimilation and forecast system (IFS), single ERS-2 observations are rejected when a backscatter triplet is too far from the (CMOD5) model cone. Due to the size of natural fluctuations this limit cannot be set too narrow. In addition, this quality control does not work where the wind cone and ice line overlap. For these reasons, quality control from an independent source is required.

At ECMWF, information on sea ice is obtained from the National Centers for Environmental Prediction (NCEP).

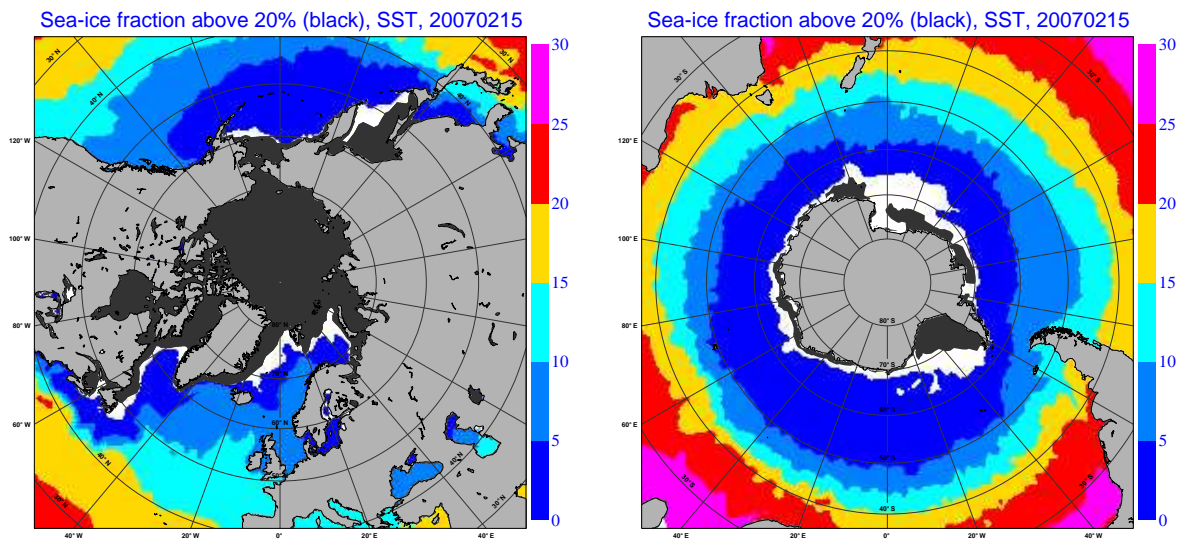


Figure 45: Sea-ice fraction exceeding 20% (in black) and sea surface temperature (in degrees Celsius) for 15 February 2007.

Fields are re-sampled from their native resolution (0.5x0.5 degrees) to the (reduced Gaussian) grid of the forecast model. Besides some other modifications, interpolated values below 20% are set to zero. More information on this procedure and an assessment of the quality of the resulting product can be found in Drusch 2006.

The NCEP based ice field is used for the screening of scatterometer data. An observation is rejected whenever the collocated sea ice concentration exceeds 1%, i.e., in practise when it exceeds 20%. Long-term monitoring of scatterometer data shows that this threshold is not sufficient. Around the ice edges, scatterometer data typically seem a few  $\text{m s}^{-1}$  too strong, as can e.g. be seen from the Cyclic coverage plots as presented in Figure 29.

Although problems in screening on sea ice have been present for a long time, the situation has worsened for ERS-2 data since February 2007. Illustration for this is given in Figure 44, where a long-term time series of the relative standard deviation between scatterometer and ECMWF wind over the Southern Hemisphere is presented. For QuikSCAT such an increase in standard deviation is not observed. A more detailed picture is presented in the top panels of Figure 46, which show the average difference in wind speed between ERS-2 (left-hand panel) respectively QuikSCAT (right-hand panel) from ECMWF FGAT winds over February 2007 in the Antarctic. Besides areas around the ice edge, it shows a larger anomalous area in the Ross Sea. According to the sea-ice map, as e.g., shown by the black area in the right-hand panel of Figure 45 for 15 February 2007, largest deviations are found for an area that is more or a less enclosed by sea ice. It does not necessarily mean that the postprocessed sea ice field is incorrect. The NCEP ice field is based on accumulated information of data from the Special Sensor Microwave Imager (SSM/I). This passive imager is less sensitive to changes in sea ice than an active scatterometer instrument. Regardless of the question whether sea-ice map accurately corresponds with the presence of sea ice, it seems clear that scatterometer data is contaminated for certain regions outside the available sea ice map.

The Arpege model of Meteo France shares the IFS code with ECMWF. In their version screening on sea ice is performed on the basis of sea-surface temperature (SST). Data is rejected at locations where SST is below 278K. At ECMWF such screening had also been performed in earlier model versions. Originally a threshold of 275K was used. In May 1997 it was replaced by a value of 273K, since the original choice was found to be too conservative. Note that all these threshold values are well above a typical freezing temperature of  $-1.5^{\circ}\text{C}$  (271.15 K) for sea water, and therefore can be regarded as safe sea-ice boundaries.

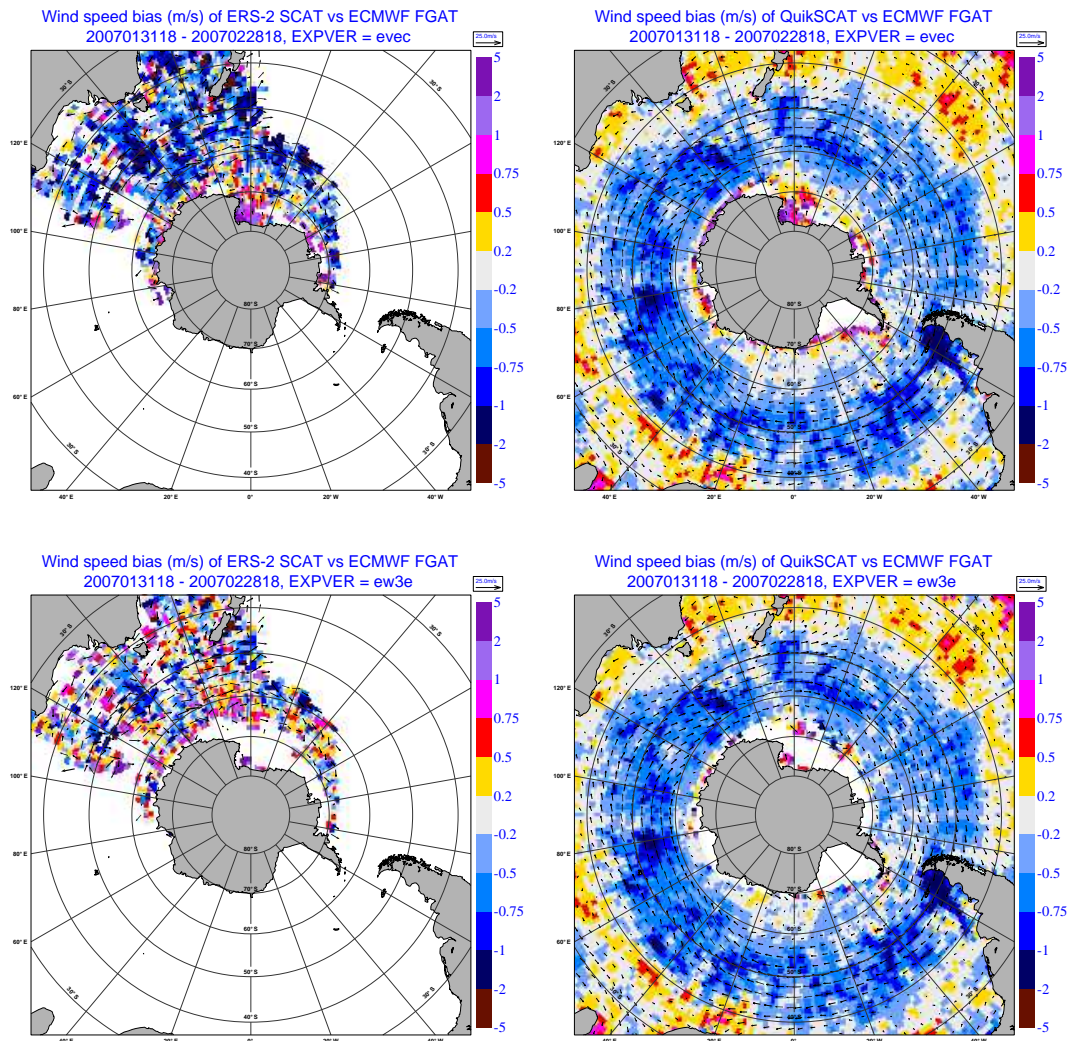


Figure 46: Monthly average (over February 2007) wind speed bias of ERS-2 (left hand panels) and QuikSCAT (right hand panels) compared to ECMWF FGAT surface winds for the control experiment (top panels) and sea-ice experiment (lower panels) over the Antarctic area.

The SST field as used at ECMWF also originates from NCEP. In Figure 45 this field is shown for 15 February 2007, together with the sea-ice map (in black) that is currently used for screening. When compared with deviation maps for scatterometer winds versus ECMWF model fields (as e.g. shown in Figure 46), it emerges that a choice of  $0^{\circ}\text{C}$  (i.e. basically the same as the threshold of 273 K used previously) provides a fair trade off between rejecting potentially poor data and retaining potentially good quality data. Instead of replacing the check on sea ice fraction by the check on SST, it was decided to screen on both criteria, i.e., data is rejected when either of the two checks fails.

The change in screening on sea ice was incorporated in the release of a new model cycle (CY32R2) on 7 July 2007.

## 6 Concluding remarks

Continuous monitoring and verification of the ERS-2 fast delivery wind and wave products from RA (URA), SAR (UWA) and scatterometer (UWI) are carried out routinely at ECMWF. Data from ECMWF atmospheric (IFS) and wave (ECWAM) models and from in-situ buoy observations are used for this purpose. As a result of the loss of gyros in early 2001, several products were degraded. The main victim was the UWI product, which became of poor quality forcing ESA to halt its dissemination. ESA managed to improve the quality of the UWI product which culminated in the public re-dissemination on 21 August 2003. The quality of the UWI product has been closely monitored at ECMWF since 12 December 2001. On 8 March 2004 ERS-2 scatterometer data was reintroduced at the ECMWF assimilation system. The degradation impact of zero-gyro mode was less pronounced on the URA and UWA products. Since the failure of the ERS-2 low bit rate tape recorders on 22 June 2003, data coverage has been restricted to the North Atlantic and western coasts of North America. More ground stations were later utilized to extend the coverage to the Southern Ocean, the eastern coasts of China and the northeastern parts of Indian Ocean. Despite the lack of the global coverage of LBR ERS-2 data, the remaining coverage represents an important area for many applications. Even positive impact on global forecast skill was found in several assimilation experiments (Hersbach 2004), which led to the re-introduction of the usage of ERS scatterometer data at ECMWF on 8 March 2004. Among others, for these reasons maximum possible continuation of the ERS-2 mission is important.

Long-term evaluation of ERS wind and wave products was carried out for the whole lifetimes of both ERS-1 and ERS-2 missions. Offline altimeter ocean product (OPR) and fast delivery products from SAR (UWA) and scatterometer (UWI) were evaluated and the following results were obtained:

- OPR SWH products from both satellites are of good quality. ERS-2 SWH product is about 30 cm higher than ERS-1. It seems, however, that ERS-1 SWH product is slightly better than ERS-2 product.
- The OPR wind speed product had several problems by time. ERS-1 OPR wind product suffered significant abrupt changes in bias at least 3 times. On the other hand, ERS-2 OPR wind speed product was rather stable for the first 4.5 years before it started to degrade (especially in the Southern Hemisphere) after the gyro problems started in early 2000. Therefore, one should handle the altimeter wind speed product with care especially for climate studies.
- SWH from ERS-1 UWA product is too high with respect to the wave model with at least two significant jumps in bias. The product seems to be degraded during Phase G (after March 1995). On the other hand, ERS-2 UWA product seems to be much better with lower bias and standard difference with respect to the wave model. However, a calibration bug (July 1998-November 2000) and the loss of the gyros (January-June 2001) degraded the product (or its inversion) during most of ERS-2 lifetime.
- A re-calibration of the ERS archive from the start until January 2001 on the basis of a collocation with ERA-40 winds suggests that there is a small difference in calibration between ERS-1 and ERS-2. Backscatter levels of ERS1 are around 0.2 dB higher than for ERS-2, which translates to a difference in wind speed of approximately  $0.2\text{m s}^{-1}$ .
- The potential quality of the AMI wind product is stable and comparable between ERS-1 and ERS-2. Changes in the behaviour of the ERS-1 and ERS-2 UWI wind product can be attributed to changes in calibration of the underlying level 1B backscatter product. By bias-correcting level 1b values before wind inversion, it appears possible to obtain an unbiased wind product of consistent high quality for all incidence angles from 15 April 1992 for ERS-1 and from 22 November 1995 for ERS-2 onwards. This analysis, therefore, indicates a high potential for a re-processing enterprise, which should result in a homogenous, unbiased high-quality wind product for the entire ERS archive.

Monthly or cyclic monitoring reports can be found at:

URA (monthly): <http://earth.esa.int/pcs/ers/ra/reports/ecmwf>  
UWA (monthly): <http://earth.esa.int/pcs/ers/sar/reports/ecmwf> (password protected)  
UWI (5-weekly): <http://earth.esa.int/pcs/ers/scatt/reports/ecmwf>

## Acknowledgements

The work presented in this paper was funded by ESRIN (Project Ref. 18212/04/I-OL). We would like to thank Peter Janssen, Jean-Raymond Bidlot, Lars Isaksen and Raffaele Crapolicchio, for support and valuable discussions. Conversion of OPR products into BUFR and the wave model hindcast using ERA-40 wind fields which was used for OPR wave product verification were carried out by Jean-Raymond Bidlot.

## A Appendix: Related Model Changes

Note: All changes were introduced for the 6-hour time-window centred at 18:00 UTC.

**21 Jun. 1992** Operational implementation of the global model on a 3 degree latitude-longitude grid (63°S to 72°N). The wave spectrum is discretized using 12 directions and 25 frequencies (from 0.041772Hz).

**15 Aug. 1993** Assimilation of ERS-1 RA wave heights in global model.

**3 Jul. 1994** The global model horizontal resolution was increased to 1.5 degree (from 81°N to 81°S).

**19 Sep. 1995** New windsea/swell separation scheme.

**30 Jan. 1996** Changes to IFS (e.g. 3DVAR operational).

**1 May 1996** Assimilation switch from ERS-1 to ERS-2 RA wave heights.

**1 Jun. 1996** Changes to IFS to switch the assimilation of scatterometer winds from ERS-1 to ERS-2.

**4 Dec. 1996** The global model horizontal resolution was changed to a 0.5 irregular latitude-longitude grid, with an effective resolution of about 55 km (from 81°N to 81°S). Change the wave-model integration scheme to accommodate Hersbach and Janssen new limiter.

**13 May 1997** Modification of the advection scheme by defining the first direction as half the directional bin.

**27 Aug. 1997** Changes to IFS (e.g. scatterometer winds are no longer blacklisted for speeds above 20 m/s and modification to the scatterometer bias).

**11 Nov. 1997** Changes to IFS (e.g. modification of the scatterometer QC).

**25 Nov. 1997** Changes to IFS to implement the 4D-Var assimilation scheme.

**1 Apr. 1998** Changes to IFS model (e.g. change horizontal resolution to T319).

**28 Jun. 1998** Operational implementation of the coupling between WAM and IFS.

**9 Mar. 1999** 10 m winds are used in coupled model. IFS changes (e.g. change vertical resolution to 50 levels, and modification of the scatterometer QC).

**13 Jul. 1999** RA wave height correction based on non-gaussianity of the sea surface elevation. Change to the frequency cut-off in the integration scheme. IFS changes (new physics/dynamics coupling).

**12 Oct. 1999** Changes to IFS model (e.g. change vertical resolution to 60 levels, and new orography)

**11 Apr. 2000** RA data quality control based on peakiness factor. Penalization of low altimeter wave heights in data assimilation. An extra iterative loop to determine the surface stress.

**27 Jun. 2000** Sea ice fraction is used for the ice mask. The buoy validation software was upgraded to use the proper anemometer height.

**11 Sep. 2000** Assimilation scheme in IFS changed to 12 hour 4D-Var.

**20 Nov. 2000** Increase the horizontal resolution of the atmospheric model to T511 (around 40 km). Increase spectral resolution in the global deterministic WAM model to 24 directions and 30 frequencies. Improved advection scheme on irregular grids. New empirical growth curves in the RA data assimilation. Bug fix of the SAR inversion software to properly use SAR data with the new calibration procedure (the bug was effective since June 1998).

**11 Jun. 2001** IFS modifications.

**21 Jan. 2002** Modified scheme for the time integration of the source terms. Assimilation of QuikSCAT data in IFS model.

**8 Apr. 2002** Inclusion of wind gustiness and air density effect. Removal of spurious values for the Charnock parameter. Blacklisting procedure for wave data.

**16 Apr. 2002** Extra quality control for QuikSCAT.

**13 Jan. 2003** Assimilation of ERS-2 SAR data. Background check for altimeter data during assimilation. Significant changes to IFS model, including a new minimisation scheme and improved background error in the assimilation part.

**22 Oct. 2003** Assimilation of ENVISAT Radar Altimeter-2 Ku-Band significant wave heights. ERS-2 RA wave height assimilation was discontinued. (This change was introduced at 6-hour time-window centred at 00:00 UTC.)

**8 Mar. 2004** Use of unresolved bathymetry in wave model. Wave model is now driven by neutral 10-metre wind. Re-introduction of ERS-2 scatterometer data based on CMOD5.

**28 Jun. 2004** The implementation of the early delivery system.

**27 Sep. 2004** Proper treatment of the initialisation of wave fields for time windows 06:00 and 18:00 UTC.

**5 Oct. 2004** Stop erroneously discarding some ENVISAT altimeter data in wave analysis.

**5 Apr. 2005** Implementation of a revised formulation for ocean wave dissipation due to wave breaking.

**1 Feb. 2006** Implementation of the high resolution atmospheric (T799) and wave ( $0.36^\circ$ ) models. ENVISAT ASAR Level 1b Wave Mode spectra replaced ERS-2 SAR in assimilation. Jason altimeter wave height data are assimilated.

**12 Sep. 2006** Revised cloud scheme, including treatment of ice supersaturation and new numerics; implicit computation of convective transports.

**5 Jun. 2007** Three outer loops for 4D-Var (T95/159/255).

**12 Jun. 2007** Active use of IASI and ASCAT from METOP.

## References

- Abdalla S. and Hersbach H. (2004). The technical support for global validation of ERS Wind and Wave Products at ECMWF, *Final report for ESA contract 15988/02/I-LG, ECMWF, Shinfi eld Park, Reading*.  
[http://www.ecmwf.int/publications/library/ecpublications/\\_pdf/esa/ESA\\_abdalla\\_hersbach.pdf](http://www.ecmwf.int/publications/library/ecpublications/_pdf/esa/ESA_abdalla_hersbach.pdf)
- Abdalla S. and Hersbach H. (2006). The technical support for global validation of ERS Wind and Wave Products at ECMWF (April 2004 - June 2006), *Final report for ESA contract 18212/04/I-LG, ECMWF, Shinfi eld Park, Reading*.  
[http://www.ecmwf.int/publications/library/ecpublications/\\_pdf/esa/ESA\\_abdalla\\_hersbach\\_18212.pdf](http://www.ecmwf.int/publications/library/ecpublications/_pdf/esa/ESA_abdalla_hersbach_18212.pdf)
- Attema, E., P., W. (1986). An experimental campaign for the determination of the radar signature of the ocean at C-band, *Proc. Third International Colloquium on Spectral Signatures of Objects in Remote Sensing*, Les Arcs, France, ESA, SP-247, 791-799, 1986.
- Bidlot, J. R., D. J. Holmes, P. A. Wittmann, R. Lalbeharry, H. S. Chen (2002). Intercomparison of the performance of operational ocean wave forecasting systems with buoy data. *Wea. Forecasting*, **17**, 287-310.
- Bidlot, J. R., Janssen, P. A. E. M., Abdalla, S. (2006). Impact of the revised formulation for ocean wave dissipation on ECMWF operational wave models. *ECMWF Technical Memorandum (In preparation)*.
- Brown, A. R., Beljaars, A. C. M., Hersbach, H., Hollingsworth, A., Miller, M., Vasiljevic, D. (2005). Wind turning across the marine atmospheric boundary layer *Quart. J. Roy. Meteor. Soc.* **607**, 233-1250.
- Brown, A. R., Beljaars, A. C. M., Hersbach, H. (2006). Errors in parametrizations of convective boundary layer turbulent moment mixing *Accepted for publication in: Quart. J. Roy. Meteor. Soc.*
- Cavanié A., and Gohin F., 1992. ERS-1 scatterometer data over sea ice, *Proc. ESA Workshop ERS-1 Geophysical Validation*, Penhors, France, Apr. 27-30 1992, ESA WPP36 (European Space Agency, Paris), 199-201.
- Crapolicchio, R., P. Lecomte, X. Neyt (2004). The advanced scatterometer processing system for ERS data: design, products and performance. Proceedings of the ENVISAT and ERS Symposium, Salzburg, Austria, 6-10 September 2004.
- Drusch M. 2006. Sea Ice concentration Analyses for the Baltic Sea and Their impact on Numerical Weather Prediction' *J. of Applied Meteorol. and Climatology*, **45**, 982-994.
- Early D. S., and Long D. G., 1997. Azimuthal modulation of C-band scatterometer  $\sigma^0$  data over Southern Ocean sea ice. *IEEE Transactions on Geoscience and Remote Sensing*, **35**, 1201-1209.
- ESA (2005). ERS-1 Mission Phases (from 1991 onwards). *An Internet web page* accessible from:  
<http://earth.esa.int/rootcollection/eo/ERS1.1.7.html>  
Last visited: 21 July 2006.
- Ezraty R., Girard-Arduin F., and Piollé J.-F., 2007. Sea Ice Drift in the Central Arctic combining QuikSCAT and SSM/I Sea Ice Drift Data, available at:  
<ftp://ftp.ifremer.fr/ifremer/cersat/products/gridded/psi-drift/documentation/merged.pdf>
- Féménias P., and Martini A. (2000). ERS-2 AOCs mono-gyro attitude software Qualification Period - Radar Altimeter Data Analysis. *ESA-ESRIN Technical Note*, accessible from:  
<http://earth.esa.int/pcs/ers/ra/events/monogyro/>
- Freilich, M. H., and Dunbar R. S. (1999). The accuracy of the NSCAT 1 vector winds: comparisons with

National Data Buoy Center buoys, *J. Geophys. Res.*, **104** (C5), 11,231-11,246.

Hersbach, H. (2003). CMOD5. An improved geophysical model function. *ECMWF Technical memorandum 395*, ECMWF, Reading, England.

Hersbach H., Janssen P. A. E. M., Isaksen, L. (2004). Re-introduction of ERS-2 scatterometer data in the operational ECMWF assimilation system. Proceedings of the ENVISAT and ERS Symposium, Salzburg, Austria, 6-10 September 2004.

Hersbach H., Stoffelen A., and Haan de S., 2007, An improved C-band scatterometer ocean geophysical model function: CMOD5, *J. Geophys. Res.*, **112** (C3) C03006.

Hersbach H., Abdalla S., and Bidlot J. R., 2007b, Long Term Assessment of ERS-1 and ERS-2 Wind and Wave Products, Proceedings of the ENVISAT and ERS Symposium, Montreux, Switzerland, 23-27 April 2007.

IFS documentation, (2004). edited by P. White, <http://www.ecmwf.int/research/ifsdocs/CY28r1/>

Isaksen, L., and Janssen P. A. E. M. (2004). The benefit of ERS Scatterometer Winds in ECMWF's variational assimilation system. *Q. J. R. Meteorol. Soc.* **130** 1793-1814,

Janssen, P. A. E. M. (2004). *The interaction of ocean waves and wind.*, Cambridge Univ. Press, 300p.

Janssen, P. A. E. M., B. Hansen, and Bidlot J. R. (1997). Verification of the ECMWF wave forecasting system against buoy and altimeter data, *Wea. Forecasting*, **12**, 763-784.

Janssen, P., Bidlot, J. R., Abdalla, S., Hersbach H. (2005). Progress in Ocean Wave Forecasting at ECMWF. *ECMWF Technical Memorandum 478*, ECMWF, Reading, UK. Available online from: [http://www.ecmwf.int/publications/library/ecpublications/\\_pdf/tm/401-500/tm478.pdf](http://www.ecmwf.int/publications/library/ecpublications/_pdf/tm/401-500/tm478.pdf)

Portabella M., and Stoffelen A., 2007. Development of a global Scatterometer Validation and Monitoring, to appear at: <http://www.knmi.nl/publications/>

Simmons A., Uppala S., Dee D., and Kobayashi S., 2007. ERA-Interim: New ECMWF reanalysis products from 1989 onwards, *ECMWF Newsletter*, **110**, 25-35.

Stoffelen, A. C. M., and Anderson D. L. T. (1997). Scatterometer Data Interpretation: Derivation of the Transfer Function CMOD4, *J. Geophys. Res.*, **102** (C3) 5,767-5,780.

Uppala, S. M., Kållberg, P. W., Simmons, A. J., Andrae, U., Da Costa Bechtold, V., Fiorino, M., Gibson, J. K., Haseler, J., Hernandez, A., Kelly, G. A., Li, X., Onogi, K., Saarinen, S., Sokka, N., Allan, R. P., Andersson, E., Arpe, K., Balmaseda, M. A., Beljaars, A. C. M., Van De Berg, L., Bidlot, J., Bormann, N., Caires, S., Chevallier, F., Dethof, A., Dragosavac, M., Fisher, M., Fuentes, M., Hagemann, S.; Hólm, E., Hoskins, B. J., Isaksen, L., Janssen, P. A. E. M., Jenne, R., McNally, A. P., Mahfouf, J. F., Morcrette, J. J., Rayner, N. A., Saunders, R. W., Simon, P., Sterl, A., Trenberth, K. E., Untch, A., Vasiljevic, D., Viterbo, P., Woollen, J. (2005). The ERA-40 re-analysis *Quart. J. Roy. Meteor. Soc.* **131**, 2961-3012.